NASA CONTRACTOR REPORT

NASA CR-40

c.1

NASA CR-400

CONTROL MOMENT GYRO OPTIMIZATION STUDY

by G. W. Yarber, K. T. Chang, Joseph Kukel, B. F. McKee, C. S. Smith, A. F. Anderson, C. J. Bertrem, and Sergel Tarhov

Prepared under Contract No. NAS 1-4439 *by*
GARRETT AIRESEARCH MANUFACTURING DIVISION
Los Angeles, Calif.
for Langley Research Center

NATIONAL AERONAUTICS AND SPACE ADMINISTRATION • WASHINGTON, D. C. • MARCH 1966

NASA CR-400

CONTROL MOMENT GYRO OPTIMIZATION STUDY

By G. W. Yarber, K. T. Chang, Joseph Kukel, B. F. McKee, C. S. Smith, A. F. Anderson, C. J. Bertrem, and Sergel Tarhov

Prepared under Contract No. NAS 1-4439 by
GARRETT AIRESEARCH MANUFACTURING DIVISION
Los Angeles, Calif.

for Langley Research Center

NATIONAL AERONAUTICS AND SPACE ADMINISTRATION

For sale by the Clearinghouse for Federal Scientific and Technical Information
Springfield, Virginia 22151 – Price $2.00

ABSTRACT

Future manned spacecraft, such as manned orbital laboratories or interplanetary spacecraft, will use momentum storage systems to minimize weight and power expenditures for their long termed missions. Primary applications of such systems will be in spacecraft stabilization systems, where control moment gyros or reaction wheels provide rate and attitude control by precessing or accelerating rotating flywheels. Secondary applications of the momentum storage concepts involve power conditioning equipment and other rotating machinery on the spacecraft.

In view of the required development of momentum storage hardware for these applications, the Langley Research Center of NASA has sponsored an optimization and preliminary design study of rotating assemblies and their associated components for minimum weight and power in the spacecraft environment. The most immediate use for these rotating components has been in the development of control moment gyroscopes for the spacecraft control systems, and control moment gyros thus provided the basis on which this optimization study was performed.

This report includes the technical approach, the solution techniques, and the results of this optimization study. The data presented comprise the preliminary design of flywheels spinning to produce a wide range of angular momenta while maintaining minimum weight, size, bearing friction, and windage loss. Other areas that were considered include the maximizing of bearing life under extreme loading conditions, proper lubrication schemes for bearings in a vacuum environment, and flywheel drive motor design for spinup and constant speed operation. The data given for these design areas should be of considerable value in the future analysis of any rotating assembly where weight and power are critical.

CONTENTS

CONTENTS (Cont).

CONTENTS (Cont)

ILLUSTRATIONS

ILLUSTRATIONS (Cont)

ILLUSTRATIONS (Cont)

SYMBOLS

ROTOR STRESS ANALYSIS

W	weight of rotor, lb
r	rim radius, in.
I	moment of inertia, lb-sec^2-in.
γ	specific weight, lb/in.^{3}
g	gravity constant, in./sec^2
σ	centrifugal stress, lb/in.^{2}
ω	angular speed, rad/sec
ν	Poisson's ratio

SELECTION OF THE MOTOR SYSTEM

P_i	power input
P_o	power output
ω_s	synchronous speed of rotating field in the stator, rad/sec
ω_r	rotor speed, rad/sec
T_l	torque, ft-lb
E_L	energy loss
α	acceleration
KE	kinetic energy
E_t	total energy
H	angular momentum
P_e	electrical power
T_o	torque
P_M	motor power rating
Δ_t	constant acceleration in time

WINDAGE LOSS FOR THE MOMENTUM WHEEL

M	moment, ft-lb
ω	angular velocity, rad/sec
ρ	mass of gas per unit volume
a	radius, ft
μ	coefficient of viscosity
ν	coefficient of kinematic viscosity
V	velocity
R	universal gas constant, ergs/^{o}K mole
T	temperature, ^{o}K
W	molecular weight
p	pressure
l	length

WINDAGE POWER LOSS FROM OIL VAPOR PRESSURE

P_o	windage power loss due to oil vapor pressure
P_{Ho}	windage power loss due to hydrogen gas at a pressure equivalent to the oil vapor pressure
W_o	molecular weight of the oil
W_H	molecular weight of hydrogen

COMPUTER PROGRAM

H	angular momentum, in.-lb-sec
R	wheel radius, in.
t_o	reference wheel thickness, in.
ω	angular speed, rad/sec
σ	maximum centrifugal stress, psi

COMPUTER PROGRAM (Continued)

γ	specific weight of wheel material, lb/in.^{3}
W	weight of wheel, lb
σ_{s_o}	maximum allowable static stress component
σ_{d_o}	maximum allowable dynamic stress component
M	gyroscopic moment
β	coefficient dependent on r/R where r is the shaft radius
t	axial depth of fiberglass windings, in.
T	torque, mm Hg
B	function of bearing size, curvature and ball complement
N	rpm
L	lubricant term proportional to (kinematic viscosity)$^{2/3}$
Q	empricial lubricant quantity factor, $\geq$ 0.4 for film lubrication
F	radial load, lb
D	pitch diameter, in.
f	ball to race osculation term, a function of curvature
n	number of balls
d	ball diameter, in.
T_h	thrust load, lb
K_t	ball race osculation term, a function of curvature and thrust
K_r	ball race osculation term, a function of curvature and radial load
α	contact angle
C	constant ball separator friction, empirically determined
P_w	windage loss, watts

COMPUTER PROGRAM (Continued)

p	pressure, mm Hg
t	rim thickness, in.
W_h	housing weight, lb
W_m	motor weight, lb
H	angular momentum, in.-lb-sec

THERMAL ANALYSIS DOUBLE-GIMBALLED GYRO

Q	heat flow Btu per min
K	thermal conductivity, Btu per min $ft^2/^oF/ft$
A	cross-sectional area of flow path, ft^2
L	length of flow path, ft
ΔT	temperature difference, ^oF
σ	Stephan-Boltzmann Constant
Σ	emissivity, dimensionless
f	radiative area, ft
T_R	bearing-motor temperature, ^oF
T_S	surrounding temperature, ^oR

STRUCTURAL ANALYSIS OF THE HOUSING (INNER GIMBAL RING)

E	modulus of elasticity
r	radius of sphere
ν	Poisson's ratio
t	thickness
H	the point load
a	radius

SECTION I

INTRODUCTION

Space vehicles, as a rule, need attitude and stability control in order to fulfill mission requirements. The control moment for this purpose can be obtained either internally (reacting against an onboard component) or externally (jet thrustors, gravity gradient). The relative merits of these schemes depend upon such factors as duration of the mission, precision and extent of control required, and frequency and nature of the anticipated disturbances. For a given mission, the engineering decision to use one control method or another must rely on the results of a study in which the best available designs from both concepts can be compared. Lack of information on what constitutes an optimum design in either concept thus will not allow such a comparative study to be made. The present study was initiated to provide the answer to one aspect of this problem--a parametric study to establish the minimum weight and power requirements for control moment gyros in the angular momentum range from 200 to 2000 ft-lb-sec.

A control moment gyro (CMG) uses a wheel which rotates at constant speed and obtains the control moment by changing the direction of its spin axis. (This should be differentiated from the mechanism of an inertia wheel, in which the moment is obtained by acceleration or deceleration of the wheel about its axis of rotation, although both are internal control devices.) Figure 1-1 illustrates one manner of application of the CMG. The wheel is mounted in two gimbal frames; a drive motor along the z-axis maintains the wheel at constant speed and is also used for initial start-up of the spin after launch. Two torquers along the x and y axes apply torques to the outer and inner gimbals, respectively, and transmit the reactive gyroscopic moment to the vehicle; the moment is produced by angular displacement of the spin axis through gimbal rotations. This arrangement allows the variable moment magnitudes to be independently specified without actively controlling the motion of the spin axis, as long as the saturation gimbal angle is not exceeded by the torquer demand (60 degrees has been assigned to avoid gimbal lock-up). Note that gimbal rotation and applied torque may be in opposite directions, since the rotation of, say, the x-gimbal depends on the direction of the moment about the y-axis, and vice versa.

The translation of this schematic system into optimized and producible hardware requires both a knowledge of component capabilities and system integration techniques. Briefly stated, a flywheel must be designed to operate at a safe speed and which possesses the specified amount of angular momentum. It must also be able to transmit gyroscopic moment through the shaft to the bearing supports. A drive motor capable of accelerating the flywheel to speed and maintaining that speed must be designed to be mounted on the same shaft. The bearings and a lubricating system are next designed for the specified speed, loading, and life requirements, paying special attention to achieving low power consumption. The inner gimbal structure in this case is a hermetically sealed housing which must be able to withstand external pressure without collapsing, as the housing must be evacuated to a low pressure in order to reduce windage loss of the gyro. The torquers must each be capable of

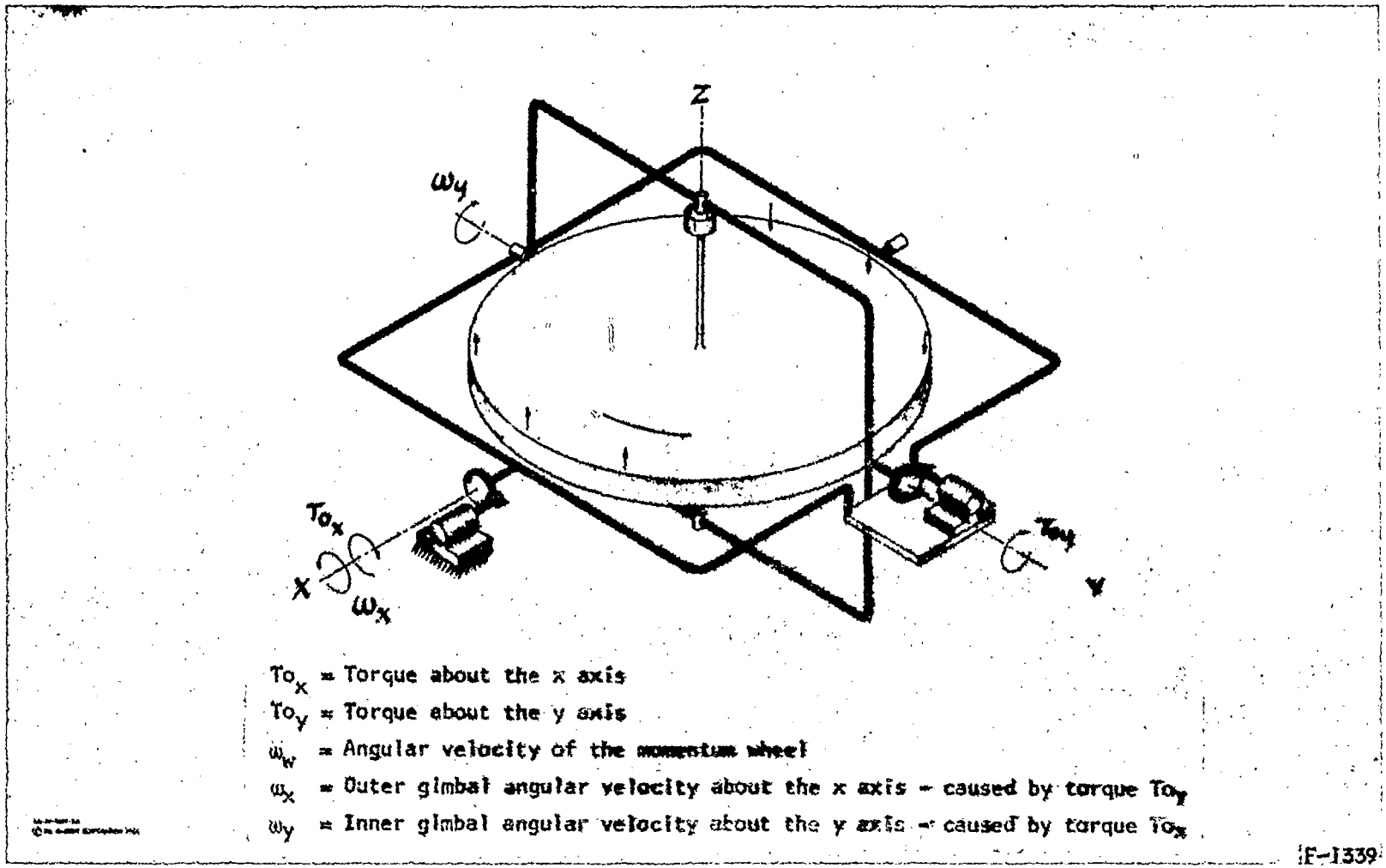

Figure 1-1. Schematic - Control Moment Gyro

delivering up to 50 ft-lb of torque with minimum weight and power demand. All structural elements must have the necessary strength and rigidity, so that reliable and trouble-free performance of the CMG can be obtained. Last, monitoring devices must be installed to detect and forewarn the occurrence of mechanical or electrical malfunctions.

The objective of this parametric study has been to establish the optimum design for momentum wheel assemblies based on the following criteria:

1. The assembly should have minimum weight and require a minimum amount of power to operate. The need to minimize pay load for any space mission is basic.

2. The design must incorporate the highest degree of reliability. Since CMG's perform a vital function in space missions, and repairs or replacement in space are costly and time consuming, the most reliable design is mandatory.

3. While scheduled services cannot be completely eliminated, a life of at least one year of continuous operation without service is a reasonable requirement.

4. Scheduled maintenance work should be designed so that it can be easily carried out and does not require special training.

5. The design should provide for a specified peak control moment. This design was based on 50 ft-lb of control torque being applied frequently for short time duration. Optimization of the design configuration should be based on the average expected moment. (In this design, 18.5 ft-lb was used).

6. The drive motor should be designed for constant synchronous speed. This requirement is consistent with the basic operating principle of a CMG where, except for initial start-up, the wheel maintains a constant speed of rotation.

7. The moment of inertia of the rotating assembly must be held to close tolerance. This requirement, together with the synchronous speed drive, allows pairs of counter-rotating CMG's to execute controls with great precision and without producing cross-coupling.

8. The lubrication system must be able to operate satisfactorily in a soft vacuum under zero "g" condition. The requirement to minimize windage loss dictates that the housing be evacuated to a low pressure.

9. The motor must be able to accelerate the flywheel from zero to full speed in the specified time. This design was based on 2 hours.

10. The design should not require heat dissipation by liquid cooling. The added weight and circuit complications of a liquid system must be avoided.

The scope of this report covers the following study areas:

1. Rotor
   - Configuration
   - Material
   - Speed
2. Housing
   - Shape
   - Material
3. Bearings
   - Type
   - Size
   - Lubrication
   - Temperature rise
   - Life
4. Motor, wheel drive
   - Acceleration
   - Continuous operation
   - Synchronous speed
5. Power requirements
   - Acceleration losses
   - Bearing
   - Windage
   - Motor
6. Torquers
   - Control torque
   - Motor
   - Power

7. Maintenance

Bearing

Motor

8. Reliability

Two approaches to the optimization of Momentum Wheel Assembly Design were made. One was based on selecting a flywheel of minimum weight which satisfies the angular momentum requirement and is run at the highest admissible speed established by the maximum safe stress limit of the material consistent with infinite fatigue life. This approach is referred to as the Stress Limited Design.

The other approach starts with the minimum weight design and increases the weight of the wheel by adding material to the outer rim while reducing speed sufficiently to maintain the same angular momentum. The reduced power loss due to reduced speed is converted to an equivalent saving in weight, and a search is conducted to determine a configuration of minimum total equivalent weight. This method is referred to as the Minimum Equivalent Weight Design.

An extensive study of material suitable for the momentum wheel was made and the following were chosen.

4340 steel, vacuum melted

Maraging steel

Titanium

Fiber glass

The Design Information presented in this report in graphic and tabulated form has been made from an extensive study of momentum wheel assemblies with 22 different angular momenta capacity over the range from 200 to 2000 ft-lb-sec.

SECTION 2

SUMMARY

This section presents the important results of the study in summary form. It serves the purpose of making available the essential design data for quick reference, and is not intended to be a summary of the entire study effort. The optimization of design configuration was made with the help of several digital computer programs; the range of angular momentum covered was from 200 to 2000 ft-lb-sec. Each momentum wheel assembly (Figure 2-1) consists of a flywheel, electric motor, and replaceable bearing cartridge, all enclosed in a hermetically sealed housing capable of being gimbal-mounted to function as a control moment gyro.

The momentum wheel sizes, weights, and speeds for selected angular momenta are given in Table 2-1. These computer determined values are the mathematical optimum, but for practical design the parameters may be varied within reasonable limits with little effect on the equivalent weight.

TABLE 2-1

COMPUTER DETERMINED VALUES

Angular Momentum (ft-lb-sec)	Flywheel Diameter (in.)	Weight, lb			Wheel Speed rpm	Peripheral Velocity ft/sec
		Fly-wheel	Housing	Complete Assembly		
200	18.8	15.1	14.2	33.9	9,368	770
500	22.4	23.4	19.7	48.0	11,153	1130
1000	25.8	33.9	25.8	64.7	12,279	1390
1500	27.8	43.3	29.7	78.4	12,803	1550
2000	29.4	51.6	33.1	90.2	13,144	1685

The momentum wheel, mounted as a control moment gyro, is shown in Section 4 in Figure 4-1. The general wheel configuration with tapered shaft is shown in Figure 2-2. It is seen to be a combination of a tapered disc and a rim which are thin in comparison to the radius. The disc thickness is about 1.3 percent of the radius while the rim ranges from 10 percent to 5 percent of the radius from smallest to largest wheels.

Since all wheels of different angular momentum capacities were designed to react to a maximum of 50 ft-lb of torque on the vehicle while in orbit, the bearing load requirements were the same. For this reason the same bearings and location were used for all wheels. For the slower speed wheels, a smaller

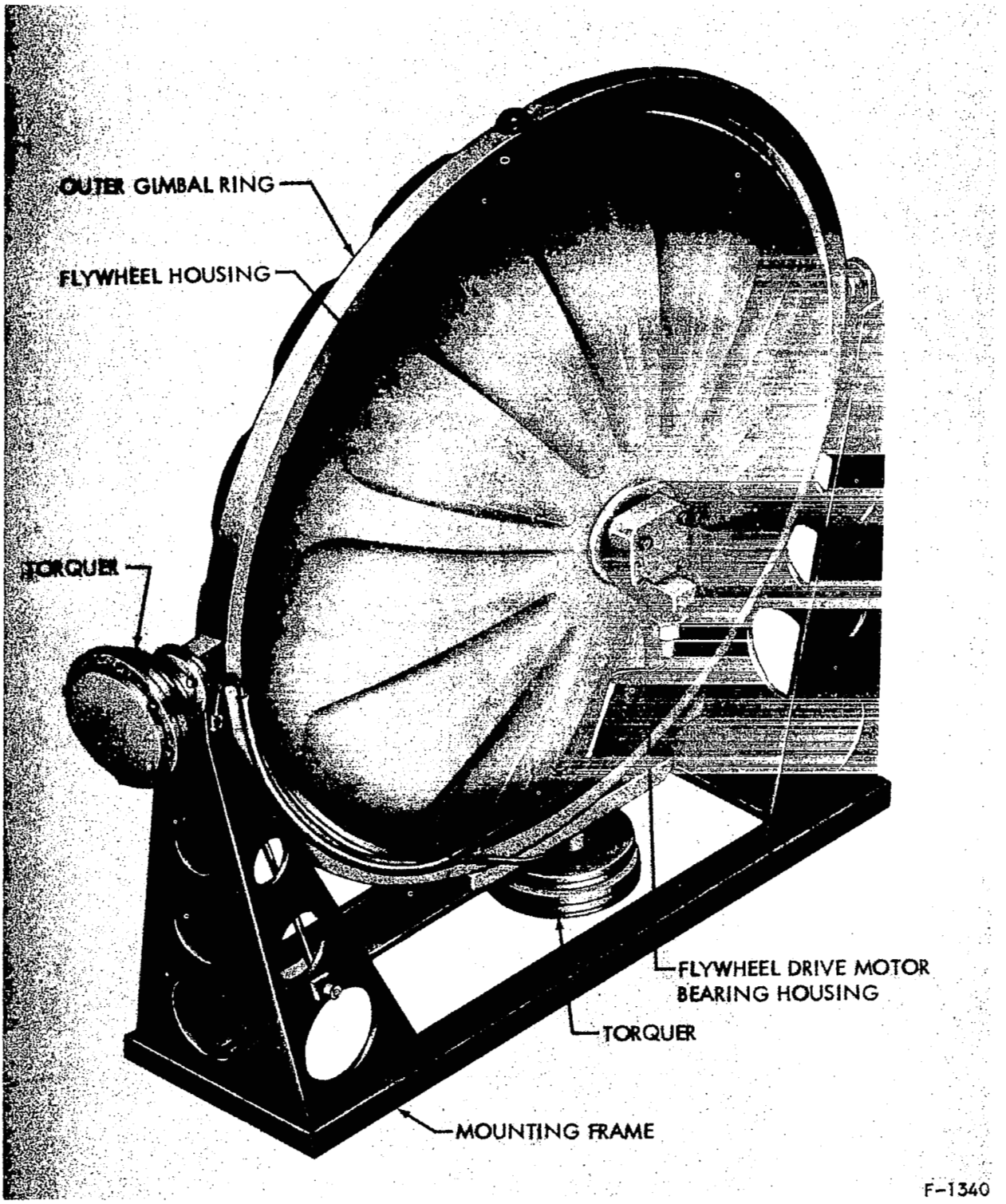

Figure 2-1. Momentum Wheel Assembly (Gimbal-Mounted).

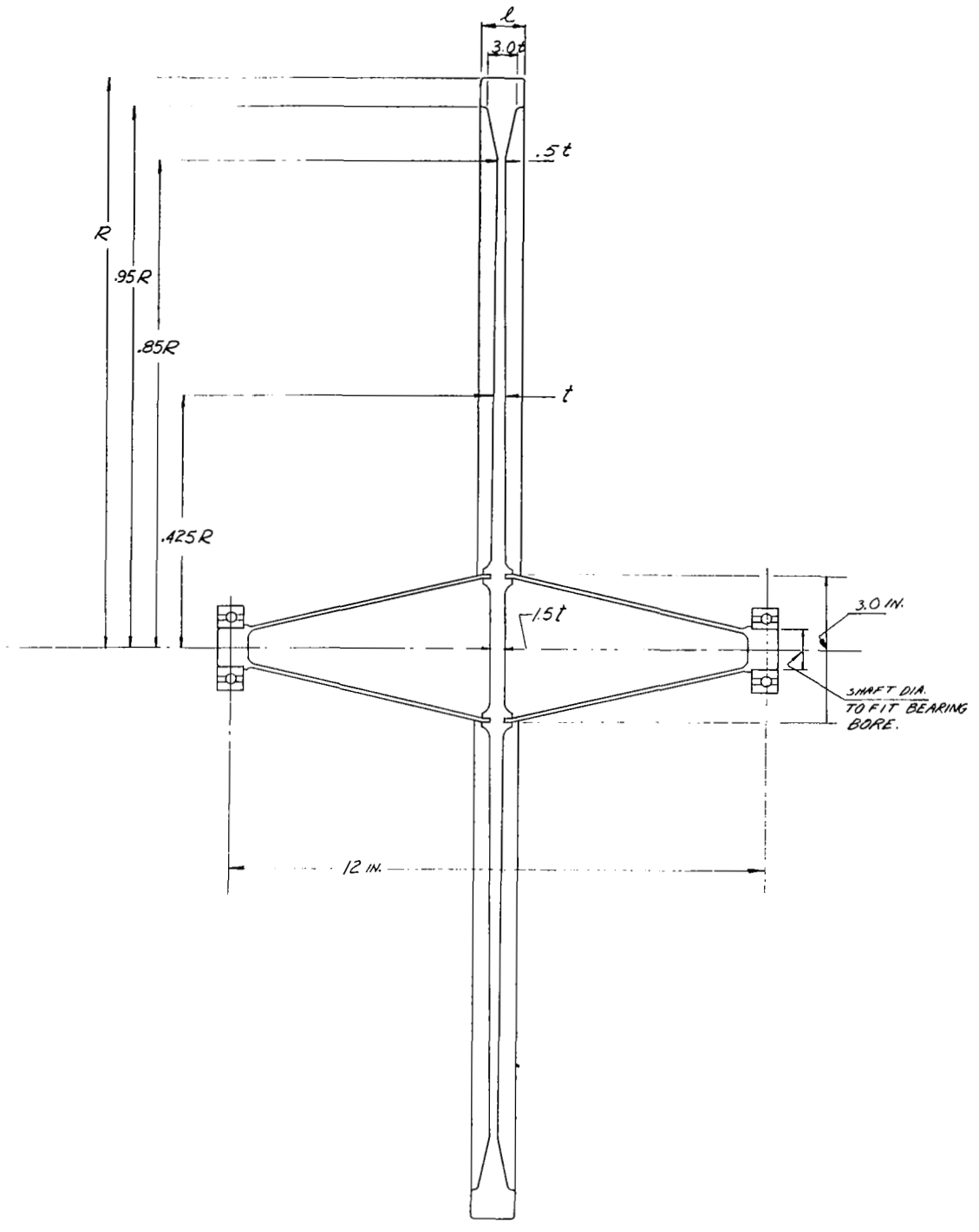

Figure 2-2. Momentum Wheel Assembly Configuration, Minimum Equivalent Weight Design, for Wheels with Angular Momentum (H) = 200 to 2000 ft-lb-sec, Gyroscopic Moment (M) = 50 ft-lb

bearing could be used but with no practical benefit in power loss. For ground testing, slightly higher bearing loads will be experienced, than for orbit conditions, due to the flywheel weight; however, the bearing selected has sufficient capacity to accommodate this additional load.

The study used an angular momentum (H) of 1000 ft-lb-sec for specific detail assembly design. Information for this capacity wheel is summarized in Table 2-2, below.

TABLE 2-2

RECOMMENDED MOMENTUM WHEEL ASSEMBLY

FOR H = 1000 FT-LB-SEC

TORQUE CAPACITY = 50 FT-LB

Wheel configuration: Shaped disc and rim

Materials:

Flywheel	4340 Steel, (vacuum melted)
Housing	Aluminum

Size:

Wheel diameter	26.2 in.
Rim thickness	0.76 in.
Disc thickness	
At hub (center line)	0.322 in.
At a radius of 5.568 in.	0.161 in.

Speed: 12,000 rpm (Chosen because of compatibility with 400 cps power supply)

Weight:

Flywheel	33.6 lb
Housing	26.5 lb
Motor	2.9 lb
Shaft and bearings	2.1 lb
Gimbal ring and bearings	6.3 lb
Torquers (2) and mounting (reduction gear type)	16.4 lb
Yoke	8.0 lb
Total	95.8 lb

TABLE 2-2 (Continued)

Flywheel drive motor:	
Type:	Permanent magnet, synchronous a-c 4-pole, 3-phase
Power Input:	
Acceleration	309.3 watts
Full speed	18.0 watts
Voltage	220 VAC 400 cps
Current	1.4 amps
Motor output	.335 hp
Torque capacity	0.14 ft-lb
Bearings:	
Ball bearings (2)	
15mm angular contact (102 H)	
M-50 tool steel races and balls	
Self-lubrication ball separators	
Location:	12 in. on center
Rated load capacity	Radial
Maximum at 12,000 rpm	130 lbs
Maximum at 100 rpm	650 lbs
Lubrication:	
Andok - C grease (channelling) with Teresso V-78 oil for evaporation makeup	
Vapor pressure at 160°F	10^{-4} mm Hg
Pressure inside the housing	10^{-3} mm Hg
Gas	Helium

ROTOR CONFIGURATION SELECTION

The analysis leading to configuration selection contained two distinct phases. The first concerned itself with determining the most favorable thickness distribution as a function of wheel radius in order to maximize the angular momentum-to-weight ratio. The second phase made use of the optimum thickness distribution so obtained and further optimized the design by selecting the most favorable slenderness ratio (thickness to radius) in order to minimize the system weight and power consumption.

MATERIAL SELECTION

Four materials with properties that gave promise of affording the least weight momentum wheel assemblies were used in the computer program. The study results showed the three metals--4340 steel, maraging steel, and titanium--to be about equal in the total weight of the assembly and power loss with an equivalent weight of 1 pound per watt. Fiberglass, the fourth material, afforded a weight reduction in the complete assembly, but required excessive power to overcome windage and bearing drag which caused the total equivalent weight to be high in comparison to metal wheels. Because of lower costs and superior ductility characteristics of 4340 steel, it was selected as the recommended material for the momentum wheels.

The housing materials considered were steel, aluminum, and magnesium. Aluminum was selected for the superior rigidity it afforded to external load, its ease in forming, and its excellent heat conducting properties.

BEARING SELECTION

Ball bearings were selected over journal bearings due to the advantage of less power loss. Journal bearings are a good second choice since their life can be made to be much greater than ball bearings.

RECOMMENDATIONS

The following action items are recommended prior to committing CMG's to actual space missions.

1. A bearing test program to prove the reliability for at least one year of continuous operation at low power loss.

2. A gimbal torquer study to establish the optimum design in regard to size, weight, power, and reliability.

3. Fabrication and ground testing of an optimum CMG to prove out design performance objectives.

The preparation and execution of these programs should be as nearly simultaneous as it is feasible.

SECTION 3

ANALYSIS

ORGANIZATION

The components which make up a control moment gyro need to be analyzed in two perspectives. First, they must be analyzed as individual pieces of hardware which are called upon to perform specific functions with adequacy and reliability; second, the interplay of component characteristics which define an optimum design must be understood through some form of "simultaneous" investigations. The presentation of analysis in this section reflects this thinking: the background knowledge for the individual important components is first presented under separate headings; the selection of an optimum design is then implemented through the use of a digital computer program which has, in the meantime, reduced the component characteristics to calculable numbers. A direct consequence of this approach to the problem is that not all analyses pertaining to a particular component will necessarily be found in a single grouping; there is the generalized information, appropriate for basic components, and there are specific equations for the trade-off studies applicable only to this program. This partitioning of analysis is aimed at retaining a reasonable presence of continuity in the development of the essential formulas contained in the computer program. A single reading of the subsection "computer program" should suffice to define the main structure of the study. The remaining treatments represent either further amplifications of the analysis or verification of the feasibility of the selected design.

ROTOR STRESS ANALYSIS

Rim Wheel vs Flat Disc

The basic function of the rotor is to provide an angular momentum vector of constant magnitude in the direction of the spin axis. As this spin axis changes direction, a control moment is produced which is proportional to the rate of change of the axis. For a given angular momentum, H, therefore, a rotor must be selected which is not stressed above its allowable stress at the most highly stressed point, and which weighs the least while providing the same angular momentum. In addition, the rotor configuration must be capable of transmitting the gyroscopic moment to the supports through the rotor shaft. Before the rotor design can be committed to a digital computer program, however, some preliminary analysis of basic simple shapes can be made to give indications of desirable features in rotor geometry.

The two basic shapes selected here are the thin hoop and the flat disc. In both cases, it is required to spin the disc to a speed determined by the allowable stress such that a total angular momentum

$$H = I\omega \qquad (1)$$

is obtained. The moment of inertia of the rotor is a function of its geometry and the material density, and the angular speed is determined by the strength-to-weight ratio of the material. For the thin-rim wheel

$$I = \frac{W}{g} r^2 \tag{2}$$

$$\sigma = \frac{\gamma}{g} \omega^2 r^2 \tag{3}$$

where W = weight of rotor, lb

r = rim radius, in.

I = moment of inertia, lb-sec^2-in.

γ = specific weight, lb/in.^{3}

g = gravity constant, in./sec^2

σ = centrifugal stress, lb/in.^{2}

ω = angular speed, rad/sec

For the flat disc

$$I = \frac{1}{2} \frac{W}{g} r^2 \tag{4}$$

$$\sigma = \frac{3+\nu}{8} \frac{\gamma}{g} \omega^2 r^2 \tag{5}$$

where σ = maximum centrifugal stress at the center of the disc, lb/in.^{2}

ν = Poisson's ratio

These equations allow the weight of the rotor to be determined in terms of H, r, σ, γ, and g (for $\nu = 0.33$)

$$W_{Rim} = \frac{Hg}{r} \sqrt{\frac{\gamma/g}{\sigma}} \tag{6}$$

$$W_{Disc} = 1.29 \frac{Hg}{r} \sqrt{\frac{\gamma/g}{\sigma}} \tag{7}$$

$$= 1.29\ W_{Rim}$$

The form of these equations shows that the weight is minimized by selecting a material with a high strength-to-weight ratio and by using the largest feasible radius r. On the other hand, the formulas only take into account centrifugal loading, so that two additional factors need be considered for the

actual rotor. First, as the rotor radius is allowed to become large, its axial thickness decreases without limit, so that eventually the transverse stiffness in bending becomes the controlling factor; second, the rim wheel design has made no allowance for moment transmittal to the shaft, so that the theoretic advantage of 29 percent savings in weight cannot be fully realized. A true optimum shape thus should contain parts of a rim wheel and a disc, and the rellzable H/W ratio should fall between 100 percent and 129 percent of that for a flat disc.

Rotor of Optimum Configuration

At this point, an analysis was made to determine the rotor shape which can yield a maximum angular momentum-to-weight ratio for a given outside radius. For high angular momentum, a rotor with a large rim is desirable. For the best rotating stress profile, a tapered disc with the thickness increasing from the rim to hub is the most desirable. These generalizations indicate that the optimum shape should consist of a tapered disc with a rim. Since gyroscopic moments will be reacted by the shaft at the wheel hub, rotating stresses in the wheel should be slightly lower in the hub region to allow for the addition of bending stresses.

Using an IBM 7074 computer program to calculate rotating stresses and inertial properties, a parametric study was initiated to determine the optimum rotor configuration. In other words, for a given radius, the radial distribution of axial thickness was determined for the highest angular momentum-to-weight ratio. Thermal stresses will be of low order of magnitude and can be neglected since the maximum thermal gradient has been estimated to be less than 40°F from hub to rim.

Figures 3-1 and 3-2 show the disc profiles that resulted from this analysis; the rotating stresses are also shown. It is noted that the stress distribution shown in each figure will be the same for any other radius when the respective configuration is used with the same peripheral velocity. The radius of 5 in. chosen for the investigation has no special significance and was only used as a convenient measure. In any case, the angular speed must be adjusted so that the desirable maximum allowable stress is obtained for each configuration.

Both profiles have about the same angular momentum-to-weight ratio for equal maximum stresses. However, gyroscopic bending will produce stresses which are highest at the hub and decrease as the radius increases. The stress distribution of Figure 3-2 provided for this and is, therefore, the more desirable configuration. The method of accounting for combined stress effects is covered under the computer program section.

Figure 3-3 shows the profile and rotating stresses for the final rotor design. The final design has the same tapered disc as that shown in Figure 3-2 (3 to 1 taper), but has an additional rim which allows a lower peripheral velocity than the rotor without the additional rim. The reason for this deviation will again be clarified under "Computer Program."

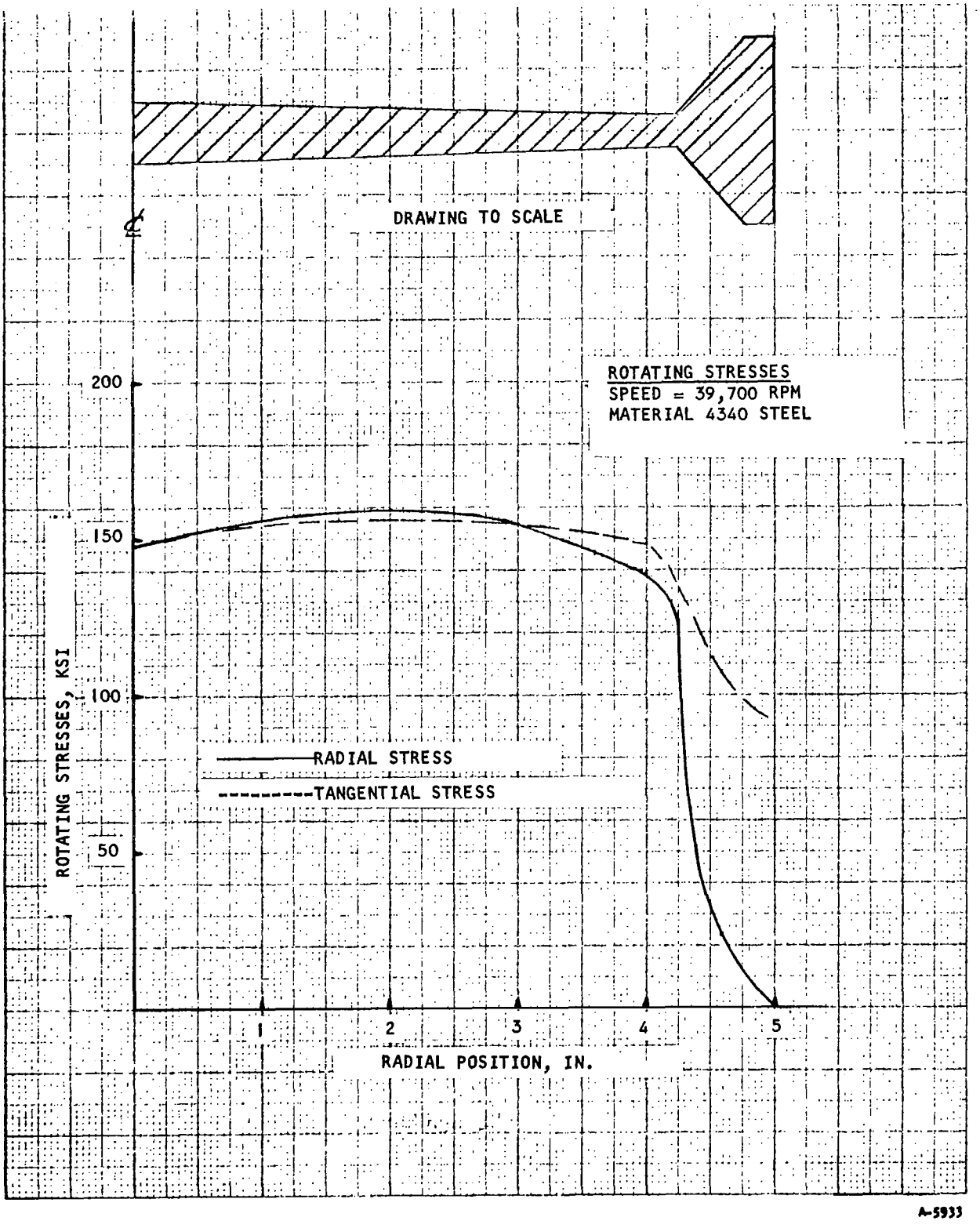

Figure 3-1. Rotating Stresses - 4340 Steel at 39,700 rpm

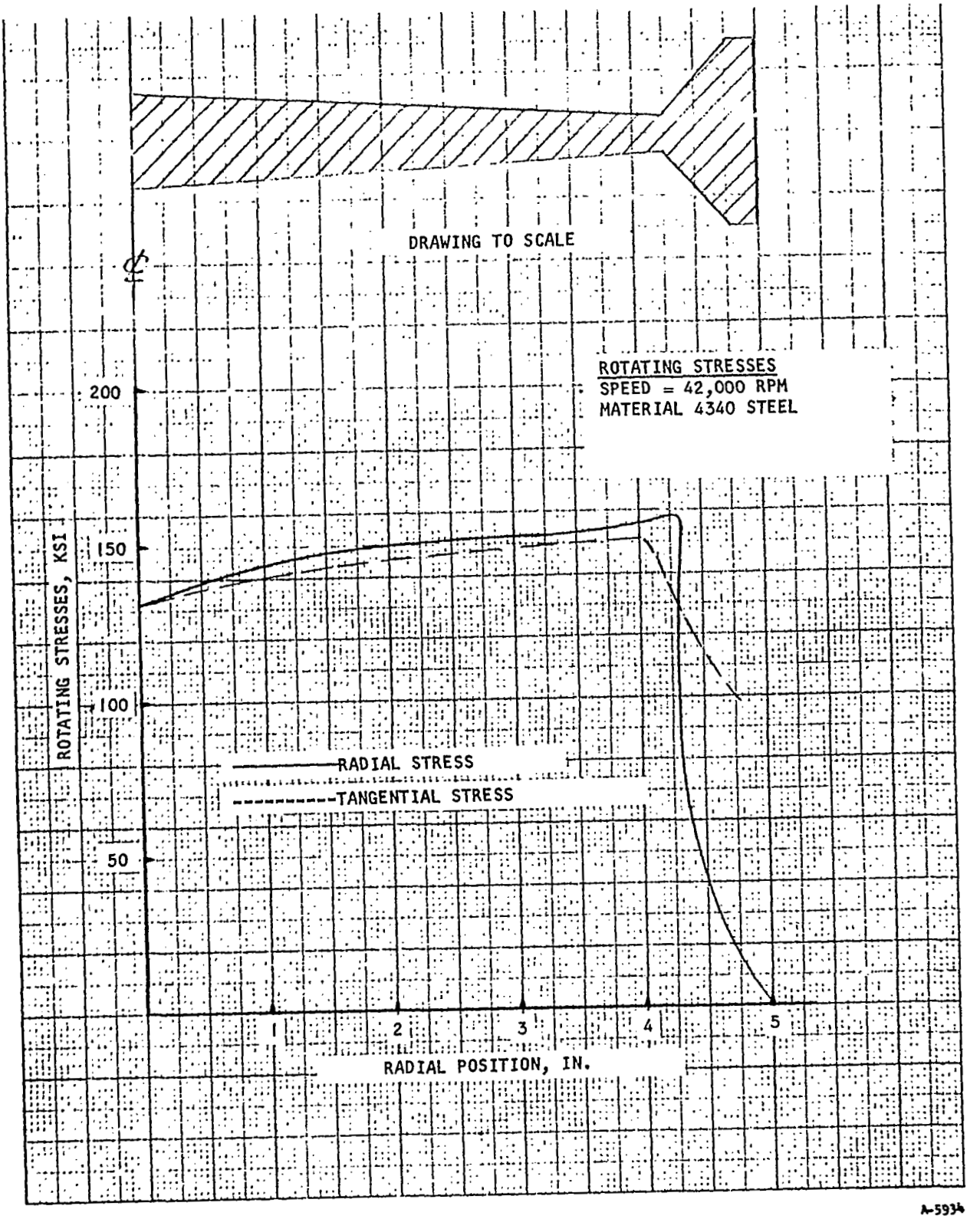

Figure 3-2. Rotating Stresses - 4340 Steel at 42,000 rpm

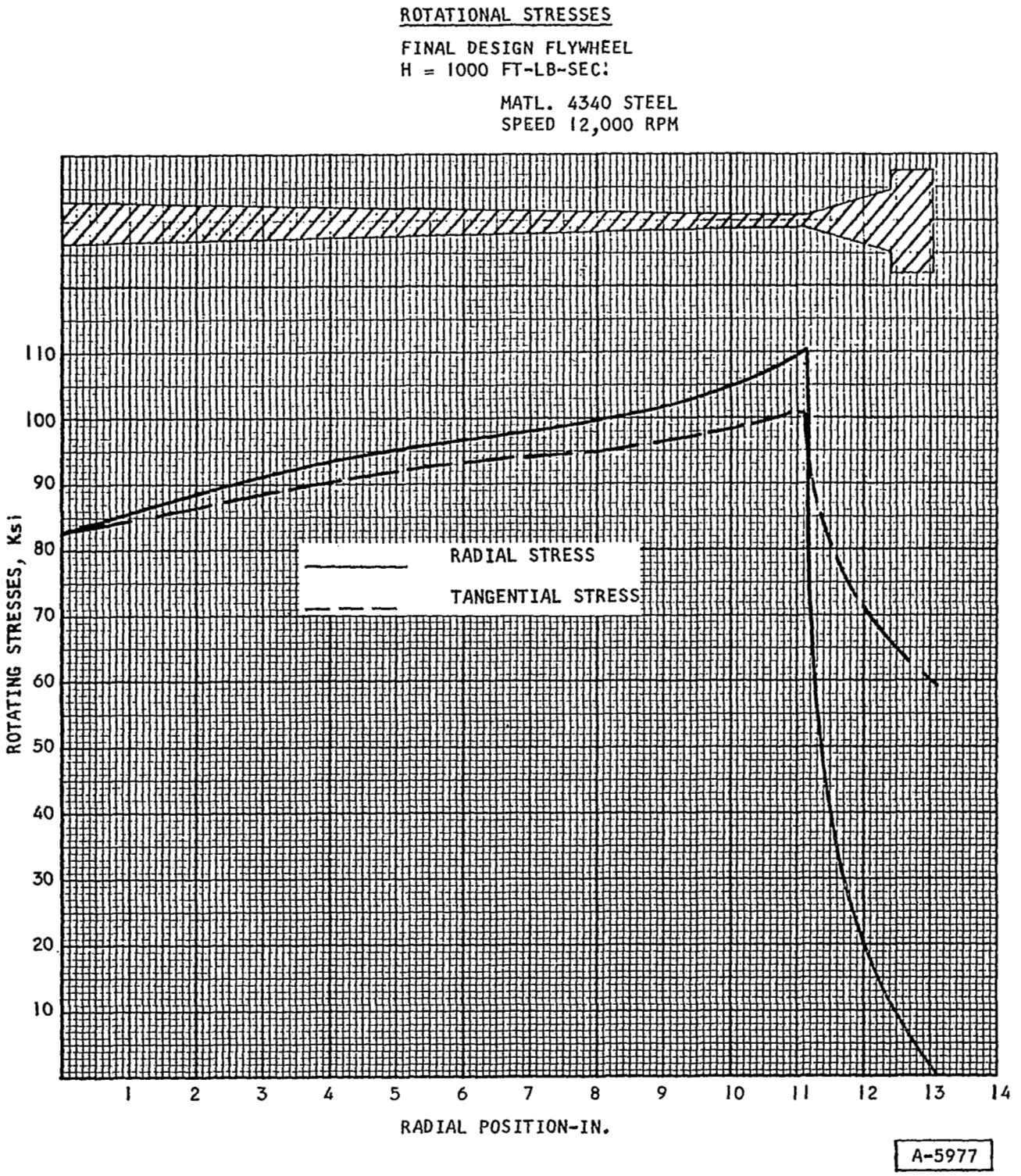

Figure 3-3. Rotational Stresses

Description of IBM Program for Rotating Stresses

The disc profile is divided into a number of radial stations (up to 50). For each station, the geometry of the disc is defined; other data include material density, modulus of elasticity, temperature variations, and coefficient of thermal expansion. The analysis assumes that each lineal element of the wheel is translated and rotated after stressing. This leads to the formulation of four simultaneous differential equations, two of equilibrium (force and moment), and two of compatibility. These equations are translated into matrix form by a numeric technique which, given the boundary conditions, can then lead to the solution of the equations.

SELECTION OF THE MOTOR SYSTEM

Four basic motor types have been evaluated to determine an optimum configuration to accelerate and drive a momentum wheel. Both fixed and variable frequency power has been considered. A permanent magnet motor operating from a variable frequency supply is selected as an optimum system. The system meets all specified requirements, and keeps power requirements to an absolute minimum.

Fixed vs Variable Frequency Power

1. Acceleration

Regardless of the type of motor used, a fixed frequency supply leads to large losses during the accelerating period. This can be shown as follows.

The power input (P_i) required for an a-c motor with a constant frequency and without losses in the stator is;

$$P_i = T_l \omega_s$$

The power output (P_o) in the rotor without mechanical losses is,

$$P_o = T_l \omega_r$$

where ω_s = synchronous speed of rotating field in the stator, rad/sec

ω_r = rotor speed, rad/sec

T_l = torque, ft-lb

The power loss is

$$P_L = P_i - P_o = T_l \omega_s - T_l \omega_r$$

$$P_L = T_l (\omega_s - \omega_r)$$

Energy loss for time dt is,

$$P_L \times dt$$

The total energy loss is,

$$E_L = \int_o^t T_l \, (\omega_s - \omega_r) \, dt$$

During acceleration, (α)

$$\alpha = \frac{d\omega}{dt} = \frac{T_l}{I}$$

I = moment of inertia of the momentum wheel, slug-ft^2

$$dt = \frac{I d\omega}{T_l}$$

By substitution for dt, the energy loss is,

$$E_L = \int_o^t T_l \, (\omega_s - \omega_r) \, \frac{I d\omega}{T_l}$$

$$E_L = I \int_o^{\omega_s} \omega_s d\omega - I \int_o^{\omega_s} \omega_r d\omega$$

ω_s = constant, full synchronous speed.

$$E_L = I \left(\omega_s^2 - \frac{\omega_s^2}{2}\right) = \frac{1}{2} I\omega_s^2$$

The energy loss equal to the kinetic energy, KE, in the momentum wheel which is,

$$KE = \frac{1}{2} I\omega_s^2$$

The total energy (E_t) required to bring the momentum wheel to full speed is

$$E_t = KE + E_L$$

$$= I\omega_s^2 = 2KE$$

The energy loss and kinetic energy (KE) of the flywheel expressed as a function of angular momentum (H) is

$$KE = \frac{1}{2} I\omega^2 = \frac{H\omega}{2}$$

For an angular momentum of

H = 1000 ft-lb-sec, and a speed of

n = 12,000 rpm

ω = 1259 rad/sec

$$KE = \frac{1000 \quad 1259}{2} = 629{,}500 \text{ ft-lb}$$

The energy loss that must be dissipated as heat (Q) in the rotor is,

$$Q = \frac{629,500}{778} = 809 \text{ Btu}$$

Bearing and motor stator losses are very small and would not have temperature rise sufficient to flow into the rotor. Windage loss is used to estimate the temperature rise in the momentum wheel.

For the three different metal materials used in this analysis, the specific heat, flywheel weights, and temperature rise are tabulated below.

Material	Specific Heat	Flywheel Weight, Lb	Temperature Rise, ^{0}F
4340 Steel	0.107	33.6	224.5
Maraging Steel	0.110	31.9	230
Titanium	0.130	30.3	205

The temperature rise does not take into consideration the dissipation of heat from the momentum wheel due to radiation during the 2-hour acceleration period. This loss will be small since the highly polished surface of the wheel affords a poor radiating surface.

The power loss associated with a constant frequency power supply during starting can be avoided by use of a variable frequency power supply. This is true because the stator equivalent speed and the rotor speed are equal.

That is,

$$\omega_s = \omega_r$$

and

$$P_L = T_l(\omega_s - \omega_r) = 0$$

Since a fixed-frequency power supply leads to large losses during the acceleration period, further effort in design in this approach is not advisable. The variable frequency power supply will be used for starting all size wheels. For momentum wheels that require other than 400-cycle power supply for full speed operation, the inverter will be used continuously.

2. Running at Full Speed

The power requirement to supply power loss due to windage and bearing drag is very small; less than 20 watts for the largest momentum wheels.

In bringing the momentum wheel to full speed, with a constant torque the motor output power (P_o) must be,

$$P_o = \frac{H}{\Delta t}\,\omega$$

For $H = 1000$ ft-lb-sec, and $\Delta t = 2$ hours, $\omega = 1259$ rad/sec

$$P_o = \frac{1000}{2\times60\times60}\ 1259 \quad \text{ft-lb/sec}$$

$$= \frac{1.259\times10^6}{7.2\times10^3} = 175 \quad \text{ft-lb/sec}$$

The electrical power (P_e) expressed in watts is,

$$P_e = 175 \times 1.356 = 237 \text{ watts}$$

The windage and bearing loss is approximately 13 watts. The total power output (P_t) of the motor will have to be,

$$P_t = 237 + 13 = 250 \text{ watts}$$

The motor power rating (P_M) will have to be

$$P_M = \frac{P_t}{\text{efficiency}}$$

The torque (T_o) required to bring the wheel from zero to full speed with constant acceleration in time (Δt) is,

$$T_o = \frac{H}{\Delta t}$$

For $H = 1000$ ft-lb-sec

and $\Delta t = 2$ hr $= 7200$ sec

$$T_o = \frac{1000}{7200} = 0.139 \text{ ft-lb}$$

The horsepower, Hp, output of the motor to accelerate the flywheel is

$$Hp = \frac{T_o\omega}{550}$$

at $n = 12{,}000$ rpm

$\omega = 1259$ rad/sec

$$Hp = \frac{0.139\times1259}{550} = 0.318$$

The windage and bearing loss of 13 watts requires 0.017 hp. The total power output requirement of the motor is

$$0.318 + 0.017 = 0.335 \text{ hp}$$

Motor Choice

Four types of motors have been evaluated:

1. Induction
2. Reluctance synchronous
3. Hysteresis synchronous
4. Permanent magnet synchronous

1. Induction Motor

An induction motor with a cage rotor operated from a variable frequency supply provides an efficient means of accelerating the rotor to running speed. The motor will not lock into synchronism with the supply, but for a constant load will operate at constant speed at 95 percent of synchronous speed. It has the advantage of maintaining a high torque output regardless of input frequency, and has no motor synchronizing problems. Its running efficiency will be slightly less than that of a PM synchronous motor. (An efficiency of 85 percent is possible.) The induction motor represents a close second choice for an optimum design where synchronous speed with another motor is not required.

2. The Reluctance Motor

The reluctance motor is a simplified salient pole synchronous motor without field windings. The synchronous torque is less than one-third that of the same motor with an externally excited field winding. The reluctance motor is a simple and very reliable motor. The rotor is a series of salient teeth equal to the number of stator poles. The rotor teeth tend to line up with the stator poles of the rotating stator field, producing the synchronous action. These rotor teeth also produce the characteristic cogging action of reluctance motors. This cogging produces undesirable current peaks.

In order to produce strong saliency effects or torque, very high magnetic densities are required which result in low power factor and poor efficiency.

The reluctance motor, because of its low torque and efficiency, was not chosen for the described application. For the size required, the efficiency would be a maximum of 60 percent.

3. The Hysteresis Synchronous Motor

The hysteresis motor has a conventional slotted and laminated stator with phase windings and a homogeneous cast sleeve of hardened permanent magnet material comprising the active part of the rotor. The magnetized rotor tends to keep in step with the rotating poles of the stator field and to resist demagnetization.

In contrast to the performance of the reluctance motor, the hysteresis motor exhibits constant torque from standstill to synchronous speed. Because the rotor is smooth, there is no tendency to cog at low speeds, and the load can be smoothly accelerated into synchronism.

For a given flux density, very high magnetizing currents are required This results in low power factor, high copper loss, and low efficiency. Here, as in the reluctance motor, the efficiency would be about 60 percent.

4. Permanent Magnet, Synchronous Motor

The permanent magnet synchronous motor is made up of a stator which produces a rotating field and an excited field rotor which follows the rotating field.

The most practical and efficient design uses permanent magnets to produce the rotor field, thus eliminating the power required for excitation.

Because efficiencies of 90 percent are possible, this is the motor that was chosen. However, the PM synchronous motor cannot accelerate by itself and develops only a small torque when not running at synchronous speed.

This problem is solved by supplying the motor with voltage and a frequency which increases at a controlled rate so that the motor is always in synchronism with its applied frequency as it accelerates. This additional power supply is a solid-state frequency inverter. The operation of the inverter is described on page 3-60 in this report.

The frequency inverter also has other advantages. The optimum momentum wheel may operate at 12,000 rpm. This is possible with a 4-pole motor when 400-cps is used. However, the frequency inverter can supply any final frequency. A frequency of 800 cps can be used with an 8-pole motor chosen, since the higher frequency affords a slight increase in the efficiency of PM synchronous motors, due to:

1. Smaller end coils

2. Smaller armature reaction (important in PM design)

3. Smaller yoke iron

The bearing friction and windage calculations at 12,000 rpm show a loss of approximately 13 watts.

This means that the motor required for acceleration is nearly 20 times larger than required for full load operation.

The use of two motors was evaluated (one for acceleration and one for full load) with the following conclusions:

1. Two motors would require additional circuitry and switching which would unduly complicate the system.

2. The improvement in efficiency of the full load motor is slight and does not warrant the additional switching circuitry.

3. The additional motor would add extra weight to the system.

Motor Design

The motor design chosen was an axial air-gap permanent magnet synchronous motor. The axial air-gap was preferred because the motor was capable of supplying the axial bearing preload of 5 pounds.

In the axial air-gap construction, two designs were analyzed:

1. Conventional toothed stator

2. Toothless design, similar to printed circuit motor

The toothless design has the following advantages over the conventional design:

1. Iron losses in teeth eliminated

2. Weight of teeth eliminated

3. Winding thickness reduced

4. Permeance of the armature reduced

5. Leakage reactance reduced

6. Armature reaction reduced

The major disadvantage of this design is that longer magnets are required. However, this is not objectionable because the rotor (PM) is part of the flywheel and the weight of the rotor is an integral part of the total moment of inertia of the flywheel.

Since weight in the rotor with a larger radius benefits the momentum, a larger motor rotor diameter has been used to reduce the magnetic flux and increase the efficiency for a specific torque.

The efficiency of one toothless design at full speed load has been calculated to be 86.5 percent. This means that the total power drawn will be 13/0.865 or 15 watts from the frequency converter. The watts lost in the frequency converter will be 2 watts, so the total system power required at full load will be 17 watts. (A more conservative efficiency of 66.7 percent was used in the computer program.)

The average efficiency of the motor during acceleration is 87 percent. Therefore, the average motor loss will be at half output or at 125 watts. The average input is then 125/0.87 = 144 watts.

The dissipation in the frequency inverter will remain practically constant during acceleration at approximately 22 watts and then drop to 2 watts at full load speed.

With a constant torque motor and a variable frequency power supply, the energy (E) required to bring the 1000-ft-lb-sec momentum wheel to full speed is:

$$E = (144 + 22)\ 2\ \text{hr} = 332\ \text{watt-hours}$$

The peak power required during acceleration is:

$$\text{Motor}_{PM} = \frac{250}{0.87} = 287.3\ \text{watts}$$

Inverter,

$$P_i = 22.0$$

$$\text{Total Power} = 309.3\ \text{watts}$$

BEARING STUDY

A study has been made of several types of bearings considered suitable for use in the momentum wheel unit. Journal and ball bearings were studied to optimize the selection of size and type for the preliminary design layout, considering the desired characteristics of long, reliable service life, low weight, and low power loss for the conditions imposed by the current specifications for the gyro unit.

Ball Bearing Design

The bearing selected for study is an angular contact, super-precision ball bearing. The materials selected are consumable electrode vacuum melt M-50 tool steel for the rings and balls, and phenolic laminate or a special self-lubricating composite for the ball separator. The size is to be 15-mm bore, 32-mm outside diameter, and 0.3543 width.

The calculated B10 life for this bearing under the following loading schedule is 8900 hours.

Load, lb	Of time, %	Speed, rpm
50	1	15,000
25	29	15,000
15	70	15,000

Correction was made for the use of vacuum melt steel, using a life multiplier based on the experience data published by the Barden Corp., SKF Industries, and New Departure Div. of GMC, all of whom have reported substantially the same findings. Typical bearing rating curves are shown in Figure 3-4.

The life multiplier used to account for the use of vacuum melted M-50 as compared to ES52100 air melted steel was 5.

To extend the probability of survival, the bearings are to be selected on the basis of low raceway waviness and raceway eccentricity below 0.000050 in. This places them in a class of reduced life scatter. Further, vibration and torque limits representing the best 10 percent of similar bearings are to be applied, further insuring freedom from defects and, finally a 50-hour prerun to establish thermal stability and torque consistency will be made. These steps constitute the greatest possible guarantee of culling out defective bearings within the current state-of-the-art, and improve the confidence of achieving at least the B10 life which itself is sufficient to the accomplishment of the intended mission.

The selection of materials is greatly simplified by the wealth of test data readily available. The M-50 tool steel is well proved in many applications, principally in gas turbine and jet engine mainshafts, high-speed turbocompressors, other high-performance equipment. AiResearch has used well over 10,000 such bearings in the recent past and this experience data is available.

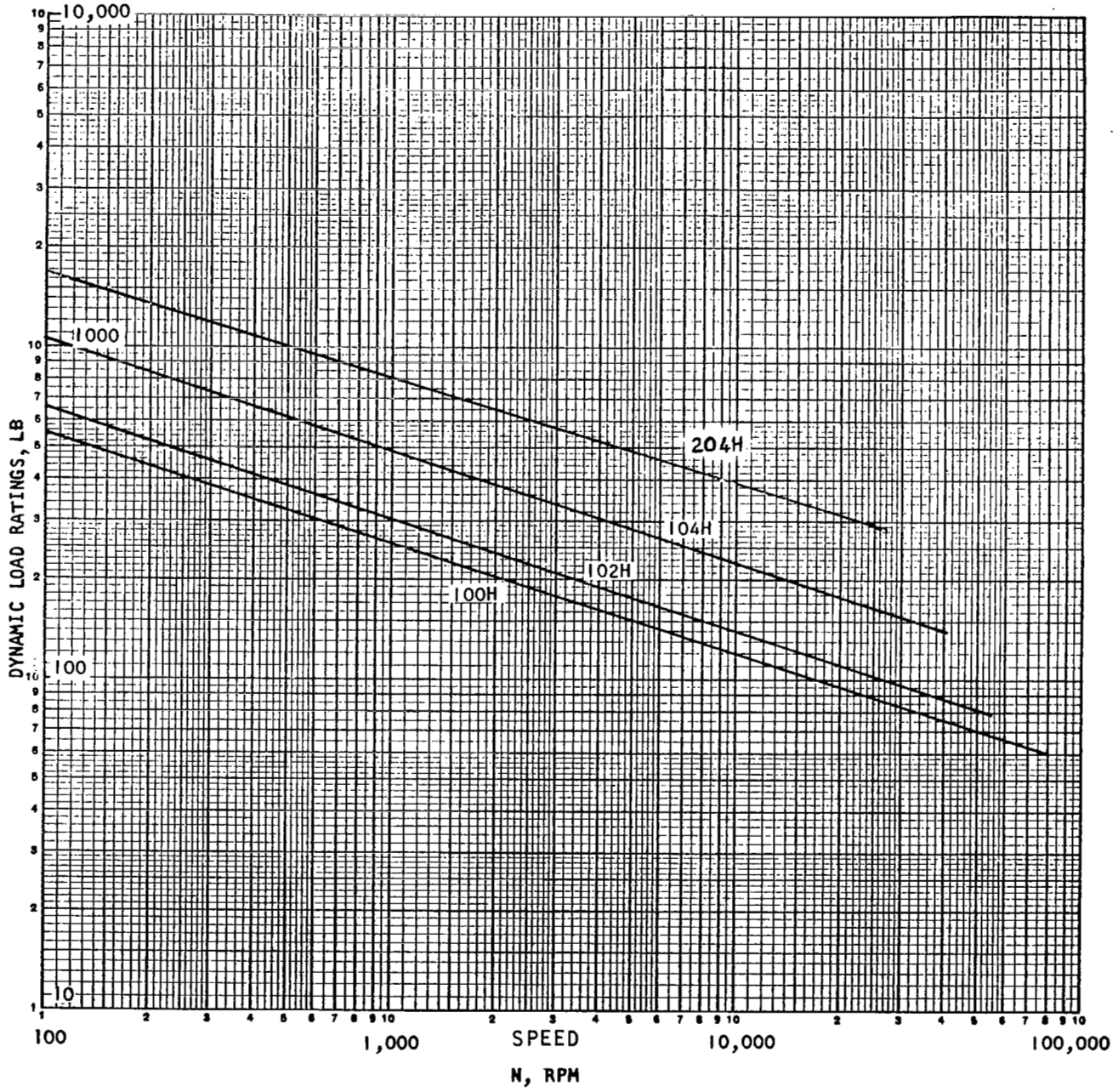

Figure 3-4. Bearing Load Rating

Phenolic laminate ball separators have, of course, a long history of application in gyros and many other devices. Their principal advantages are (1) porosity to permit lubricant storage, (2) insensitivity to marginal lubrication, and (3) minimized damage to the bearing in the event of failure.

A composite material developed by Westinghouse has been investigated. Preliminary tests of this material have shown it to be a promising material for a ball bearing separator. More extensive testing is suggested during the development phase of the gyro unit to verify its attractive characteristics for aerospace application.

Lubrication is the crux of the design and for the speeds considered; Andok-C grease with periodic make-up oil added to replenish the grease is chosen. The oil is to be Teresso V-78, a well tested gyroscope bearing lubricant, as is the Andok-C grease. Finally, prior to use, the separator is to be vacuum-impregnated with oil to prevent outgassing and to insure the maximum storage utility of the porous structure of the material.

At present, bearing curvatures of 53 percent at the inner race and 54 percent at the outer race are specified. A distinct torque reduction is possible with a wider inner ring curvature (of 55 percent to 57 percent) but a reduction in the theoretical B10 will occur. Other investigators have results suggesting the B10 calculations to be inappropriate to a predominately thrust-loaded bearing with wide curvatures, but only testing will prove or disprove this point. In essence, a better bearing design is indicated, but there is insufficient certainty as to the life to permit proposing its usage. Power loss values for the bearing selected will be found in Figures 4-13, 4-14, and 4-15.

In conclusion, the bearing specified, the lubrications, and the fitting practice recommended have proved successful in other equipment, the most notable of which is a 22,000-rpm fan which has accumulated over 18,000 hours of operation with grease.

Total ball bearing torque is the sum of the torque due to load, torque due to lubricant viscous effects, and the separation friction. Only the lubricant torque is speed dependent, varying approximately as the 2/3 power of the speed. With minimum film conditions, the magnitude of the lubricant torque is insignificantly small and the torque of a bearing so lubricated will be independent of speed for all practical purposes. This condition represents the minimum power loss of ball bearings. Using properly channelled grease, the same result can be obtained with extremely long life. The power loss due to bearing torque are included in the computer portion of Section 3 on page 3-42.

Figure 4-2 and 4-3 show the recommended ball bearing removable cartridges in detail. Opposite the motor end of the shaft, is also an oil reservoir and solenoid control valve to provide a positive means of replacing the oil lost by evaporation into the flywheel chamber The labyrinths will keep the evaporation of oil from the grease at a very low rate. About 1 drop of oil per week should keep the bearing grease saturated with oil.

Journal Bearing Design

Since the unit is required to have a very long life potential when operating at a constant speed, a simple journal bearing running with a hydrodynamic oil film is another type of bearing worthy of consideration. The bearing must be capable of maintaining the hydrodynamic film separating the relatively moving surfaces at the peak transient and high short-duration loads encountered during manuevering of the space vehicle. Most of the operation would be at considerably smaller bearing loads where the oil film separating the bearing surfaces becomes thicker and power loss somewhat smaller than at the maximum loading condition. This characteristic in a well-designed journal bearing installation leads to exceptionally long life with no metallic contact, rubbing or fatigue of the bearing surfaces. Suitable bearing materials and lubrication provisions, as well as adequate but not excessive sizing of the bearing are necessary.

The determination of journal bearing proportions shown in Figure 3-5 was based on previous satisfactory experience in the selection of the following parameters:

1. Bearing Diameter

The smallest diameter journal deemed practical considering peak loads, manufacturing feasibility, mounting, and installation in the complete unit assembly.

2. Bearing Length

The shortest effective axial length, which together with the diameter, oil film viscosity, and bearing clearance will carry the peak loads to minimize power loss at the design rotative speed; these proportions would be used in the first prototype of a unit designed with journal bearings; it should be understood that modification may be needed to further optimize the bearing when actual oil film temperatures (determined by test) affecting oil viscosity, tolerance requirements affecting clearances and alignment conditions become more accurately known during development.

3. Oil Film Viscosity

In the unit under consideration, for the long-duration operation when not making rapid attitude changes, the bearing heating effects are small and provisions can be made to conduct heat away from the bearings to relatively extensive surfaces from which the heat can be radiated. The oil film temperature has been estimated at 200^0F. This temperature gives an absolute viscosity of 0.5 $(10)^{-6}$ reyns, (pound-second per square inch units) for a typical very low vapor pressure oil such as Octoil-S. If other suitable oils having different temperature-viscosity characteristics are found later to be even better, then the journal bearing proportions may have to be correspondingly modified.

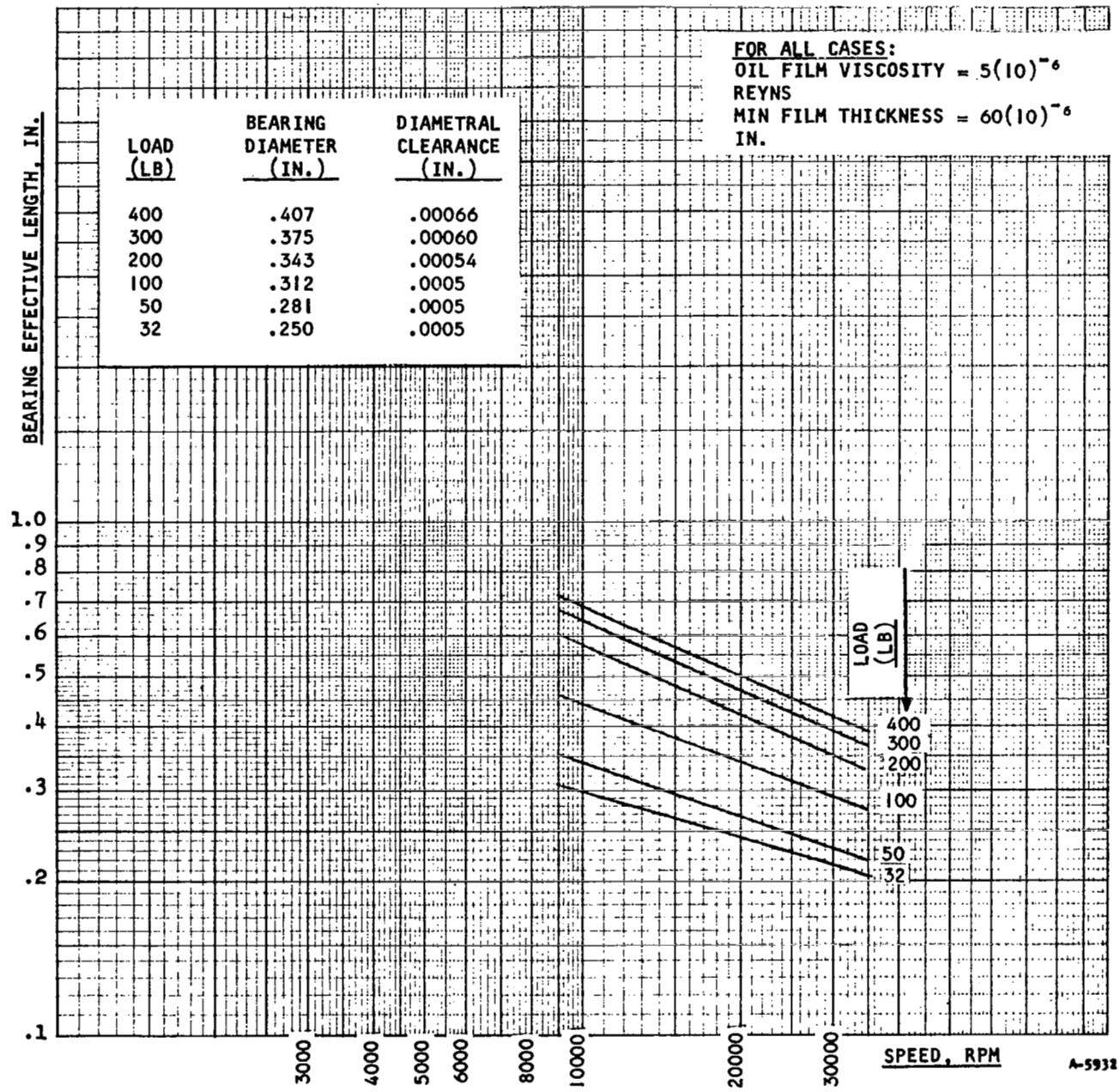

Figure 3-5. Journal Bearing Dimensions for Various Speed and Load

4. Minimum Oil Film Thickness

An important parameter which was chosen from experience with consideration of the bearing materials, quality of manufacture, and film viscosity, is the minimum oil film thickness to be allowed. If this parameter is too great, the bearing becomes larger, heavier, will be capable of higher maximum loads but will consume excessive power. If the parameter is too small, the bearing may be too marginal in maximum load capacity, and may be too sensitive to surface finish and shaft alignment, but would consume less power. The minimum oil film thickness for the peak load condition selected for this study was based on experience with the kind of materials and quality of manufacture that would be used. It still has some conservatism for the high-speed bearing capacity being considered. The minimum film thickness used in this study is $60\ (10)^{-6}$ inch. At the long duration nominal loading conditions, this minimum film thickness would approach the radial clearance with the journal concentric with the bearing or one-half the allowed diametral clearance.

5. Material Selection

The journal would, in all cases, be a high-strength, hard material. It would have a surface hardness of 60 to 64 Rockwell C, obtainable by case hardening, nitriding, or equivalent treatment. The preferred bearing bushing material would consist of a steel or beryllium backing with a silver bearing suitable, there are Alcoa B750-T5 aluminum, or Clevite trimetal (high lead bronze with a tin base babbitt overlay).

6. Other Considerations

Certain other configurations of journal type bearings are the floating bushing and shoe types. These and other types of bearing geometry would be given serious consideration in a final design if there were any indication of an oil film whirl problem. These introduce somewhat greater complexity and cost which may not be justified in this application.

It is likely in a final design that any bearings used would be resiliently mounted to permit operation above the first critical speed of the rotor assembly. This would materially reduce any peak transient loads and what is more important, would permit the already very well balanced rotor to rotate almost exactly about the principal axis through its mass center of gravity.

An important part of a final design would be the development of the bearing lubrication system to minimize the power loss required to perform this function. One means for pressurizing a journal bearing is to use a nonrotating scoop tube of very small size with minimum depth of immersion in oil which is rotating at rotor speed. Other types of pumps or means for transporting oil to the bearing could be devised. In all cases, the final design and development work would be concerned with providing adequate oil to the bearing at the smallest power consumption.

7. Journal Bearing Design

Figure 3-7 shows a journal bearing design that would be suitable for the momentum wheel. It includes its own oil pump in the form of a nonrevolving pitot tube. This journal bearing was not incorporated in the final assembly due to it having slightly greater power loss.

8. Power Loss

Power loss equations are included in the computer portion of this section on page 3-43. Power loss values are shown in Figure 3-6.

Summary of Journal Bearing Study

In addition to the various items pertinent to journal bearings discussed previously, there remains the presentation of the bearing size selection, calculated power losses and diametral clearances. This information is presented in the following figures:

Figure 3-5 shows selected bearing diameters for various maximum allowable radial loads from 32 to 400 lb and bearing lengths for a range of rotative speeds.

Figure 3-6 shows the journal bearing power loss at various speeds for the bearing sizes to be selected in Figure 3-5. Also indicated in this figure is the power loss to be expected for a very lightly loaded bearing having the proportions selected and at various speeds. Figure 3-6 includes power losses required for supplying oil to the bearing.

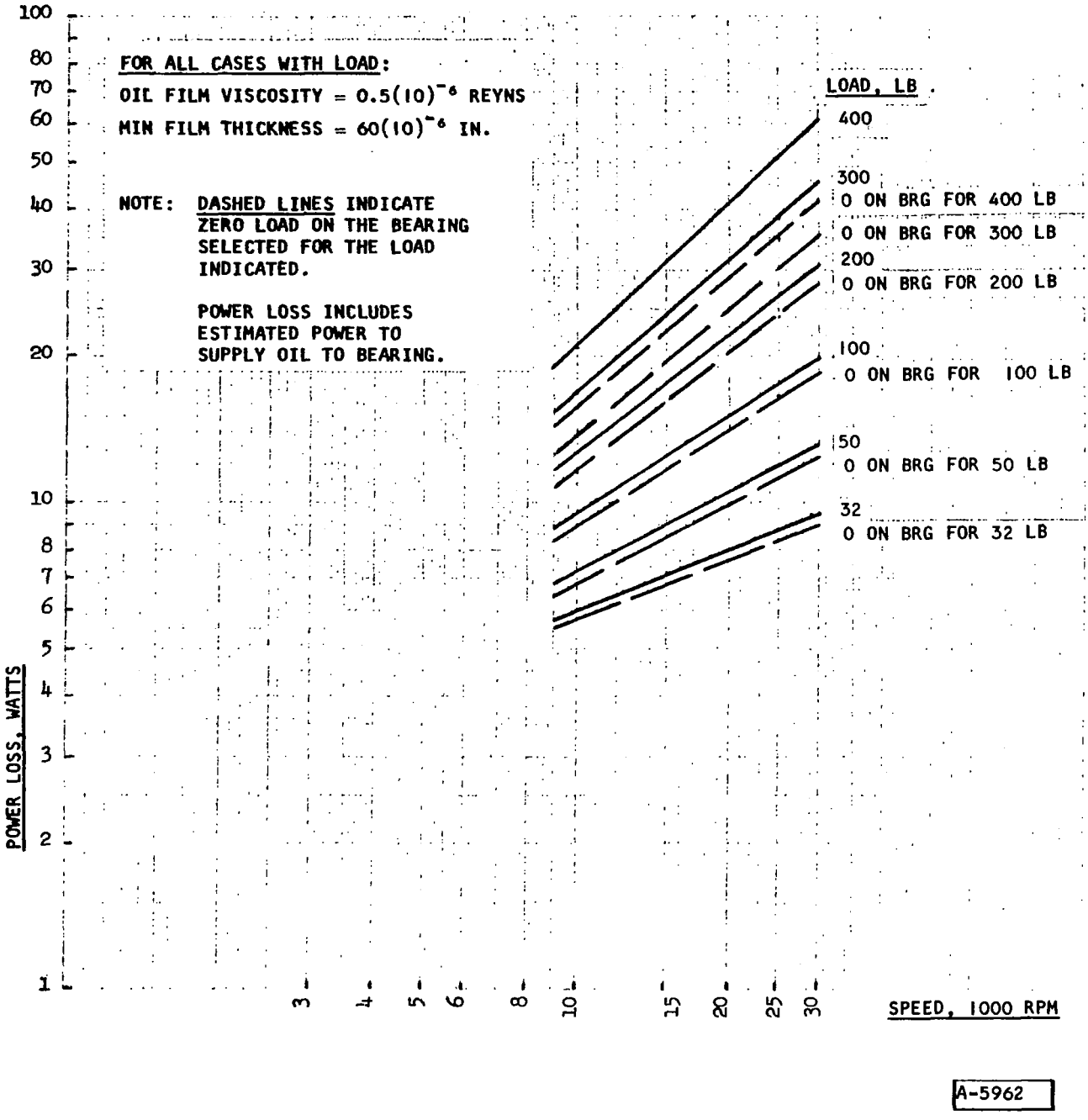

Figure 3-6. Power Loss Per Journal Bearing for Various Speeds and Loads

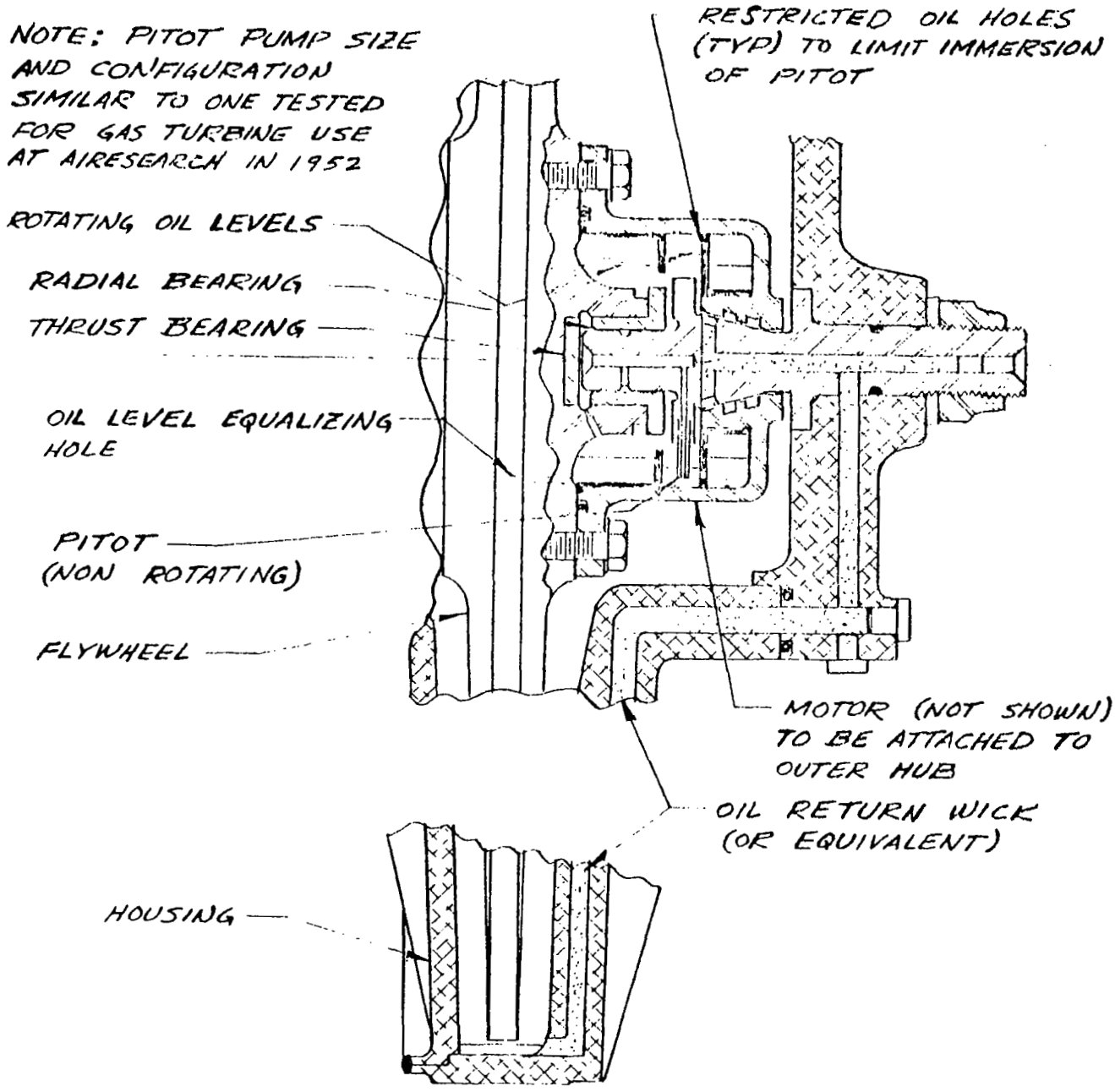

Figure 3-7. Journal Bearing with Lubrication System

WINDAGE LOSS FOR THE MOMENTUM WHEEL

The power loss due to aerodynamic drag must be considered for various pressures inside the housing and for different gases. Since equations for our specific design wheels were not available, the following derivation of the equations used in the computer program is given.

There are three different aerodynamic flow conditions in which the wheel could operate, each requiring a different set of equations to express the power loss. These flow conditions are turbulent, laminar, and free molecular regions.

Turbulent Region

For a disc,

$$\text{Power} = M\omega = C_M \left(1/2\ \rho a^5 \omega^3\right) \frac{\text{ft-lb}}{\text{sec}}$$

M = moment, ft-lb

ω = angular velocity, rad/sec

ρ = mass of gas per unit volume

a = radius, ft

μ = coefficient of viscosity

ν = coefficient of kinematic viscosity

$$\nu = \frac{\mu}{\rho}$$

$$C_M = 0.146 R^{-1/5}$$

R = Reynolds number

$$R = \frac{\omega a^2}{\nu} = \frac{\omega a^2 \rho}{\mu}$$

$$C_M = 0.146 \left(\frac{\omega a^2 \rho}{\mu}\right)^{-1/5}$$

$$M\omega = 0.073 \left(\rho^{0.8} a^{4.6} \omega^{2.8} \mu^{0.2}\right) \frac{\text{ft-lb}}{\text{sec}}$$

Electrical power,

$$P = 1.356 \times M\omega$$

$$= 0.099 \left(\rho^{0.8} a^{4.6} \omega^{2.8} \mu^{0.2}\right) \text{ watts}$$

Reference NASA report No. 793, Appendix B, page 15.

For a smooth cylinder,

$$\text{Power} = M\omega = C_D \pi \rho a^4 \omega^3 \ell$$

C_D = drag coefficient

ℓ = length, ft

$$\frac{1}{\sqrt{C_D}} = -0.6 + 4.07 \log_{10} R \sqrt{C_D}$$

Electrical power,

$$P = 1.356\ \pi\ C_D \rho a^4 \omega^3 \ell \text{ watts}$$

Total electrical power

P = disc power + cylinder power

$$P = 0.099\ (\rho^{0.8} a^{4.6} \omega^{2.8} \mu^{0.2}) + 4.26\ (C_D \rho a^4 \omega^3 \ell) \text{ watts}$$

For helium at 15^0C,

$$\mu = 4.065 \times 10^{-7} \text{ slugs/ft-sec}$$

The density of helium at 0^0C and 760 mm Hg is

$$\rho_o = 0.000346 \text{ slug/ft}^3$$

At 15^0C

$$\rho = \rho_o\ 0.3595\ \left(\frac{\rho \text{mm Hg}}{t^0\text{C} + 275^0\text{C}}\right)$$

$$= 3.46 \times 10^{-4}\ \left(\frac{760}{15+273}\right)\ 0.3595$$

$$= 3.28 \times 10^{-4} \text{ slugs/ft}^3$$

Determine the Reynolds No. for

p = 760 to 0.00076 mm Hg

$$R = \frac{\omega a^2 \rho}{\mu} = \frac{\omega a\ a\rho}{\mu}$$

The peripherial velocity of the wheel is

$$V = \omega a$$

Then $R = \frac{va\rho}{\mu}$

For the stress-limited wheel, using 4340 steel,

$V = 1800$ ft/sec, approximately

$R = 1$ ft, approximately

$p = 760$ mm Hg

$$R = \frac{1800 \cdot 1 \cdot 3.28 \times 10^{-4}}{4.065 \times 10^{-7}} = 1.445 \times 10^{6}$$

For $V = 1250$ ft/sec

and $R = 1$ ft

$p = 760$ mm Hg

$$R = \frac{1250 \cdot 1 \cdot 3.28 \times 10^{-4}}{4.065 \times 10^{-7}} = 1.01 \times 10^{6}$$

For $R = 1.445 \times 10^{6}$

$C_D = 2.5 \times 10^{-3}$ (Shown in Figure 3-9)

Laminar Region

For a disc,

$$\text{Power} = M\omega = C_M \left(1/2\ \rho a^5 \omega^3\right) \frac{\text{ft-lb}}{\text{sec}}$$

$$C_M = 3.87 R^{-1/2}$$

$$M\omega = 1.935 \frac{\rho a^5 \omega^3}{\sqrt{R}}$$

Electrical Power

$$P = 1.356 \times 1.935 \frac{\rho a^5 \omega^3}{\sqrt{R}}$$

$$= 2.61 \frac{\rho a^5 \omega^3}{\sqrt{R}}, \text{ watts.}$$

Reynolds No. $R = \frac{\omega a^2 \rho}{\mu}$

$$P = 2.61 \frac{\rho a^5 \omega^3 \mu^{.5}}{\omega^{.5} a \rho^{.5}}$$

$$= 2.61\ \rho^{.5} a^4 \omega^{2.5} \mu^{.5}, \text{ watts}$$

For a smooth cylinder,

The electrical power is

$$P = 4.26\ C_D\ \rho a^4 \omega^3 \ell$$

$$C_D = \frac{4}{R}$$

$$P = \frac{17.04}{R}\ \rho a^4 \omega^3 \ell, \text{ watts}$$

The total electrical power is,

$$P = 2.61\ \frac{\rho a^5 \omega^3}{\sqrt{R}} + 17.04\ \frac{\rho a^4 \omega^3 \ell}{R}, \text{ watts}$$

Substituting for Reynolds No.

$$P = 2.61\ \rho^{0.5} a^4 \omega^{2.5} \mu^{0.5} + 17.04\ a^2 \omega^2 \mu \ell, \text{ watts}$$

Free Molecular Flow Region

In the free molecular flow region, where the mean free path is in the same order of magnitude as the characteristic length, (Figure 3-8) the major flow phenomenon is governed by the collision between gas molecules and the wetted surfaces. The free molecular viscosity may be defined (Ref. 1) as

$$Z = \frac{pW^{\frac{1}{2}}}{(2\pi RT)^{\frac{1}{2}}}\ \frac{\text{gram}}{\text{cm}^2 \text{ sec}} \qquad (1)$$

where p = pressure, $\frac{\text{dyne}}{\text{cm}^2}$

R = universal gas const., ergs/^{0}K mole

T = temperature, ^{0}K

W = molecular weight

For a plate moving at velocity V, cm/sec, the shearing stress is

$$ZV = \frac{pW^{\frac{1}{2}}V}{(2\pi RT)^{\frac{1}{2}}} \text{ dyne/cm}^2$$

Thus, the total moment acting on both sides of a rotating disc may be integrated as

---

Ref. 1 Kennard, E. H., "Kinetic Theory of Gases" New York, McGraw Hill Book Co.

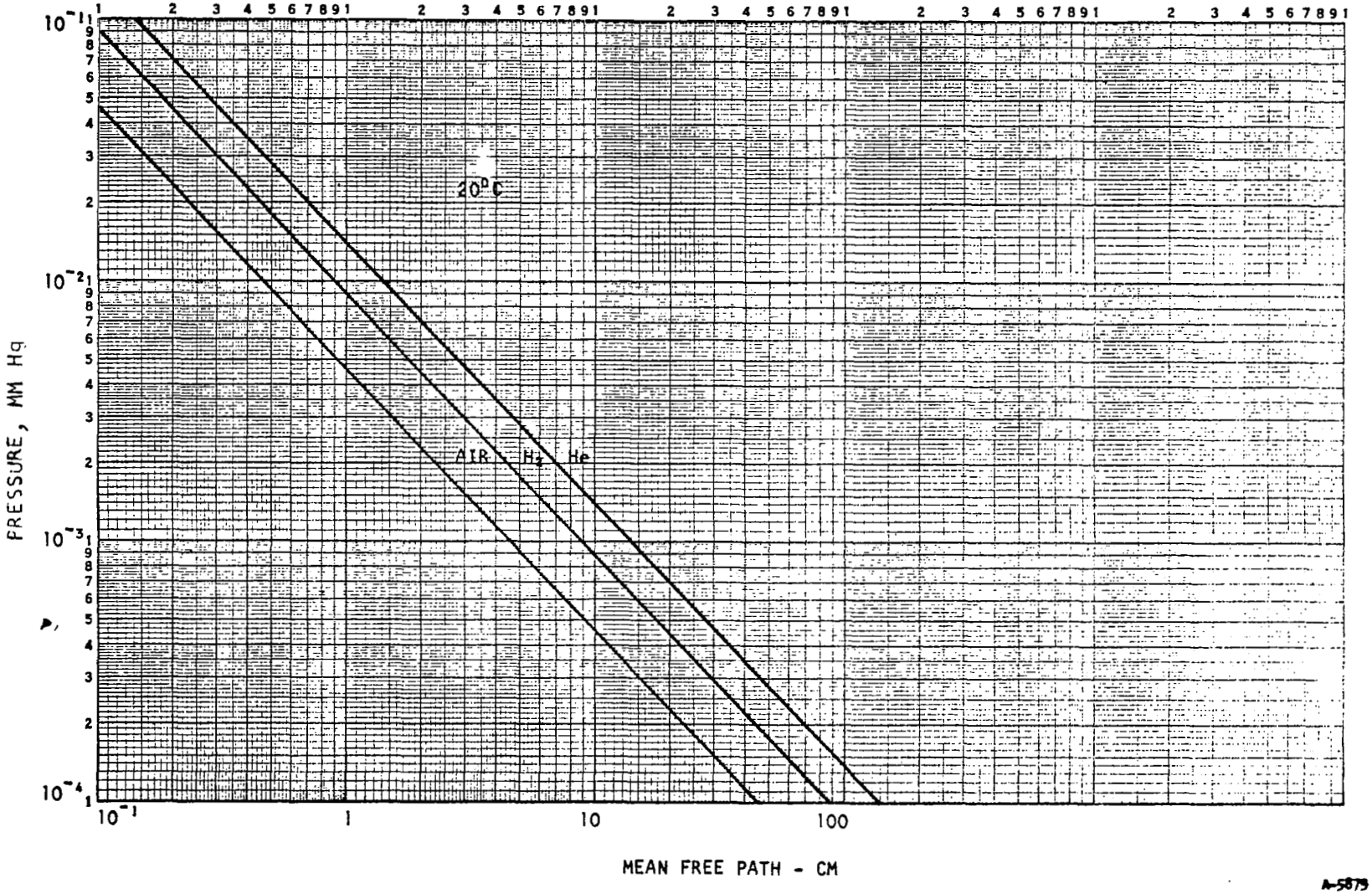

Figure 3-8. Free Molecular Flow Region

$$M = 2\int_0^a \frac{pW^{\frac{1}{2}}}{(2\pi RT)^{\frac{1}{2}}} 2\pi r^3 \omega \, dr \quad \text{dyne/cm} \tag{3}$$

and the power loss as

$$P = 2\int_0^a \frac{pW^{\frac{1}{2}}}{(2\pi RT)^{\frac{1}{2}}} 2\pi r^3 \omega^2 \, dr \text{ ergs/sec}$$

$$= \frac{\pi p W^{\frac{1}{2}}}{(2\pi RT)^{\frac{1}{2}}} a^4 \omega^2 \times 10^{-7} \text{ watts}$$

or $$\boxed{P = 0.0158 \times \frac{pW^{\frac{1}{2}}}{T^{\frac{1}{2}}} a^4 \omega^2 \text{ watts}} \tag{4}$$

where p = pressure, mm Hg

W = molecular weight

T = ^{0}K

a = radius, ft

ω = rad/sec

Similarily, the drag on the circumferential area may be calculated as follows:

$$P = \frac{p W^{\frac{1}{2}}}{(2\pi RT)^{\frac{1}{2}}} 2\pi a^3 \ell \omega^2 \times 10^{-7} \text{ watts}$$

where p = pressure, $\frac{\text{dyne}}{\text{cm}^2}$

a = radius, cm

ℓ = length, cm

ω = rad/sec

or $$\boxed{P = 0.0314 \times \frac{p a^3 \ell \omega^2 W^{\frac{1}{2}}}{T^{\frac{1}{2}}} \text{ watts}} \tag{5}$$

where p = pressure, mm Hg

a = radius, ft

ℓ = length, ft

ω = rad/sec

$T = {}^{0}K$

W = molecular weight

The total windage loss, therefore, can be expressed as

$$P_{total} = \frac{\rho a^3 W^{\frac{1}{2}} \omega^2}{T^{\frac{1}{2}}} \left[0.0158a + 0.0314\ell\right] \qquad (6)$$

As shown in equation (6), the total windage loss is proportional to the square root of the molecular weight of the gas; therefore, it is recommended that helium be used because it would have approximately 1/3 loss compared with air. (Hydrogen would have the least loss but has not been used because of the hazard its flamability introduces.)

Windage Loss Equations

Power Loss, Watts

Flow Region	Portion of Wheel	
	Disc	Smooth Cylinder
Turbulent	$0.099\ (\rho^{0.8} a^{4.6} \omega^{2.8} \mu^{0.2})$	$4.26\ C_D \rho a^4 \omega^3 \ell$
Laminar	$2.61\ (\rho^{.5} a^4 \omega^{2.5} \mu^{.5})$	$17.04\ a^2 \omega^2 \mu \ell$
Free Molecular	$0.0158 \frac{p W^{\frac{1}{2}}}{T^{\frac{1}{2}}} a^4 \omega^2$	$0.0314 \frac{p \ell W^{\frac{1}{2}} a^3 \omega^2}{T^{\frac{1}{2}}}$

For C_D values, see Figure 3-9.

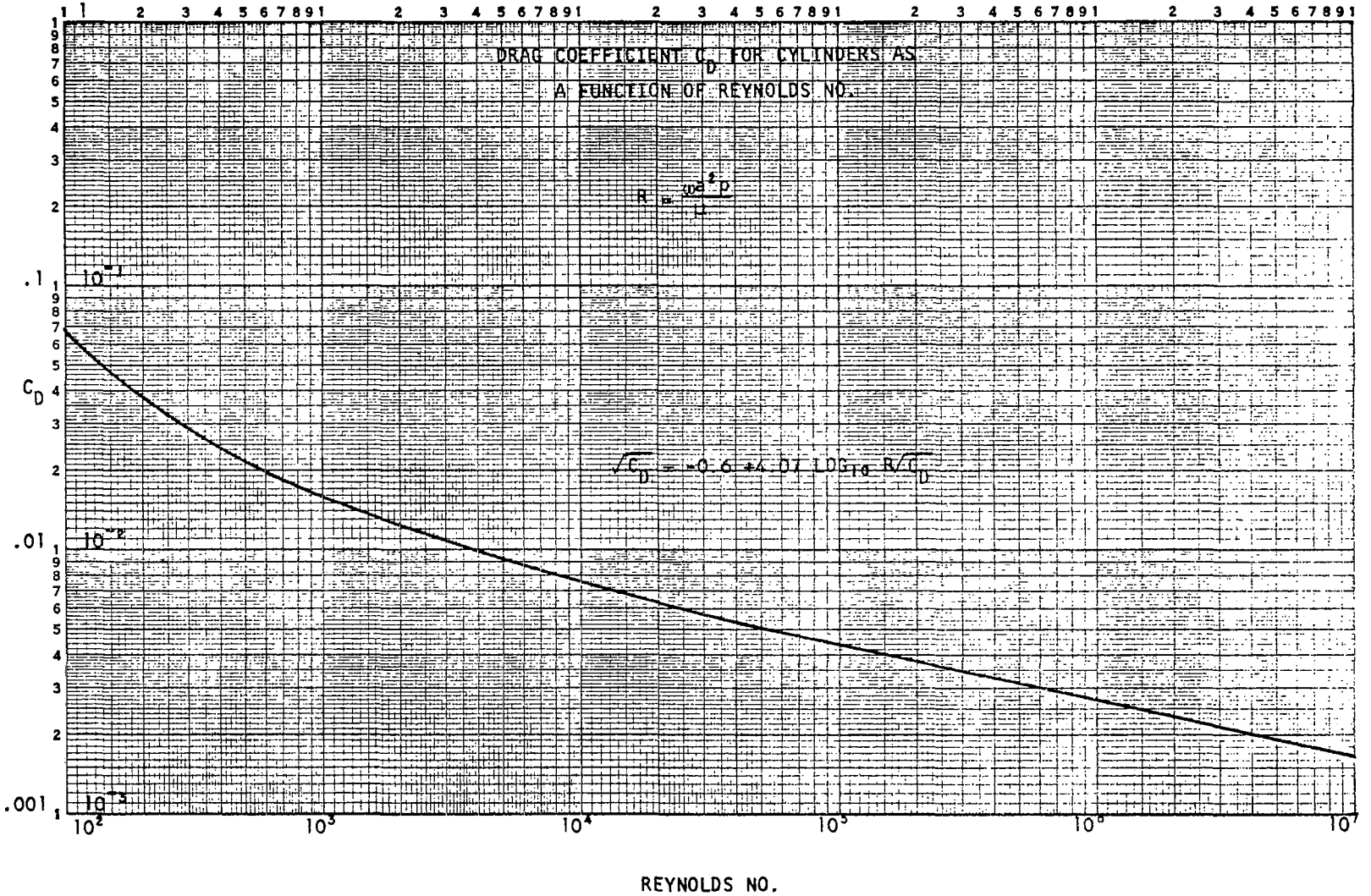

Figure 3-9. Drag Coefficient for Revolving Cylinders as a Function of Reynolds No.

WINDAGE POWER LOSS FROM OIL VAPOR PRESSURE

The rotor-bearing oil-lubricant will supply molecules to the gas inside the momentum wheel, and in the steady state, according to Dalton's Law,* the pressure contribution will be the vapor pressure of the oil. Although the vapor pressures of typical oils for vacuum operation are rather small (1.5 to 3×10^{-8} mm Hg at 25°C), the molecular weight is high (typically 429) which might nevertheless contribute a significant portion of the windage loss. A calculation was made and for the minimum equivalent weight design at 12,000 rpm and 10^{-3} mm Hg pressure, the windage loss due to the oil vapor pressure alone is 1.8×10^{-3} watts versus 0.8 watts for hydrogen gas, 3.6 watts for helium, and 7.8 watts for air. The vapor pressure can be expected to increase by a factor of 100 at the nominal working temperature of 160°F. For this, the loss is 0.13 watts. Consequently, the additional windage loss caused by the oil is negligible and need not be considered when determining total CMG loss.

To calculate the oil vapor pressure loss, use is made of Equation 6 on page 3-31. The oil vapor molecules are in the free molecular flow region. Using hydrogen gas as a basis,

$$P_o = \frac{W_o}{W_H} P_{Ho}$$

where P_o = windage power loss due to oil vapor pressure

P_{Ho} = windage power loss due to hydrogen gas at a pressure equivalent to the oil vapor pressure

W_o = molecular weight of the oil

W_H = molecular weight of hydrogen

---

*Dalton's Law: A mixture of several gases which do not react chemically exerts a pressure equal to the sum of the pressures which the several gases would exert separately if each were allowed to occupy the entire space alone at the given temperature.

COMPUTER PROGRAM

Introduction

Design optimization refers to the selection of flywheel material, flywheel geometry, operating speed, and bearing configuration, such that a minimum equivalent weight design is obtained. The equivalent weight includes the actual weights of the flywheel, the housing, the electric drive motor, and the shaft; and also the power demand figured at 1 pound of weight per watt. The power demand is that required to maintain a constant speed of the flywheel, and is, therefore, equal to the losses due to the bearings, flywheel windage, and motor.

General Approach

For a specified angular momentum vector and magnitude of control moment, various designs are examined, starting with an assigned radius of the flywheel. First, a minimum weight flywheel is designed from given strength properties and specific weight of the selected material. The corresponding weight of the housing and bearing losses, etc., in support of this flywheel operation are then calculated. This represents the best design for a given radius with the lightest weight flywheel. However, for materials possessing a high strength-to-weight ratio the speed needed to develop the limiting stresses for small wheel radius may be excessive in the sense that power losses at that speed, when converted to weight penalty, more than offset the weight savings offered by the wheel alone. In such a case, it is more advantangeous to use a heavier wheel which can be operated at a lower speed for the same angular momentum. The added weight of the wheel must, of course, be more than compensated for by the reduction in power made possible by the lower speed. A search is made at this time for the best combination of wheel weight and speed which results in a minimum equivalent weight design.

The entire procedure is now repeated for another radius of the flywheel; this is continued until the feasible range of sizes has been exhausted. Automated machine plotting of various design parameters vs radius then presents the user with a graphic picture of the tradeoff factors affecting weight, power, and speed.

This program is now applied to a range of angular momentum magnitudes (200 to 2000 ft-lb-sec), and then to various materials and bearing designs. The final selection of material and bearing design is made by the responsible engineer.

Detailed Analysis

1. Wheel Geometry

To eliminate unnecessary bending stresses, the wheel profile will be made symmetrical about a radial line. The geometry is then defined by the thickness variation as a function of radius, or $t = t(r)$. An important concept in wheel geometry is the slenderness ratio, defined as the ratio

of a reference thickness, e.g. t(0), to the maximum radius r_{max}. The parameter to be maximized in a wheel design is the angular momentum to weight ratio (H/W). It can be shown that this ratio increases without limit as the slenderness ratio is allowed to approach zero. Practical considerations, however, place limits on both the size of the wheel and its minimum thickness so that it is inadequate to attempt to maximize H/W by reducing the slenderness ratio alone. A higher level of maximization involves searching for a profile shape t(r) which, for the same allowable working stress of the material, would yield the largest ratio of H/W. The shape factor here must be understood to designate the thickness ratios between various parts of the wheel at different radial stations inasmuch as wheels with the same thickness ratios, independent of actual thicknesses, have the same stress distribution and hence the same H/W for a given tip speed. This fact allows the search for an optimum shape (or relative thickness distribution) to be made independent of either the radius of the wheel or the total angular momentum H. Wheels of various shapes but having the same OD were investigated for their H/W values by a computer program which calculated the stresses at an arbitrarily assigned speed. The speed is subsequently adjusted to correspond to the same allowable stress in each wheel, thus yielding the maximum angular momentum H for that shape. The profile in Figure 3-10 was selected as a result of such a comparative study; it has very nearly the optimum thickness variation for maximum H/W, and is the geometry adopted for all the wheels investigated in this study (excepting the fiberglass design).

The governing equations for this shape are represented in terms of dimensionless coefficients C_1, C_2, and C_3:

$$H = C_1 R^4 t_o \gamma \omega \qquad (1)$$

$$\sigma = C_2 (R\omega)^2 \gamma \qquad (2)$$

$$W = C_3 R^2 t_o \gamma \qquad (3)$$

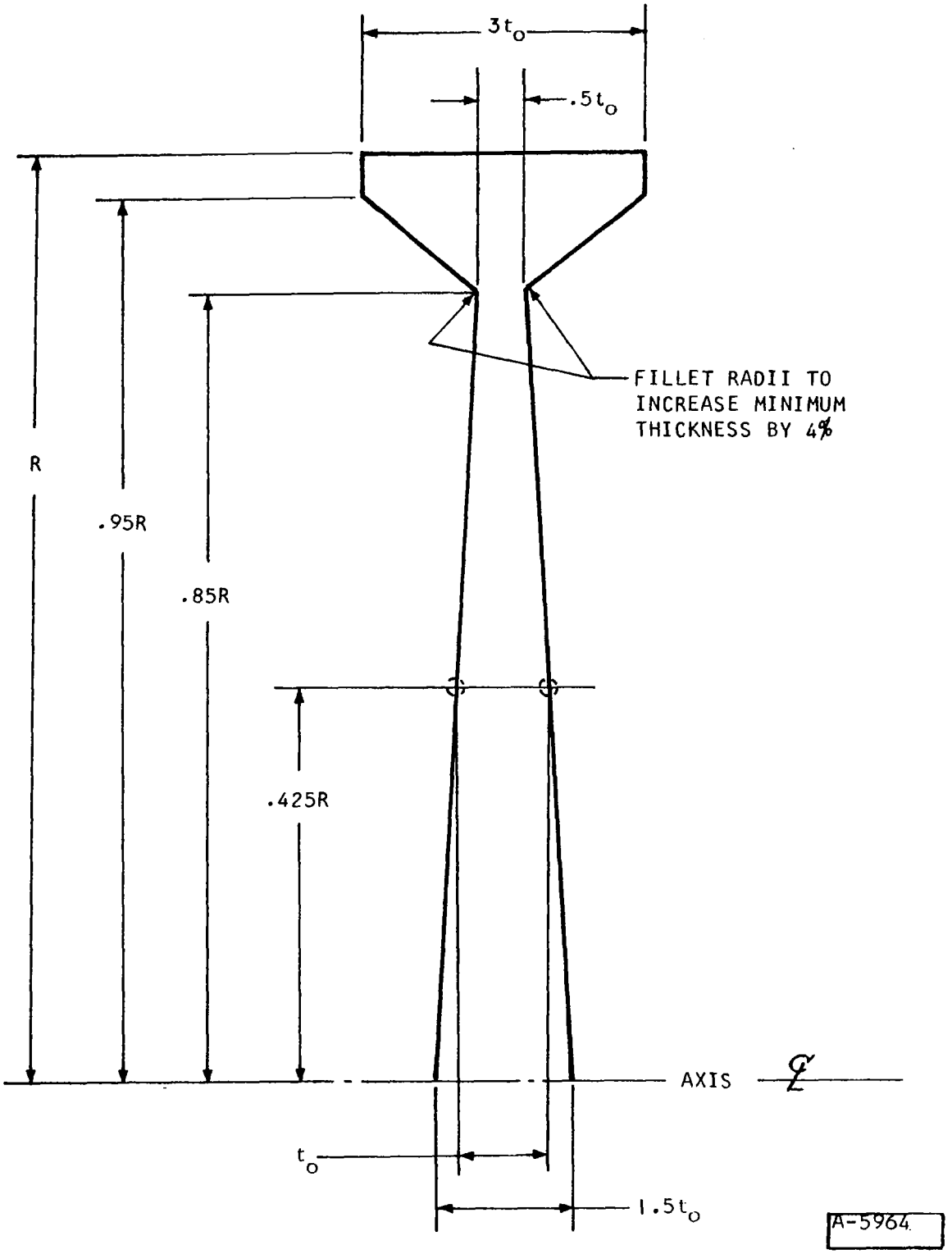

Figure 3-10. Profile of Optimum Shaped Momentum Wheel

where

H = angular momentum, in-lb-sec

R = wheel radius, in

t_o = reference wheel thickness, in

ω = angular speed, rad/sec

σ = maximum centrifugal stress, psi

γ = specific weight of wheel material, lb/in^3

W = weight of wheel, lb

Once the three coefficients have been calculated for a sample wheel, another wheel of different radius, wheel material, and slenderness ratio can be quickly designed as long as the thickness distribution is unchanged.

2. Combined Stresses (Stress Limited Design)

In addition to the centrifugal stresses of rotation, there are some small but not negligible bending stresses in the wheel, occasioned by the transmission of gyroscopic moments to and from the bearing supports. This latter stress condition is, furthermore, cyclic in nature, as opposed to the centrifugal stress, which is uniform at a uniform speed. Since cycling occurs at the rotational speed of the wheel, these stresses must be considered for infinite fatigue life. The total allowable stress can be specified conservatively through the use of a modified Goodman Diagram shown below in Figure 3-11.

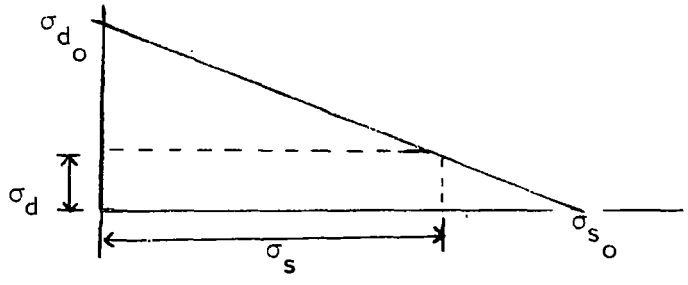

Figure 3-11. Modified Goodman Diagram

σ_{s_o} = maximum allowable static stress component

σ_{d_o} = maximum allowable dynamic stress component

The maximum stresses allowable for either type of loading alone are laid out on two cartesian axes. Combined allowable stressing is then indicated by

the straight line joining the two points, σ_{s_o} and σ_{d_o}. For bending of a circular plate by a moment applied through a central shaft, the maximum radial stress occurs at the junction of the shaft and the plate, and its magnitude may be given by

$$\sigma_d = \beta \frac{M}{Rt^2} \qquad (4)$$

where

M = gyroscopic moment

R = wheel radius

β = a coefficient dependent on r/R, where r is the shaft radius

From reference (1), the following table for β is obtained.

r/R	0.1		0.15	0.20		0.25	0.30	0.35	
β	4.36-5.05		3.80-3.70	3.27-2.75		2.80-2.30	2.37-2.00	2.10	
r/R	0.40	0.45	0.50	0.55	0.60	0.65	0.70	0.75	0.80
β	1.84	1.58	1.41	1.16	1.07	0.90	0.78	0.70	0.57

The solution given here is only approximately applicable to the problem on hand; but subsequent analysis has shown that the optimum design is only slightly influenced by the cyclic stress component because of the small moment specified for the control moment gyro. For this reason, it is the conclusion that refined and time-consuming analysis of a more exacting nature cannot be justified for this problem statement.

In the design of the stress-limited wheel, conservative allowable stresses were used, as shown in the following table:

Material	σ_{s_o}	σ_{d_o}
4340 Steel	150,000	60,000
Maraging Steel	170,000	60,000
Titanium	110,000	50,000

Reference (1) Roark, "Formulas for Stress and Strain," 2nd Edition, McGraw-Hill, N.Y., 1954, pp 195 - 216

An additional margin of safety is provided through the selection of β and t in equation (4). The average web thickness t(0.425R) rather than the hub thickness is used, while β is assigned the value 5.05 for r/R = .1.

Referring again to the preceding Goodman diagram, it is seen that

$$\sigma_s = \sigma_{s_o} - \frac{\sigma_{s_o}}{\sigma_{d_o}} \sigma_d \tag{5}$$

By selecting a material and assigning the radius "R", equations (1) through (5) allow the speed and wheel thickness to be calculated such that the given angular momentum is satisfied and with the stress components riding the allowable limits set forth by the modified Goodman diagram:

$$t^2 = \frac{1}{\sigma_{s_o} \sigma_{d_o} R} \left(\frac{C_2 H^2 \sigma_{d_o}}{C_1{}^2 R^5 \gamma} + \sigma_{s_o} \beta M \right) \tag{6}$$

$$\omega = \frac{H}{C_1 R^4 t \gamma} \tag{7}$$

and weight $W = C_3 R^2 t \gamma$

The minimum weight flywheel so designed requires an operating speed ω and physical dimensions t and R. These parameters are necessary information for the calculation of bearing and windage losses.

3. Fiberglass Design

Since a minimum weight flywheel can be obtained from a material with the highest strength-to-weight ratio, fiberglass was investigated as a possible wheel material, its F_{tu}/γ ratio being nearly 2.5 times that of the high strength alloy steel. This apparent advantage, however, must be tempered with the fact that the fiberglass can only be fabricated easily into a ring which can effectively provide high hoop tension against rotational stresses. Some type of attachment must be incorporated into the design to tie the rim to the hub and to transmit the gyroscopic moments. Another disadvantage is that comparatively high speeds are required to develop the full strength of the fiber, and this causes power losses which must be reckoned against the actual weight of the wheel.

The accompanying sketch indicates a possible design configuration wherein the moment is transmitted via two aluminum discs.

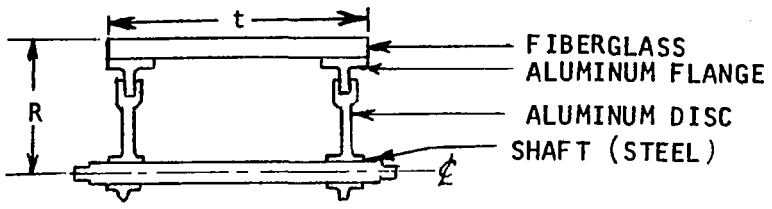

The design formulas, derived from the basic equation $H = I\omega$ and $W = \Sigma$ (volume) x (specific weight), are

$$H = \omega \left\{0.432R + 0.244t \quad R^4 \times 10^{-4}\right\} \tag{8}$$

and

$$W = (0.02775R + 0.00943t)\, R^2$$

where

H = angular momentum, in.-lb-sec

R = wheel radius, in

t = axial depth of fiberglass windings, in

W = weight of assembly, lb

In general, the construction requires that $t \geq R/2$

4. Minimum Equivalent Weight Design

In the course of the design analysis, some heavy and paired ball bearing configurations were investigated as to their effect on the selection of the optimum system. The large power losses associated with these bearings indicated that under certain combination of design requirements it is advantageous to operate a flywheel below the speed of the maximum allowable stress. This entails a heavier wheel and housing for a given angular momentum; but the reduction in power loss due to the lowered speed can more than make up the difference. The computer program which implements this phase of the study uses a search routine which, starting with the minimum weight flywheel, examines the possible merits of adding various amounts of flange material to the stress-limited wheel. The search proceeds in the direction of reducing total equivalent weight until a minimum has been located.

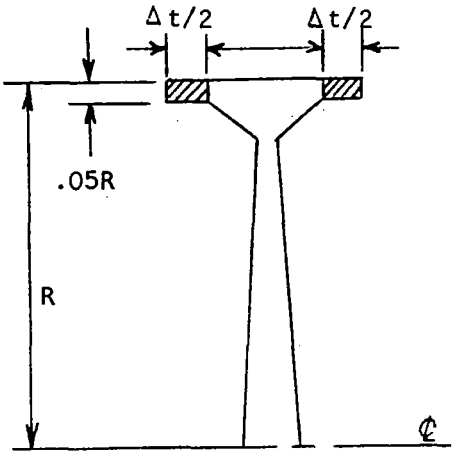

Referring to the drawing, the amount of flange addition is specified by the weight increase ΔW:

$$\Delta W = \alpha W \tag{10}$$

where α is initially assigned some value, about 0.1 at the beginning of the search, and is later reduced to 0.01 toward the end of the search. The width of the additional rim is then given by

$$\Delta t = \frac{\alpha W}{\gamma \pi R^2 \ (.0975)} \tag{11}$$

The increase in moment of inertia is, correspondingly,

$$\Delta I = \frac{\alpha W R^2}{g} \ (.95125) \tag{12}$$

Therefore, to obtain the same angular momentum, the speed must be reduced:

$$\Delta\omega = -\frac{\omega}{1 + I/\Delta I} \tag{13}$$

The new geometry and speed are used to recalculate the power requirements.

This procedure is based on the condition that the speed reduction to maintain constant angular momentum is more than needed to offset the stress increase caused by the introduction of non-optimum wheel geometry. This condition has been verified through a series of calculations by the computer program for disc stresses, where it was established that these wheels can be run from 6 percent to 30 percent faster and still remain within the stress limits, the margin being larger for the smaller angular momentum designs.

5. Bearing Formulas

a. Angular Contact Ball Bearings--The torque in a ball bearing may be assigned to various causes:

1. Lubricant drag - recent development in the use of channeling greases can reduce this item to almost zero. In the computer program a conservatively large drag is assumed, using a proven light oil.

2. Radial load - the bearings are sized to take the maximum specified loads, but the optimization is carried out using a weighted average load due to the specified control moment schedule.

3. Thrust load - this is introduced to prevent the separation of the balls from their races on the unloaded side of a bearing. This loading is necessary to insure reliable and smooth performance and for long life.

4. Ball separator drag - the use of new separator materials designed for vacuum operation will practically eliminate this item. Again, the computer program conservatively included a quantity based on conventional material.

The following bearing torque formulas used in the calculations were empirically derived and verified through extensive laboratory tests.

$$\begin{cases} T_a = BN^{\frac{2}{3}} LQ \text{ (Lubrication drag torque)} \\ T_b = 6400 \ (F^{\frac{4}{3}} Df)/(n^{\frac{1}{3}} d^{\frac{2}{3}}) \text{ (Radial load torque)} \\ T_c = 3600 \ (T_h^{\frac{4}{3}} d^{\frac{1}{3}}) \ (K_t + DK_r/d)/(n\sin\alpha)^{\frac{1}{3}} \text{ (Thrust load torque,} \\ T_d = C \text{ (Ball separator drag)} \end{cases}$$

where

T = torque in mg-mm

B = function of bearing size, curvature and ball complement

N = rpm

L = lubricant term proportional to (kinematic viscosity)$^{\frac{2}{3}}$

Q = empirical lubricant quantity factor, ≥ 0.4 for film lubrication

F = radial load, lb

D = pitch diameter, in.

f = ball to race osculation term, a function of curvature

n = no. of balls

d = ball diameter, in.

T_h = thrust load, lb

K_t = ball-race osculation term, a function of curvature and thrust

K_r = ball-race osculation term, a function of curvature and radial load

α = contact angle

C = constant ball separator friction, empirically determined.

b. Journal Bearings--Journal bearings have the advantage of offering practically infinite life when operated under design conditions. However, they consume slightly more power than the ball bearings. They also require some type of oil pump to circulate the lubricant and, when sized for the maximum load, do not afford a substantial torque reduction when operated under a light load condition. Several journal bearings designed for a range of radial loads yielded the following formula:

$$P_b = (.0002 + .000026F)N^{\frac{1}{4}}\omega/8.8512 \qquad (15)$$

$$P_p = 4.8F^{\frac{1}{5}}$$

where

P_b = power loss in one bearing, watts

F = radial load, lb

N = RPM

ω = speed in rad/sec

P_p = pump power, watts

6. Windage Loss Formulas

The windage loss in a soft vacuum is discussed in more detail starting on page 3-25 of this report; for calculation at a pressure of 0.001 mm Hg of helium, the following equation was used:

$$P_w = 0.5297145 \times 10^{-10} \sqrt{p}\, R^4\omega^{2.5} + .4008 \times 10^{-8} R^2 t\, \omega^2 \qquad (16)$$

where

P_w = windage loss, watts

p = pressure, mm Hg

R = wheel radius, in

ω = speed, rad/sec

t = rim thickness, in

7. Housing and Electric Motor Weights

Several aluminum housing designs led to the following empirical formula: (The equation was derived by log-log plotting shown in Figure 3-12.)

$$W_h = 0.14583\ R^2\ (1 + t/R) \qquad (17)$$

where

W_h = housing weight, lb

R = wheel radius, in.

t = rim thickness, in.

Aluminum was selected as the best material for fabricating the wheel housing for the following reasons.

1. It is superior to steel in withstanding collapsing external load because its lower density permits a larger cross-sectional area than steel to give it greater elastic stability.

2. The thermal conductivity of aluminum is superior to steel and will permit lower bearing temperature.

3. It forms more readily than magnesium. Otherwise, magnesium and aluminum are about equal.

4. The temperature of the housing will be at least 250°F under that which aluminum is capable of withstanding.

The electrical motor is conservatively programmed, allowing for 35 percent power loss for its load. Motor weights have been calculated for momentum wheel drives, covering the range of the parametric study, and are expressed in the following emperical equation.

$$W_m = 2.389 + .0000463H \qquad (18)$$

where

W_m = motor weight, lb

H = angular momentum, in.-lb-sec

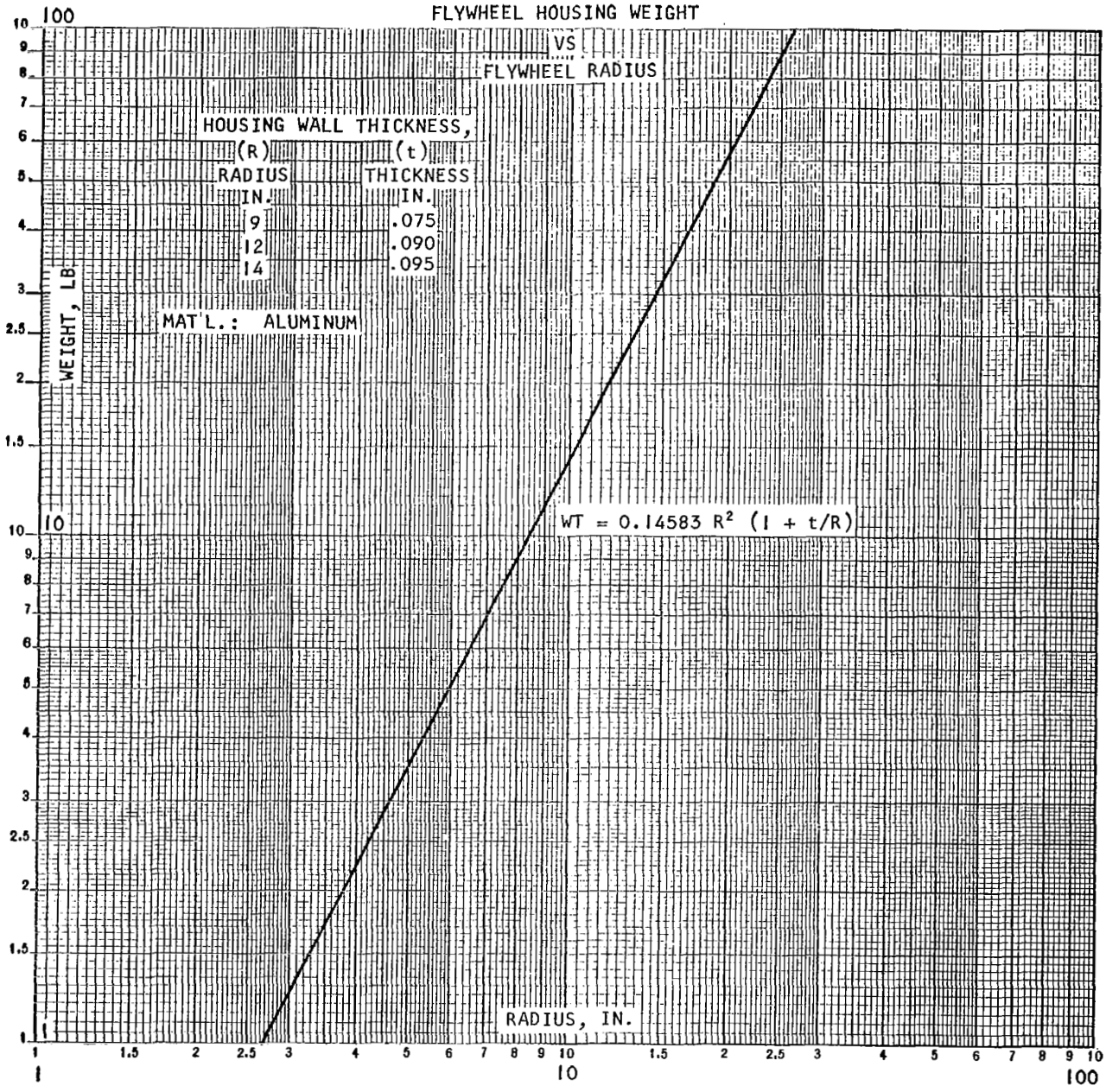

Figure 3-12. Flywheel Housing Weight

A-5974

CRITICAL SPEED ANALYSIS

Introduction

An analysis was performed on the final design unit (1000 ft-lb-sec angular momentum) to determine the critical speed characteristics of the rotating assembly. Also, the shaft deflections and bearing loads at the operating speeds were determined. An IBM 7074 computer program was used to make the calculations required for the analysis.

For a rotating assembly of the type considered in this study, the critical speeds that must be investigated are those associated with the lateral vibration of the wheelshaft system. A critical speed is characterized by amplified lateral vibrations of the rotating assembly accompanied by high bearing loads. The amplified motion is the resultant of a resonant condition which occurs when the frequency of the wheelshaft rotating unbalance coincides with the natural frequency of the elastic system--the elastic system consisting of the flywheel, shaft, bearings, and bearing mounts.(Figures 4-1, 4-2, and 4-3).

The most desirable rotating assembly design operates at a speed with a large margin from the nearest critical speed and encounters criticals at the lowest possible speeds during the start-up period. Critical speed characteristics can be adjusted to the above requirement by changing the mass-stiffness relationship of the rotating assembly and supports.

Discussion of Results

Analysis shows that for the shaft support stiffness and speed ranges considered, there is little shaft bending during lateral vibration, and, therefore, the critical speeds are almost entirely dependent upon the relationship of the shaft support stiffness (a combination in series of the bearing stiffness and the bearing mount stiffness) to the rotating assembly mass. Figure 3-13 shows critical speed as a function of shaft support stiffness as calculated by the IBM computer program. The values of support stiffness considered range from those values representative of resilienty mounted bearings (10,000 to 100,000 lbs/in.) to those representative of rigidly mounted Barden 102H bearings (200,000 to 300,000 lb/in.). The results show that only one critical speed occurs below the operating speed. The mode shape of the critical speed is shown in Figure 3-14. All other critical speeds for the system occur above 50,000 rpm.

Final Design

For the final flywheel design, a resiliently mounted bearing was chosen so that the bearing loads at operating speed would be low. With a bearing support stiffness of about 30,000 lb/in., the unit will have to pass through a critical at a relatively low speed of 6,200 rpm. Experience with rotating machinery shows that damping inherent in the system will prevent shaft vibration and bearing loads from becoming prohibitive as the unit passes through the critical speed during start-up. Bearing loads and shaft deflections for the operating speed range are shown in Figure 3-15..

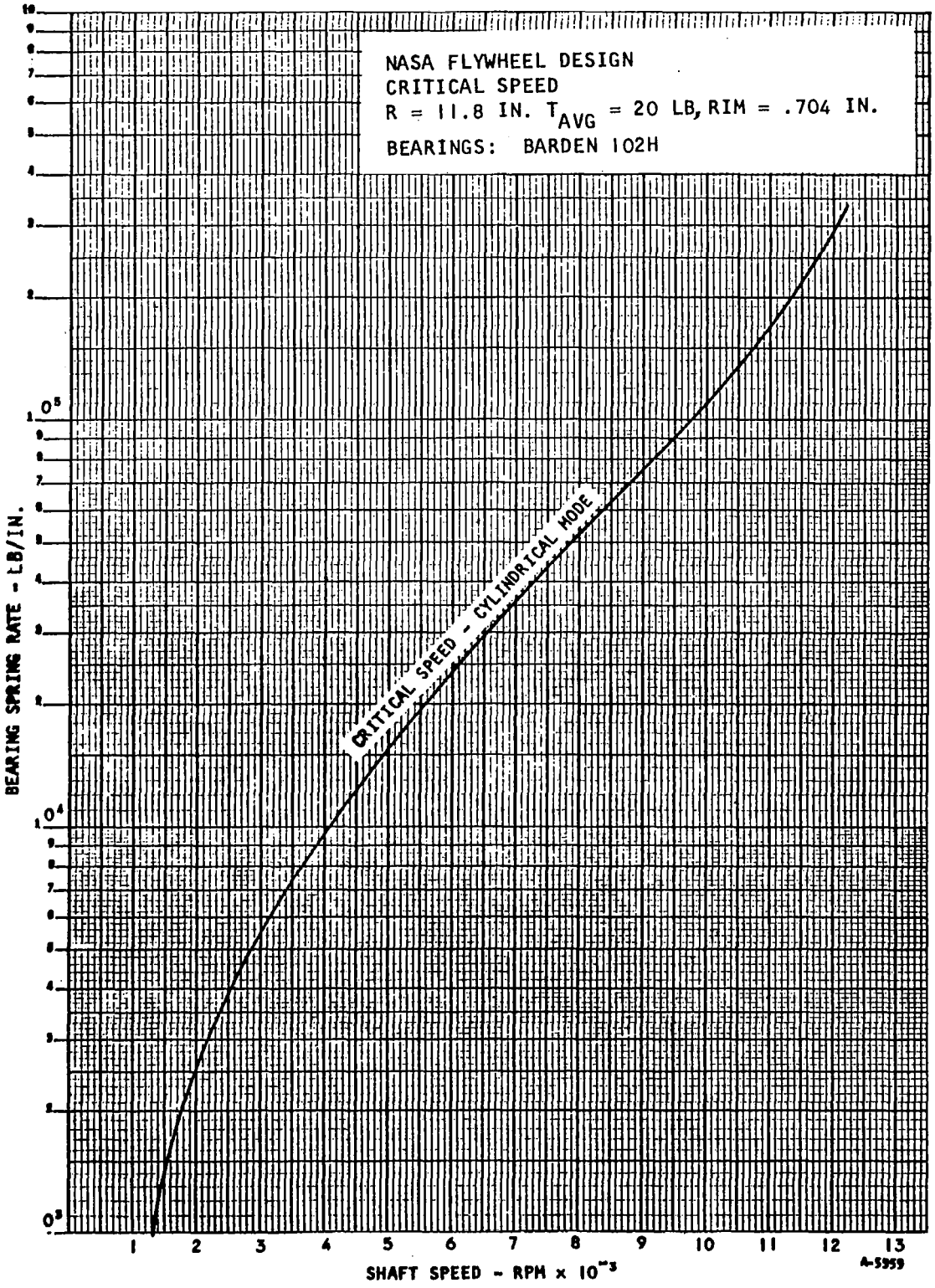

Figure 3-13. NASA Flywheel Design Critical Speed

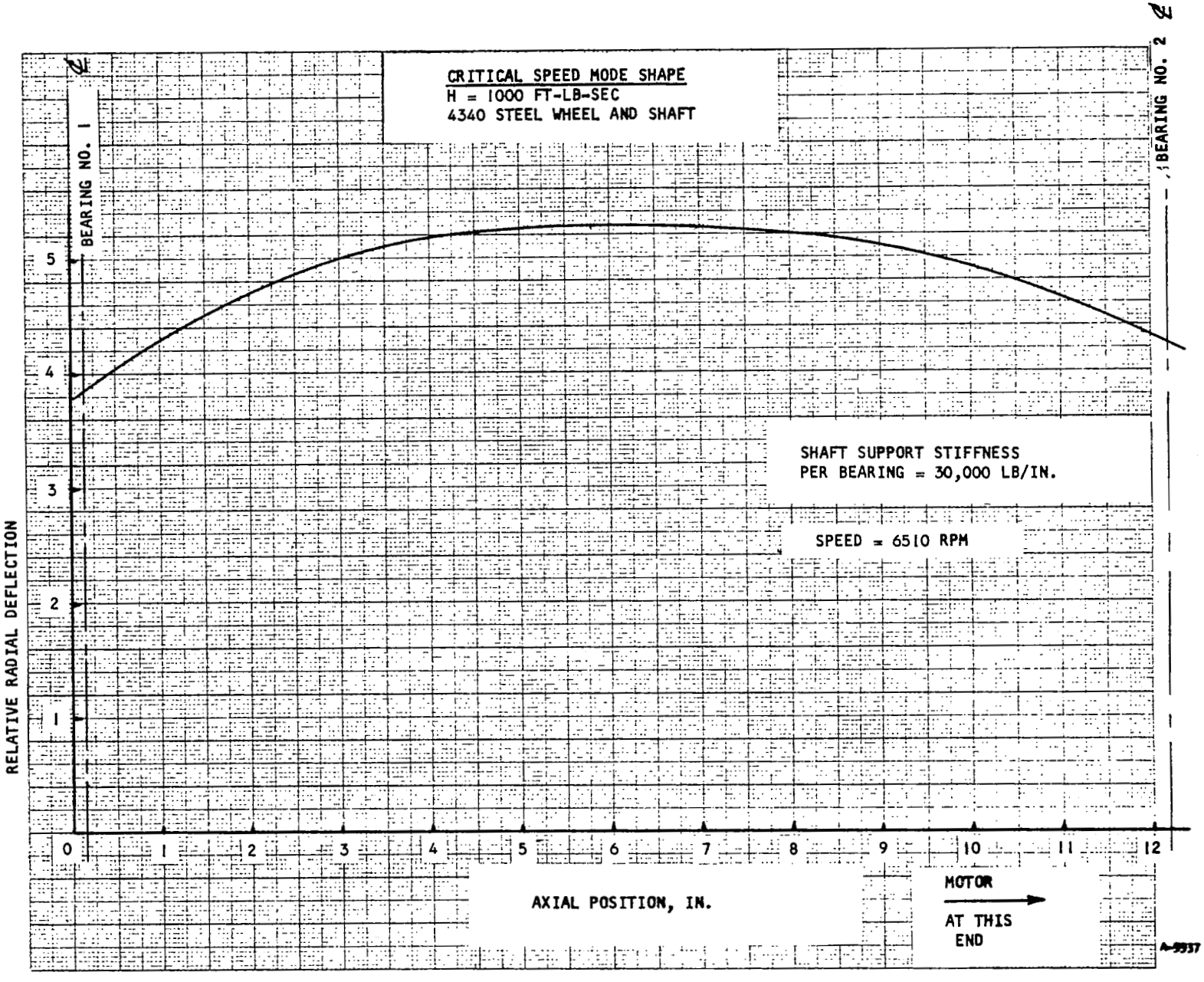

Figure 3-14. Critical Speed Mode Shape

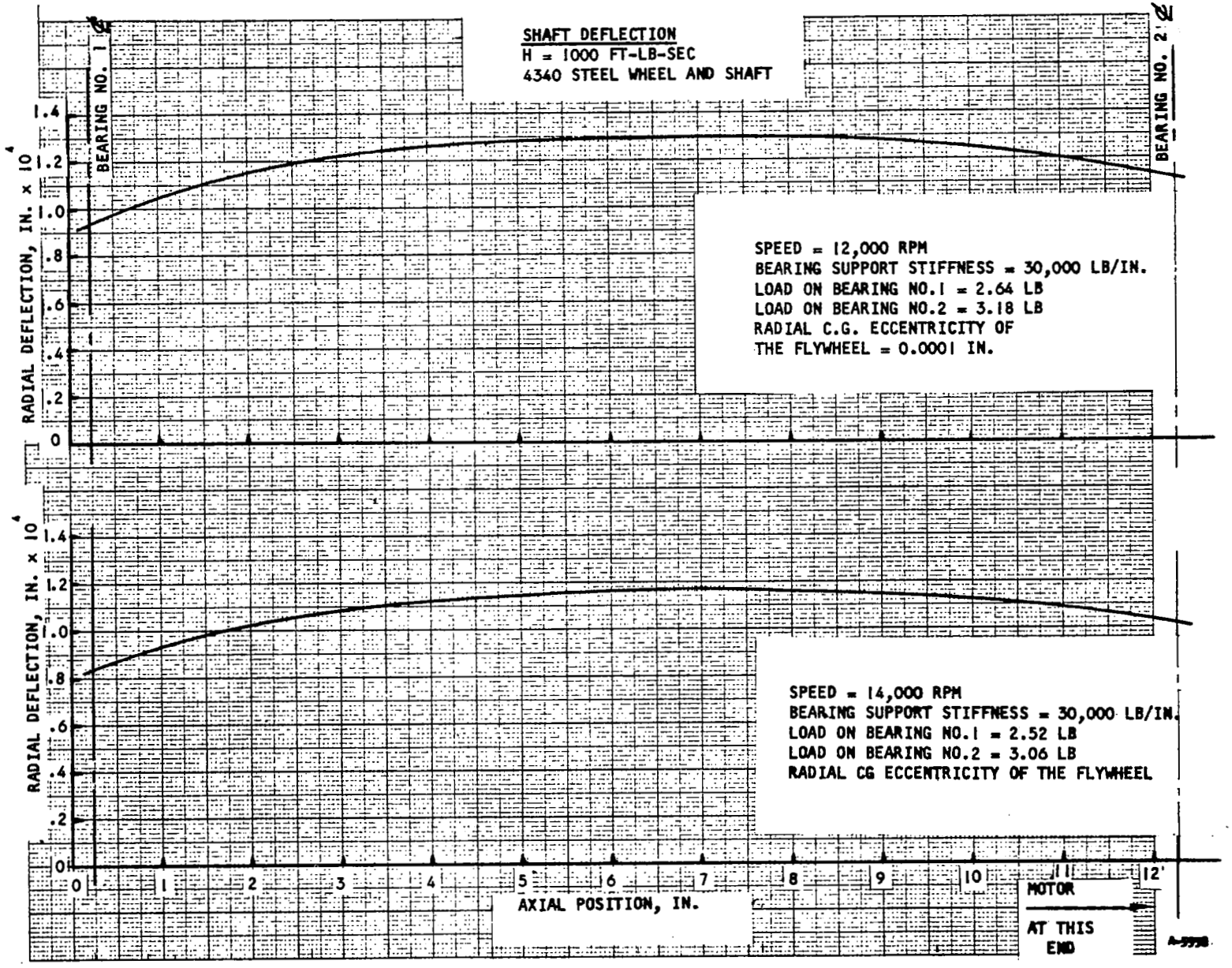

Figure 3-15. Shaft Deflection

Description of the Computer Program for Critical Speed Analysis

The IBM program used to determine the critical speeds in the analysis calculates the shaft whirl amplitudes as functions of the speed of rotation with specified built-in unbalance. A search subroutine finds the critical speeds as peaks of the speed-dependent whirl loads, and critical deflections. The program prints out shaft deflections and bearing loads as functions of shaft speed, as well as the discrete critical speeds.

The program accommodates a large number of degrees of freedom of any system through the use of a matrix formulation of Myklestad's method for beams.

The general program idealizes the system as a beam containing as many as 30 lumped masses and 60 lumped area moments of inertia. Each of the mass stations is also a possible point of support for the beam. Each support may be flexible, with specified linear and torsional spring characteristics. The 30 lumped masses may be entered as input to the program, or the program will calculate them from a specified distribution of an unlimited number of mass elements. The elastic influence coefficients of the shaft element between adjacent stations are calculated from geometric input specification. For this stiffness calculation, there may be as many as 10 cylindrical elements of different diameters between stations. There may be a specified unbalance at each of the 30 stations. Both mass unbalance and lack of straightness of the shaft may be accepted.

THERMAL ANALYSIS, DOUBLE-GIMBALLED GYRO

To preclude overheating of the motor or bearings during the anticipated operating life of the double-gimballed gyro, AiResearch conducted a thermal analysis. It is understood that this device will operate in a space environment, or at least in an environment where no heat may be rejected by normal convection methods. Two modes of heat dissipation are therefore available: radiation and conduction. No matter which of these modes of heat dissipation is used, the temperature of the surroundings is important. If the heat is transferred by conduction, it must eventually be absorbed by the vehicle structure; if the heat is to be dissipated by radiation, the surroundings must absorb the waste heat. Throughout the analysis it was assumed that the temperature of the entire surrounding structure would be 120°F.

Other information used in analysis included the specified geometry and the specified heat loads. The heat dissipated in each of the two bearings was taken to be 5.5 watts. The maximum heat load which could be anticipated from the motor was taken to be 10.3 watts, which was twice the motor loss determined by computer analysis. The windage losses were taken to be 3.6 watts. These windage losses will be distributed over the entire housing ellipsoid surface area, but for the purposes of the analysis it was assumed that half of this heat flowed through the motor end bearing and the other half through the bearing on the opposite end of the shaft. This is a conservative approach. The geometry used in the analysis was as shown in the supplied drawing.

It was understood that NASA would prefer heat dissipation by conduction into the vehicle structure. The first stage in the analysis was, therefore, to determine the temperatures that would exist at the motor and bearings if all the heat had to be removed by conduction alone. Consider the path which must be followed by heat conduction from the motor-bearing combination to reach the vehicle structure. From the localized source (motor and bearings), the heat must flow through the aluminum ellipsoid shell down to the first gimbal. The temperature drop estimated for this section of the heat path was 107°F. The next obstacle in the flow of heat conduction is through the rotating joint of the gimbal. Since this joint has a very small area and no metallurgical bond, the temperature drop across this joint is high. If an air gap of 0.002-in. width is assumed, the temperature drop across this gap would be approximately 1000°F. If a conventional lubricated joint is assumed, where the gap is filled with a lubricant, this temperature drop decreases to approximately 300°F. With this latter condition, this gives a total temperature drop between the first gimbal and the motor-bearing combination of at least 400°F. Even if no further temperature drop is encountered in flowing from the first gimbal to the second gimbal and then from the second gimbal into the structure, the temperature of the motor and bearings is much higher than is allowable. Conduction alone is, therefore, not sufficient to provide adequate cooling of the motor-bearing combination.

The next stage in the analysis was to investigate the heat dissipation capabilities of radiation. Radiation is basically an attractive idea for this application, since there is a large area available (the entire curved surface

of the ellipsoid). Assuming an emissivity of 0.1 (typical of aluminum plate) for this entire surface and with the maximum heat load being generated by the motor and bearings radiating to 120°F surroundings the estimated motor and bearing temperature is 300°F. This value is still slightly higher than required; however, the use of a high emissivity coating on the ellipsoid surface can substantially reduce this temperature. It is, therefore, recommended that the entire ellipsoid surface be painted with a black paint manufactured by the Minnesota Manufacturing and Mining Company. This paint is marketed under the trade name of 3M-Black Velvet, Trade Number C10. Data available for this coating indicate that the coating has any emissivity of 0.99 through the entire infrared radiation spectrum. This coating has been widely used in the space industry and no troubles have been encountered due to high vacuum or high temperature. The paint exhibits no tendencies to outgas or to flake under normal space environmental conditions. This coating has, therefore, not only the required thermal capabilities, but is highly suited for the space type of applications. With the entire ellipsoid surface painted with this black paint, the estimated maximum motor temperature is 160°F. If the previously mentioned lower motor heat load is used (5.15 watts), the estimated maximum temperature will be 150°F. On the opposite side of the ellipsoid (only bearing and windage losses) the estimated maximum bearing temperature is 134°F.

From the analysis, radiation is superior to conduction in dissipating the heat from this device. Conduction alone is not adequate to maintain the desired temperatures in the motor and bearings. Radiation from an untreated surface of the ellipsoid is also inadequate to maintain the required temperatures; however, it does maintain temperatures much lower than those obtained by conduction alone. If the recommended coating is utilized, no difficulty will be encountered in maintaining temperatures well below those required throughout all anticipated operating conditions. Where this coating is utilized, the effect of conduction on overall heat dissipation will be completely negligible.

To determine the heat flow from the motor-bearing combination by conduction, only the basic conductor equation is required

$$Q = \frac{K A \Delta T}{L}$$

where
- Q = Heat flow, Btu per min
- K = Thermal conductivity, Btu per min $ft^2/^oF/ft$
- A = Cross-sectional area of flow path, ft^2
- L = Length of flow path, ft
- ΔT = Temperature difference, ^oF

For motor-bearing to first gimbal, a two-dimensional heat conduction analysis is required; however, for the purpose of the present analysis, a simpler approach was used. A flow path width of 8 in. was assumed and applied to the above equation. The inaccuracies in this method are slight, particularly in view of the fact that the main loss is across the rotating joint of the gimbal. The loss in this joint was calculated for both an air gap and a lubricated joint using the above equation.

For radiation, the main relationship used was:

$$Q = \sigma \Sigma \eta_f A (T_R^4 - T_S^4)$$

where
- σ = Stephan-Boltzmann Constant (0.1712×10^{-8}) $Btu^2/hr\ ft^2\ {}^oR^4$
- Σ = Emissivity, dimensionless
- η_f = Radiative fin effectiveness, dimensionless
- A = Radiative area, ft^2
- T_R = Bearing-motor temperature, ^oR
- T_S = Surroundings temperature, ^oR

This assumes black body characteristics for the surroundings and a view factor of 1.0 from radiative surface to surroundings. In order to calculate radiative fin effectiveness the relationship of Bartas and Selbis* and of Mackay** were used.

*J. G. Bartas and W. H. Selbis "Radiation Fin Effectiveness" Trans ASME, Journal of Heat Transfer, 82, 73-75, (1960)

**D. B. Mackay, "Radiant Heat Transfer from Extended Surfaces" presented in 1961 to Institut Francais des Combustibles et de l' Energie

STRUCTURAL ANALYSIS OF THE HOUSING (INNER GIMBAL RING)

For the structural analysis the housing was considered to be a thin-walled ellipsoidal shell of revolution made of two halves connected through a rigid circular ring. The actual shell will be stiffened by radial corrugations. The corrugations will improve the efficiency of the structure; therefore, the following analysis will tend to be conservative. A minimum thickness for the shell was determined such that the collapsing pressure of the shell is at least two atmospheres. Stresses and deflections in the shell due to a 50 ft lb gyroscopic moment of the wheel were then checked.

The minimum thickness for the shell is assumed to be the same as that required by a spherical shell with a radius equal to the maximum radius of curvature of the ellipsoid of revolution. The following expression for the buckling stress was used in the analysis (Reference 1).

$$\sigma_{cr} = \frac{pr}{t} = \frac{1}{3} \frac{Et}{r\sqrt{3(1-\nu^2)}}$$

where:

E = modulus of elasticity

r = radius of sphere

ν = Poisson's ratio

t = thickness

Using the preceding relationship, the minimum thickness required to withstand 2 atmospheres of external pressure was calculated to be 0.067 in. for the proposed 356-T aluminum casting. The actual thickness used was 0.090 in.

The gyroscopic moment produced by the flywheel will be reacted by the shell at the ends of the shaft. The stresses in and the deflection of a 0.090-in. thick shell were roughly estimated. Equations for the membrane stresses in a hemisphere due to a point load at the apex were used for this analysis (Reference 2). The stresses are:

$$\sigma_{\phi} = -\sigma_{\theta} = -\frac{H}{\pi a t} \frac{\cos\theta}{(1+\cos\phi)\sin\phi}$$

$$\sigma_{\phi_\theta} = \frac{H}{\pi a t} \frac{\sin\theta}{(1+\cos\phi)\sin\phi}$$

where

H = the point load

t = thickness

a = radius

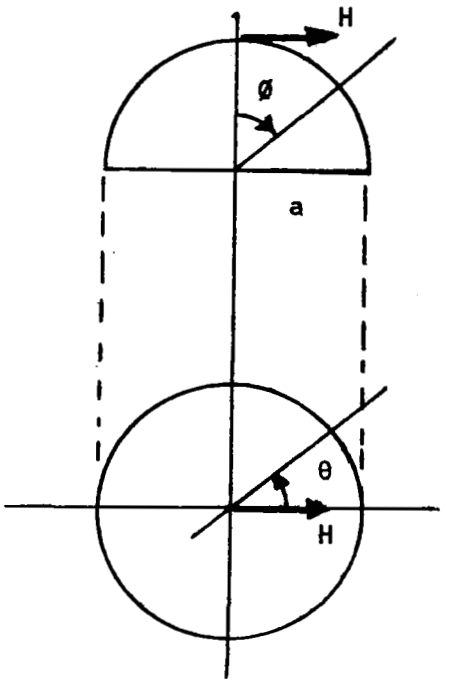

The region around the apex where the above equations give infinite stresses was disregarded, since this region in the actual housing consists of a relatively heavy boss that supports the shaft and bearings. An estimate of the nominal stresses in the shell was made by letting the radius "a" in the stress equations be equal to the semi-major axis of the ellipsoid. This approximation gives a maximum effective stress, defined by the Von Mises theory of combined stress, of 140 psi for the maximum gyroscopic moment of 50 ft lb. Local discontinuity stresses in the region of the bosses could be higher, but not prohibitively high.

An approximation of the deflection of the shaft supporting boss in the direction of the gyroscopic loading was made using the strain energy approach. Again, a sphere with a radius equal to the semi-major axis was assumed in place of the actual ellipsoidal shell, and the stresses defined in Reference 2 and stated above were utilized. The calculation gives a deflection of the apex of 0.0000446 in.

Since the values roughly calculated in this analysis for the stresses and deflection of the housing are low, a more rigorous and exact analysis of the unit is not required to ensure reliability.

References:

1. Timoshenko, S., Theory of Elastic Stability, 1936
2. Flügge W., Handbook of Engineering Mechanics, 1962

DEFLECTION ANALYSIS, OUTER-GIMBAL

For dimensional stability, this ring will be fabricated from 0.060 in. aluminum sheet stock, forming a rectangular cross-section 1 x 1.5 in. outside dimension.

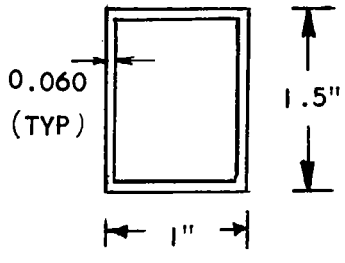

SECTION A-A

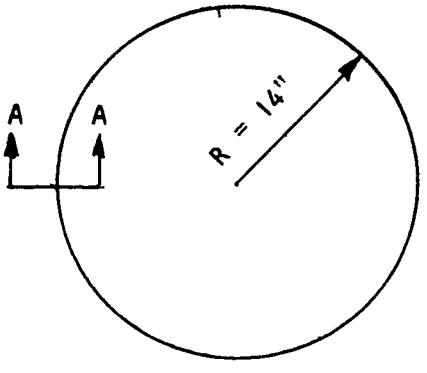

The structural strength of this ring is many times more than the loading requires. Therefore, only an approximate deflection analysis will be performed to establish the order of magnitude of deformations.

(1) Out of Plane Loading

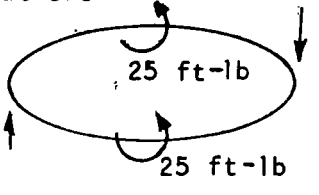

A maximum moment of 50 ft-lb has been specified for the torquer. This moment is resisted by a gyroscopic moment of the flywheel through the inner gimbal mount points. The exact mechanism of moment application has not been defined. For this analysis, it will be assumed that each end of the outer gimbal exerts 25 ft-lb, or the loading is symmetrical. Then Ref. 1 gives a solution approximately applicable to this case:

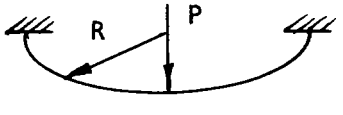

$$\delta = \frac{.514\ PR^3}{2EI_x}$$

where $P = \frac{50 \times 12}{28} = 21.4$ lb

$R = 14$ in.

$E = 10 \times 10^6$ psi

$$I_x = \frac{.12}{12}(1.5)^3 + (.72)^2 + (.88)(.12)$$

$$= .0885 \text{ in.}^4$$

$$\delta = .017 \text{ in.}$$

The total rotation of the inner gimbal supports is 2δ or .034 in. The angular error is

$$\frac{.017}{14} \times 57.3 = .07 \text{ deg}$$

For ground testing, the weight of the rotor assembly adds 20.3 lb to the support load. The weight of the gimbal ring itself accounts for another 1.25 lb. These figures indicate that on the ground the deflection can be twice the amount calculated when under the most unfavorable combination of loads. Whether or not these deflections are excessive can only be determined after receiving a more explicit control requirement specification.

(2) In-Plane Loading

The in-plane loading of the outer gimbal occurs when the spin axis of the flywheel is displaced from its direction normal to the plane of the outer gimbal. The maximum moment is

$$50 \tan 60^0 = 86.6 \text{ ft-lb}$$

for a maximum gimbal angle of 60 degrees. Then

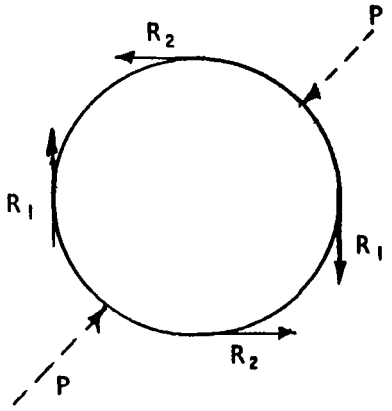

$$R_1 = R_2 = \frac{86.6}{28/12} = 37.2 \text{ lb}$$

The couples may be resolved into two equal and opposite forces P acting on the ring for an approximate deflection analysis.

$$P = 37.2/2 = 52.5 \text{ lb}$$

The diametral deflection is(from Ref. 2)

$$\delta = -.149 \frac{PR^3}{EI}$$

$$I = \frac{1}{12}(1)^3(.12) + (.47)^2(1.38)(.12)$$

$$= .0466$$

$$\delta = -.149 \frac{(52.5)(14)^3}{10^7 \times .0466} = -.042 \text{ in.}$$

The weight of the ring is

$$W = (4.76)(.06)(\pi)(28)(.1)$$

$$= 2.51 \text{ lb}$$

References

1. Timoshenko, "Strength of Materials," Part I, 3rd edition, D. Van Nostrand Co. N. Y., pp 412-415.

2. Roark, "Formulas for Stress and Strain," 3rd Ed, McGraw Hill Book Co. N.Y. 1954, p. 156.

SHAFT DESIGN AND ANALYSIS

Two major design considerations for the shaft are: (1) adequate bending stiffness to prevent the occurrence of a bending mode of vibration at the operating speed, and (2) adequate strength to transmit bending and torsional moments. Since resilient bearing mounts have been recommended for this design, the first critical speed was intentionally lowered by allowing the supports to become flexible. The shaft stiffness thus has little effect on the first critical; and the second critical was found to occur at about 75,000 rpm, beyond the range of interest.

The requirement of strength in this case was satisfied by making the shaft cross-section follow approximately the moment diagram due to a centrally applied load on a simply supported beam. As shown in Figure 4-1, the shaft has a total span of 12 in. from center to center of the ball bearings, it has two hollow conical sections starting with a 1.5 in. radius at the center line of the rotor, and tapering off to 0.4 in. radius at 5.0 in. toward the bearings. The wall thickness is .060 in. minimum. Recommended material is 4340 steel, and the method of joining to the rotor is by welding. At the center of the shaft, the area moment of inertia is

$$I = \frac{\pi}{64}(d_o^4 - d_i^4)$$

$$= \frac{\pi}{64}(3^4 - 2.88^4)$$

$$= .599 \text{ in}^4$$

For a bending moment of 1200 in. lb, the maximum stress is only

$$\sigma = \frac{MC}{I} = \frac{1200 \times 1.5}{.599} = 3{,}000 \text{ psi}$$

at the center of span. The stresses will become higher toward the supports due to a more rapid decrease in section modulus of the shaft than the moment, until the minimum section is reached. At that point, the linearly varying moment would have decreased to

$$M = \frac{1}{6} \times 1200 = 200 \text{ in. lb}$$

and the section modulus is

$$\frac{I}{C} = \frac{1}{0.4}\frac{\pi}{64}(0.8^4 - 0.68^4) = 0.0241 \text{ in}^3$$

The bending stress is now

$$\sigma = \frac{200}{0.0241} = 8300 \text{ psi}$$

which still affords a large margin of safety. Torsional vibration does not present a problem because of the absence of tangential periodic excitation. The acceleration torque also produces negligible stresses. The minimum thickness of .060 in. selected for fabrication and welding purposes, should not be reduced although the stresses are low.

No further analysis of the shaft can be justified in view of the low stresses obtained.

POWER SUPPLY

Description of the Frequency Converter

A block diagram of the proposed system is shown in Figure 3-16. To keep the motor torque constant, the current into the motor is held constant. During acceleration, this is accomplished by current feedback to the controlled power supply.

When the motor is operating from a constant current source, the voltage across the motor is a function of the motor speed. The voltage is, therefore, low when the frequency is low. As the motor accelerates, the voltage across it increases and the frequency of the voltage-controlled oscillator increases proportionally.

During this period, the power dissipation in the converter is constant and will be held to 22 watts.

The converter package should be mounted to a reasonable heat sink. If this is not available, then the package size will have to be increased to prevent overheating during acceleration.

The package weight has been estimated as 4.75 lb.

When the momentum wheel reaches the desired operating speed, the mode of operation is changed. For a constant speed, only enough current must be supplied to the motor to overcome friction and windage losses in the wheel and motor losses. The motor must also be supplied by a constant frequency.

The mode of operation, therefore, changes from constant current to constant voltage and frequency.

By careful motor design, the voltage chosen will provide unity power factor to motor. This is a very desirable operating point because the inverter losses due to circulating currents will be kept to a minimum. We have calculated a power dissipation of two watts for this operating condition.

To control the power supply voltage and inverter operating frequency, the output frequency of the inverter is compared in a frequency discriminator to a frequency standard. When the output frequency approaches the frequency of the frequency standard, a d-c voltage overrides the current feedback signal from the current detector and the voltage feedback to the voltage-controlled oscillator. The gain of this loop will be great enough to maintain the desired momentum wheel speed to 0.25 percent of maximum speed for variations in bearing load, motor torque, and windage losses.

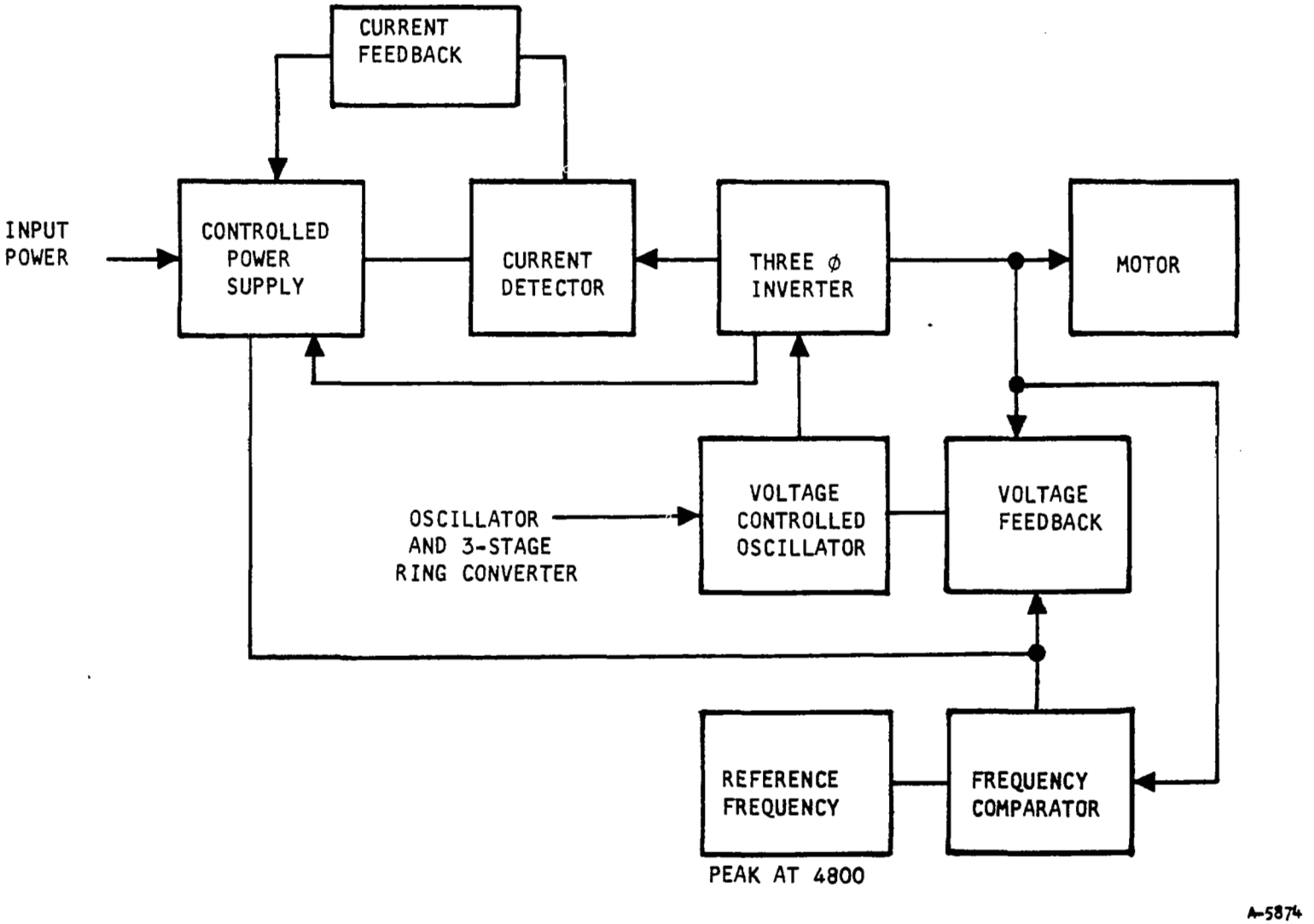

Figure 3-16. Block Diagram of Proposed System

NOISE LEVEL

Two factors in the design of the momentum wheel assure a low acoustic noise level in its operation: (1) resilient mounting of the bearings with hydraulic damping action; (2) evacuated chamber for the flywheel to revolve in. From experience with test equipment running bearings at a pressure of 10^{-2} mm Hg and less, it can be expected that the noise level of the control moment gyro will be barely audible.

A component currently in production for submarine use that has gears and a 10-hp motor running at 23,600 rpm on two 205H bearings has a noise level of only 56 db. This level is less than that of a quiet reading room in a library. This fact gives assurance that a quiet running control moment gyro can be designed and fabricated.

MONITORING DEVICES

Noise Level

An acoustic monitoring device of microphone type should be installed in the vicinity of the bearings as shown in Figures 4-2 and 4-3. Continuous monitoring of the noise level through an electronic amplifier can detect failure and set off a warning device or cause automatic shut-down.

Bearing Temperature

Change of the bearing temperature relative to the ambient is a good indication of incipient failure. Experience with bearing tests have proved failure is indicated by either increase or decrease of the temperature differential. A change of $\pm 25^{0}$F almost invariably indicates that the bearing has encountered a problem that can lead to its destruction. This fact can be used in a failure warning system. This method can predict failure in advance of the acoustic warning device where the adverse change is taking place slowly such as a gradual loss of lubricant. In this case, the bearing temperature drops slowly, first, before it experiences a rapid rise. The location of thermocouples for monitoring bearing temperature is shown in Figures 4-2 and 4-3.

MATERIAL COST

The materials considered for use in fabricating the flywheel require cost consideration. Forging metal material costs are approximately as listed below:

4340 Steel, vacuum melted	$0.75 per lb
Maraging Steel	10.00 per lb
Titanium	5.00 per lb

SECTION 4

STUDY RESULTS

The information and data resulting from this study is presented in this section in detail for study and use as a basis for drawing conclusions and making recommendations for optimum design momentum wheels.

COMPUTER RESULTS

The computer program provided information as shown in Table 4-1 which is a photo copy of digital computed values for a 4340 steel momentum wheel with an angular momentum of 1,000 ft-lb-sec. The first line of numbers in a horizontal line across from each radius is for the "stress limited design" and the next line gives the values for the " minimum equivalent weight design." A total of 218 such sheets of digital computer runs were made and analyzed in this program.

The design values of momentum wheel size, assembly weight, wheel speed, and total power loss resulting from the parametric study for angular momenta over the range of 200 to 2000 ft-lb-sec, are presented in Table 4-2, and shown in graphic form in Figure 4-8. These values are for assemblies that have been optimized on the basis of the minimum combined total assembly weight and power loss, i.e., "minimum equivalent weight design." (The speed used does not take into account the availability of 400-cycle a-c power the use of which would result in a speed of 12,000 rpm. For wheels with speeds near 12,000 rpm, as will be shown in a later curve, there is only a very slight increase of weight when the speed is changed to 12,000 rpm.)

DESCRIPTION - MOMENTUM WHEEL ASSEMBLY

The design for a momentum wheel assembly for an angular momentum of 1000 ft-lb-sec is shown in Figure 4-1. The wheel is made of 4340 steel and the ball bearings are size 102H. Figures 4-2 and 4-3 show how the bearings are mounted in replaceable cartridges for ease in annual maintenance. The aluminum housing is hermetically sealed by metal to metal sealing. Helium gas used in assembly, is evacuated to a pressure of at least 10^{-3} mm-Hg.

The motor as shown in detail in Figure 4-4 is a 4-pole, 3-phase, permanent magnet, synchronous motor. It is an axial gap type with a magnetic thrust of about 4 lbs. It is capable of driving at speeds far in excess of that required by any design speeds set forth in this report.

MATERIAL SELECTION

Information pertinent to the selection of material suitable for the flywheel is shown in Figures 4-5 and 4-6 for the two design approaches used in this analysis. Figure 4-5 is for "stress limited design" wheels and 4-6 is for "minimum equivalent weight design" wheels. Four materials, 4340 steel, maraging steel, titanium, and fiberglass are compared. Flywheel, housing, and total assembly weight and power loss are summed to give the total equivalent weight associated with each material. Material selection is facilitated by use of these two graphs.

CHARACTERISTICS

The influence of the flywheel material characteristics in regards to size and speed is shown in Figure 4-7. This information is useful where space and angular velocity is an important consideration.

POWER LOSS

Power loss vs wheel speed due to bearing torque, windage, and motor inefficiency is shown in Figure 4-9 for a 4340 steel wheel using two 102H ball bearings. This set of curves shows the influence of speed on each of the sources of power loss and gives a comparison in these losses.

Windage

Further study of windage power losses is possible by use of Figures 4-10, 4-11, and 4-12. Figures 4-10 and 4-11 show the influence of the gas pressure around the spinning momentum wheel with an angular momentum of 1000 ft-lb-sec and makes a comparison of the windage losses for air, helium, and hydrogen. Wheels resulting from the two design methods are covered. Figure 4-12 shows the influence of wheel speed on windage loss for each of the three gasses at a pressure of 10^{-3} mm-Hg at 15^{0}C.

Bearings

Power loss due to bearing torque for three sizes of ball bearings is covered for three different loads in Figures 4-13, 4-14, and 4-15.

The bearing sizes used in the study are listed below with their inside and outside diameter dimensions.

Identification No.	Diameter			
	Bore		Outside	
	(in.)	(mm)	(in.)	(mm)
204H	0.7874	20	1.8504	42
102H	0.5906	15	1.2598	32
100H	0.3937	10	1.0236	26

The bearing loss, in watts, vs wheel speed for each of these bearings, is shown in each of the three figures. The loads studied are shown as listed below:

Figure No.	Load, lbs	
	Radial	Thrust
4-13	18.5	20
4-14	50.0	20
4-15	112.	40

MOTOR LOSS

Motor loss is a function of other power loss load, such as that caused by bearing and windage drag. A typical curve of motor loss vs speed is shown in Figure 4-9. This curve is for wheels with 1000 ft-lb-sec capacity for various operating speeds, ranging from 10,000 to 31,000 rpm.

MOMENTUM WHEEL CHARACTERISTICS

The curves shown in Figures 4-16 through 4-19 are very useful in the optimization study for comparing the two design approaches stress-limited, and minimum equivalent weight, angular momentum from 200 to 2000 ft-lb-sec.

These figures cover the following designs:

Figure No.	Material	Bearings Type	Qty.	Size	Identification No.
4-16	4340 Steel	Ball	2	15 mm.	102H
4-17	Maraging Steel	Ball	2	15 mm.	102H
4-18	Titanium	Ball	2	15 mm.	102H
4-19	4340 Steel	Journal	2	.25 in. dia x .3 in. lg.	-

Figure 4-20 is very closely related to the above four sets of curves. These curves show the effect of designing the wheels to run at 12,000 rpm. The minimum weight design wheels are plotted on the same graph for comparison purposes.

SPEED EFFECT ON MOMENTUM WHEEL DESIGN

The effect of speed on flywheel weight, size, total assembly weight, and total equivalent weight for wheels with an angular momentum of 1000 ft-lb-sec is shown in Figures 4-21 through 4-24.

These figures cover both stress-limited and minimum equivalent weight designs. They all use 2-15 mm ball bearings. They are divided up as to material as listed below.

Figure No.	Material
4-21	4340 Steel
4-22	Maraging Steel
4-23	Titanium
4-24	Fiberglass

These curves are useful in comparing the two design approaches as well as determining trade-off values required to shift the operating speed. The flatness of the total actual weight and equivalent weight curves in the minimum range is very interesting and beneficial where a shift in speed from optimum is necessary.

DIRECT PLOT OF COMPUTER DATA

The digital computer program made large amounts of data available that were printed in numerical form as shown in Table 4-I. All optimum data has been transcribed into the curves shown in Figures 4-5 through 4-24, however some of the same computer tapes were selected to show these data in graphic form. These curves are useful in that they show the characteristic effect of the flywheel radius on weight, size, and speed. Figures 4-25 through 4-35 are correlated with angular momentum, material, design method, and bearing type and size as listed below.

Figure No.	Angular Momentum (ft-lb-sec)	Material	Design Method	Bearing Type	Bearing Identification
4-25	1000	4340 Steel	Stress Limited	Ball	102H
4-26	500	4340 Steel	Min Equiv Wt	Ball	102H
4-27	1000	4340 Steel	Min Equiv Wt	Ball	102H
4-28	1500	4340 Steel	Min Equiv Wt	Ball	102H
4-29	1000	4340 Steel	Stress Limited	Journal	0.25 in. dia 0.3 in. lg.
4-30	500	Maraging Steel	Min Equiv Wt	Ball	102H
4-31	1000	Maraging Steel	Min Equiv Wt	Ball	102H
4-32	1500	Maraging Steel	Min Equiv Wt	Ball	102H
4-33	500	Titanium	Min Equiv Wt	Ball	102H
4-34	1000	Titanium	Min Equiv Wt	Ball	102H
4-35	1500	Titanium	Min Equiv Wt	Ball	102H

The curves shown in this section can be used as a very strong tool for designing wheels where departure from the optimum is desirable.

TABLE 4-1

FLYWHEEL OPTIMIZATION
4340 STEEL, SHAPED DISC, TWO 102H BRGS, H=1000 FT-LB-SEC
PRESSURE=.001 MM HG, THRUST LOAD = 20 LBS, RADIAL LOAD = 18.5 LBS

H= 12CC0.0 IN-LB-SEC ONE WATT = 1.COO LB

RADIUS IN.	THICK. IN.	T/R	RPM	WHEEL LBS	HOUSING LBS.	BEARING WATTS	WINDAGE WATTS	MOTOR WATTS	ACTUAL W LBS	EQUIV. W LBS	LOSS WATTS
6.800	1.068	0.1571	30578.5	52.57	9.92	32.90	8.17	14.37	67.52	122.96	55.44
	5.029	0.7395	25017.5	59.88	11.73	24.85	7.65	11.39	76.64	120.52	43.88
7.000	0.980	0.1400	29689.8	51.09	10.15	31.56	7.75	13.76	66.27	119.33	53.06
	4.612	0.6589	24290.4	58.20	11.85	23.86	7.17	10.86	75.08	116.97	41.89
7.200	0.901	0.1251	28848.7	49.70	10.40	30.31	7.38	13.19	65.13	114.02	50.89
	4.241	0.5890	23602.3	56.61	12.01	22.93	6.75	10.39	73.66	113.72	40.06
7.400	0.830	0.1122	28051.2	48.39	10.67	29.14	7.07	12.67	64.10	112.98	48.89
	3.909	0.5282	22949.8	55.12	12.20	22.06	6.38	9.95	72.35	110.74	38.39
7.600	0.767	0.1009	27293.7	47.15	10.97	28.05	6.79	12.20	63.15	111.19	47.04
	3.611	0.4751	22330.1	53.70	12.42	21.24	6.05	9.55	71.16	108.01	36.84
7.800	0.710	0.0910	26573.1	45.97	11.30	27.02	6.56	11.75	62.30	107.64	45.33
	3.343	0.4285	21740.5	52.37	12.67	20.48	5.76	9.18	70.08	105.49	35.42
8.000	0.659	0.0823	25886.4	44.86	11.64	26.06	6.35	11.34	61.54	105.29	43.75
	3.101	0.3876	21178.7	51.10	12.95	19.76	5.50	8.84	69.09	104.19	34.10
8.200	0.612	0.0747	25230.9	43.81	12.00	25.15	6.17	10.96	60.85	104.13	42.28
	2.882	0.3515	20642.4	49.90	13.25	19.08	5.27	8.52	68.19	101.06	32.87
8.400	0.570	0.0679	24604.3	42.81	12.39	24.28	6.02	10.61	60.23	101.14	40.91
	2.684	0.3195	20129.8	48.77	13.58	18.43	5.07	8.23	67.38	99.11	31.73
8.600	0.532	0.0619	24004.4	41.87	12.79	23.47	5.89	10.28	59.69	99.32	39.64
	2.504	0.2912	19639.0	47.69	13.93	17.82	4.90	7.95	66.65	97.32	30.67
8.800	0.497	0.0565	23429.2	40.97	13.21	22.70	5.78	9.97	59.21	97.65	38.44
	2.340	0.2659	19168.4	46.66	14.30	17.25	4.74	7.69	65.99	95.67	29.68
9.000	0.465	0.0517	22877.0	40.11	13.64	21.96	5.69	9.68	58.79	96.12	37.33
	2.190	0.2434	18716.6	45.69	14.69	16.70	4.60	7.45	65.41	94.16	28.75
9.200	0.436	0.0474	22346.1	39.30	14.10	21.26	5.61	9.41	58.43	94.71	36.28
	2.054	0.2232	18282.2	44.76	15.10	16.17	4.48	7.23	64.90	93.78	27.88
9.400	0.410	0.0436	21834.9	38.52	14.57	20.60	5.55	9.15	58.13	93.42	35.30
	1.929	0.2052	17864.0	43.88	15.53	15.68	4.37	7.02	64.45	91.51	27.06
9.600	0.385	0.0401	21342.2	37.79	15.06	19.97	5.49	8.91	57.88	92.25	34.37
	1.814	0.1889	17460.9	43.04	15.98	15.20	4.27	6.82	64.06	90.35	26.29
9.800	0.363	0.0370	20866.5	37.09	15.56	19.36	5.45	8.68	57.68	91.18	33.49
	1.708	0.1743	17071.7	42.25	16.45	14.75	4.19	6.63	63.73	89.29	25.57
10.000	0.342	0.0342	20406.8	36.42	16.09	18.78	5.42	8.47	57.54	90.20	32.66
	1.659	0.1659	16448.1	41.91	17.00	14.03	4.04	6.32	63.94	88.33	24.39
10.200	0.323	0.0317	19961.9	35.79	16.61	18.22	5.39	8.26	57.44	89.31	31.88
	1.567	0.1537	16089.6	41.18	17.50	13.62	3.97	6.16	63.72	87.46	23.75
10.400	0.306	0.0294	19530.9	35.18	17.16	17.69	5.37	8.07	57.38	88.51	31.13
	1.482	0.1425	15742.2	40.48	18.02	13.23	3.91	6.00	63.54	86.67	23.14
10.6C0	0.289	0.0273	19112.8	34.61	17.73	17.18	5.36	7.89	57.37	87.79	30.42
	1.403	0.1324	15405.2	39.82	18.55	12.85	3.86	5.85	63.41	85.97	22.56
10.800	0.274	0.0254	18706.9	34.06	18.31	16.69	5.35	7.71	57.40	87.15	29.74
	1.331	0.1232	15078.0	39.19	19.11	12.49	3.81	5.70	63.33	85.34	22.00
11.000	0.261	0.0237	18312.2	33.54	18.90	16.21	5.34	7.54	57.48	86.58	29.10
	1.263	0.1148	14759.9	38.60	19.67	12.14	3.77	5.57	63.30	84.78	21.48
11.200	0.248	0.0221	17928.1	33.05	19.51	15.75	5.34	7.38	57.59	85.07	28.48
	1.200	0.1072	14450.3	38.03	20.25	11.81	3.73	5.44	63.31	84.29	20.97
11.400	0.236	0.0207	17554.0	32.58	20.13	15.31	5.34	7.23	57.74	85.63	27.88
	1.142	0.1002	14148.7	37.49	20.85	11.48	3.70	5.31	63.37	83.86	20.49
11.600	0.224	0.0193	17189.1	32.13	20.76	14.88	5.35	7.08	57.93	85.24	27.31
	1.088	0.0938	13854.6	36.97	21.46	11.17	3.67	5.19	63.47	83.50	20.02

TABLE 4-1 (Cont)

11.800	0.214	0.0181	16832.9	31.71	21.41	14.47	5.35	6.94	58.16	84.92	26.76
	1.038	0.0879	13567.6	36.49	22.09	10.86	3.64	5.08	63.61	83.19	19.58
12.800	0.204	0.0170	16485.0	31.31	22.07	14.07	5.36	6.80	58.42	84.64	26.23
	0.991	0.0826	13287.2	36.03	22.73	10.57	3.62	4.96	63.79	82.94	19.15
12.200	0.195	0.0160	16144.8	30.93	22.75	13.68	5.36	6.67	58.71	84.42	25.71
	0.947	0.0776	13012.9	35.59	23.39	10.28	3.59	4.86	64.01	82.74	18.73
12.400	0.187	0.0151	15811.9	30.57	23.44	13.31	5.37	6.54	59.04	84.25	25.21
	0.906	0.0731	12744.6	35.17	24.06	10.00	3.57	4.75	64.27	82.60	18.33
12.600	0.179	0.0142	15485.9	30.23	24.14	12.94	5.37	6.41	59.40	84.13	24.72
	0.842	0.0669	12669.6	34.44	24.70	9.93	3.65	4.75	64.17	82.50	18.33
12.800	0.172	0.0134	15166.3	29.91	24.85	12.59	5.37	6.29	59.80	84.05	24.25
	0.808	0.0631	12408.2	34.07	25.40	9.66	3.63	4.65	64.51	82.45	17.94
13.000	0.165	0.0127	14853.0	29.61	25.58	12.24	5.37	6.17	60.23	84.01	23.78
	0.775	0.0596	12151.8	33.73	26.11	9.40	3.61	4.55	64.88	82.44	17.57
13.200	0.158	0.0120	14545.5	29.33	26.32	11.91	5.37	6.05	60.68	84.02	23.33
	0.745	0.0564	11900.3	33.41	26.84	9.15	3.60	4.46	65.28	82.48	17.20
13.400	0.152	0.0113	14243.6	29.06	27.08	11.58	5.37	5.93	61.17	84.06	22.89
	0.716	0.0534	11653.3	33.10	27.58	8.90	3.58	4.37	65.72	82.56	16.84
13.600	0.146	0.0108	13947.0	28.81	27.84	11.26	5.37	5.82	61.69	84.14	22.45
	0.689	0.0507	11410.6	32.82	28.34	8.66	3.56	4.28	66.19	82.69	16.49
13.800	0.141	0.0102	13655.6	28.58	28.62	10.95	5.36	5.71	62.24	84.26	22.02
	0.664	0.0481	11172.2	32.56	29.11	8.42	3.54	4.19	66.70	82.85	16.15
14.000	0.136	0.0097	13369.1	28.36	29.42	10.65	5.35	5.60	62.82	84.41	21.60
	0.640	0.0457	10937.8	32.31	29.89	8.20	3.52	4.10	67.23	83.05	15.81
14.200	0.131	0.0092	13087.3	28.17	30.22	10.36	5.33	5.49	63.42	84.60	21.18
	0.600	0.0422	10869.2	31.76	30.65	8.13	3.60	4.11	67.44	83.28	15.84
14.400	0.127	0.0088	12810.2	27.98	31.04	10.07	5.32	5.39	64.05	84.83	20.77
	0.579	0.0402	10639.0	31.55	31.46	7.91	3.58	4.02	68.04	83.55	15.51
14.600	0.123	0.0084	12537.4	27.81	31.87	9.79	5.30	5.28	64.71	85.08	20.37
	0.560	0.0384	10412.5	31.36	32.28	7.69	3.56	3.94	68.67	83.86	15.18
14.800	0.119	0.0080	12269.0	27.66	32.71	9.52	5.27	5.18	65.40	85.37	19.96
	0.542	0.0366	10189.6	31.19	33.11	7.48	3.53	3.85	69.34	84.20	14.86
15.000	0.115	0.0077	12004.9	27.52	33.57	9.25	5.24	5.07	66.12	85.68	19.57
	0.525	0.0350	9970.2	31.03	33.96	7.27	3.50	3.77	70.03	84.57	14.55
15.200	0.111	0.0073	11744.9	27.39	34.43	8.99	5.21	4.97	66.86	86.03	19.17
	0.493	0.0325	9902.5	30.58	34.79	7.21	3.59	3.78	70.40	84.98	14.58
15.400	0.108	0.0070	11488.9	27.28	35.31	8.74	5.18	4.87	67.63	86.41	18.78
	0.479	0.0311	9686.7	30.45	35.66	7.01	3.56	3.70	71.15	85.41	14.26
15.600	0.105	0.0067	11237.0	27.18	36.21	8.49	5.14	4.77	68.42	86.81	18.39
	0.465	0.0298	9474.3	30.34	36.55	6.81	3.52	3.62	71.92	86.88	13.95
15.800	0.102	0.0065	10989.1	27.09	37.11	8.25	5.10	4.67	69.24	87.25	18.01
	0.438	0.0277	9406.8	29.94	37.41	6.75	3.60	3.62	72.39	96.37	13.98
16.000	0.099	0.0062	10745.1	27.02	38.03	8.01	5.05	4.57	70.08	87.71	17.63
	0.426	0.0266	9197.9	29.86	38.33	6.56	3.57	3.54	73.22	86.89	13.67
16.200	0.097	0.0060	10505.0	26.96	38.96	7.78	5.00	4.47	70.95	88.20	17.25
	0.414	0.0256	8992.4	29.80	39.25	6.37	3.53	3.46	74.08	87.45	13.36
16.400	0.094	0.0057	10268.8	26.91	39.90	7.55	4.95	4.38	71.84	88.72	16.88
	0.391	0.0238	8925.1	29.45	40.16	6.31	3.60	3.47	74.64	88.03	13.39
16.600	0.092	0.0055	10036.4	26.87	40.85	7.33	4.89	4.28	72.76	89.26	16.50
	0.381	0.0229	8723.2	29.41	41.11	6.13	3.56	3.39	75.55	88.63	13.08

TABLE 4-1 (Cont)

FINE DIVISION RUN

H= 12000.0 IN-LB-SEC ONE WATT = 1.000 LB

RADIUS	THICK.	T/R	RPM	WHEEL	HOUSING	BEARING	WINDAGE	MOTOR	ACTUAL W	EQUIV. W	LOSS	
12.500	0.183	0.0146	15648.0	30.40	23.79	13.12	5.37	6.47	59.22	84.18	24.96	
	0.886	0.0709	12612.5	34.98	24.40	9.87	3.56	4.70	64.41	82.54	18.13	
12.600	0.179	0.0142	15485.9	30.23	24.14	12.94	5.37	6.41	59.40	84.13	24.72	
	0.842	0.0669	12669.6	34.44	24.70	9.93	3.65	4.75	64.17	82.50	18.33	
12.700	0.175	0.0138	15325.3	30.07	24.49	12.76	5.37	6.35	59.60	84.08	24.48	
	0.825	0.0649	12538.3	34.25	25.05	9.79	3.64	4.70	64.33	82.47	18.13	
12.800	0.172	0.0134	15166.3	29.91	24.85	12.59	5.37	6.29	59.80	84.05	24.25	
	0.808	0.0631	12408.2	34.07	25.40	9.66	3.63	4.65	64.51	82.45	17.94	✓
12.900	0.168	0.0130	15008.9	29.76	25.22	12.41	5.37	6.23	60.01	84.02	24.01	
	0.791	0.0613	12279.4	33.90	25.76	9.53	3.62	4.60	64.69	82.44	17.75	MIN. WT.
13.000	0.165	0.0127	14853.0	29.61	25.58	12.24	5.37	6.17	60.23	84.01	23.78	
	0.775	0.0596	12151.8	33.73	26.11	9.40	3.61	4.55	64.88	82.44	17.57	
13.100	0.161	0.0123	14698.5	29.47	25.95	12.07	5.37	6.11	60.45	84.01	23.56	G
	0.760	0.0580	12025.5	33.56	26.48	9.27	3.60	4.51	65.08	82.46	17.38	
13.200	0.158	0.0120	14545.5	29.33	26.32	11.91	5.37	6.05	60.68	84.02	23.33	
	0.745	0.0564	11900.3	33.41	26.84	9.15	3.60	4.46	65.28	82.48	17.20	
13.300	0.155	0.0117	14393.9	29.19	26.70	11.74	5.37	5.99	60.92	84.03	23.11	
	0.730	0.0549	11776.2	33.25	27.21	9.02	3.59	4.41	65.50	82.52	17.02	
13.400	0.152	0.0113	14243.6	29.06	27.08	11.58	5.37	5.93	61.17	84.06	22.89	
	0.716	0.0534	11653.3	33.10	27.58	8.90	3.58	4.37	65.72	82.56	16.84	
13.500	0.149	0.0111	14094.7	28.93	27.46	11.42	5.37	5.88	61.43	84.10	22.67	
	0.702	0.0520	11531.4	32.96	27.96	8.78	3.57	4.32	65.95	82.62	16.67	

TABLE 4-2

COMPUTER SELECTED SIZES, WEIGHTS AND SPEED OF THE FLYWHEEL

MINIMUM EQUIVALENT WEIGHT DESIGN

Angular Momentum (H) ft-lb-sec	Wheel Size, in.				Weight, lb			Speed rpm	Power Loss Watts
	Radius	Dia	(ℓ) Rim	(t) Disc	Flywheel	Housing	Assembly		
200	9.4	18.8	.957	.109	15.1	14.2	33.9	9,368	10.0
250	9.85	19.7	.933	.113	16.7	15.5	36.8	9,742	10.8
300	10.2	20.4	.922	.118	18.2	16.5	39.4	10,089	11.4
350	10.45	20.9	.927	.124	19.7	17.3	41.7	10,446	12.2
400	10.8	21.6	.882	.126	20.8	18.4	43.9	10,703	12.8
450	11.0	22.0	.899	.132	22.3	19.1	46.1	10,873	13.2
500	11.2	22.4	.888	.137	23.4	19.7	47.95	11,153	13.8
600	11.7	23.4	.843	.142	25.6	21.4	51.8	11,410	14.7
700	12.0	24.0	.849	.150	28.0	22.5	55.4	11,661	15.4
800	12.3	24.6	.843	.158	30.2	23.6	58.7	11,862	16.2
900	12.6	25.2	.827	.163	32.2	24.7	61.9	12,035	16.9
1000	12.9	25.8	.791	.168	33.9	25.8	64.7	12,279	17.9
1100	13.1	26.2	.800	.175	36.1	26.6	67.7	12,367	18.2
1200	13.3	26.6	.779	.182	37.8	27.3	70.2	12,630	19.2
1300	13.6	27.2	.762	.183	39.5	28.5	73.2	12,575	19.5
1400	13.7	27.4	.773	.192	41.6	28.9	75.7	12,750	20.1
1500	13.9	27.8	.764	.196	43.3	29.7	78.4	12,803	20.6
1600	14.1	28.2	.752	.200	45.0	30.5	80.9	12,852	21.1
1700	14.3	28.6	.738	.204	46.6	31.4	83.3	12,900	21.6
1800	14.4	28.8	.750	.210	48.6	31.8	85.8	12,949	21.9
1900	14.6	29.2	.731	.213	50.0	32.6	88.1	12,994	22.4
2000	14.7	29.4	.724	.219	51.6	33.1	90.2	13,144	23.1

Configuration - Shaped Disc and Rim
Material - 4340 Steel
Bearings - 2 Ball Bearings, Size 102H

Weights are made up as follows:
Flywheel - Basic wheel
Housing - Complete Shell
Assembly - Flywheel, Housing, Bearings, Shaft, Motor

TABLE 4-2 (Cont)

H ft-lb-sec	Thickness Ratio	
	Disc (t/R)	Rim (ℓ/R)
200	.012	.100
250	.012	.095
300	.012	.090
350	.012	.089
400	.012	.082
450	.012	.082
500	.012	.079
600	.012	.072
700	.0125	.071
800	.013	.069
900	.013	.066
1000	.013	.063
1100	.013	.061
1200	.014	.059
1300	.014	.056
1400	.014	.056
1500	.014	.055
1600	.014	.053
1700	.014	.052
1800	.015	.052
1900	.015	.050
2000	.015	.049

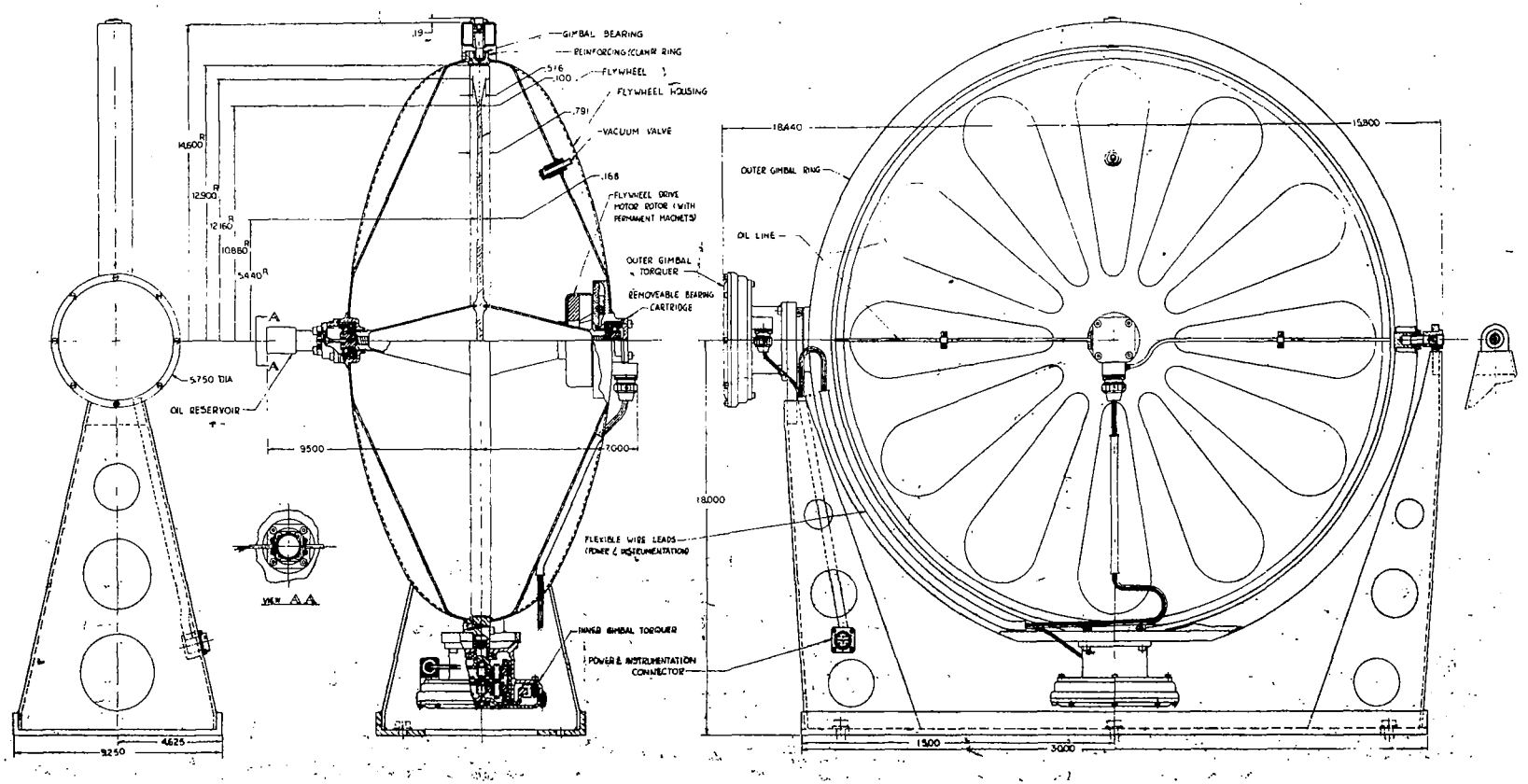

Figure 4–1. Control Moment Gyro Assembly.

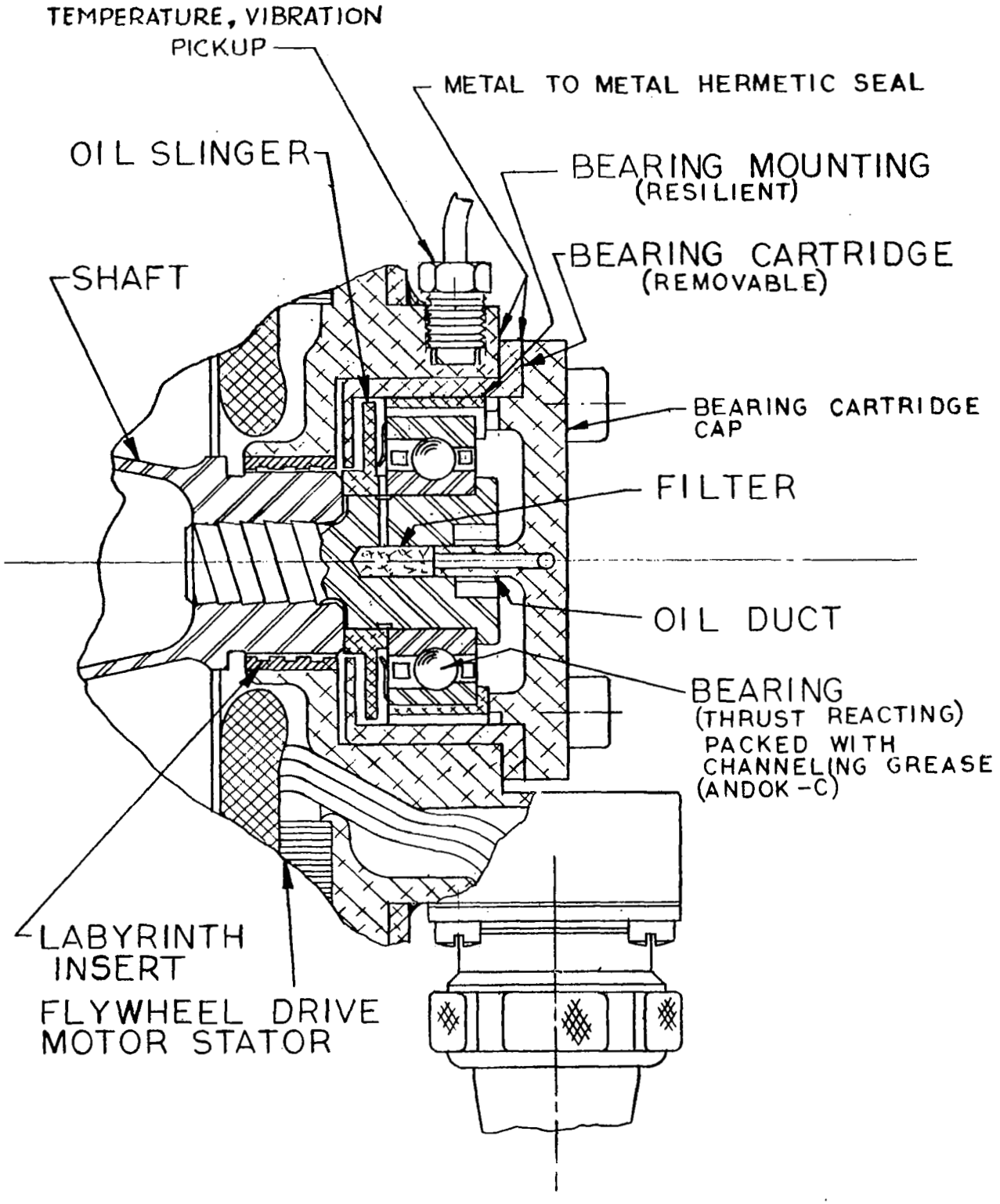

Figure 4-2. Bearing Cartridge With Oiling System

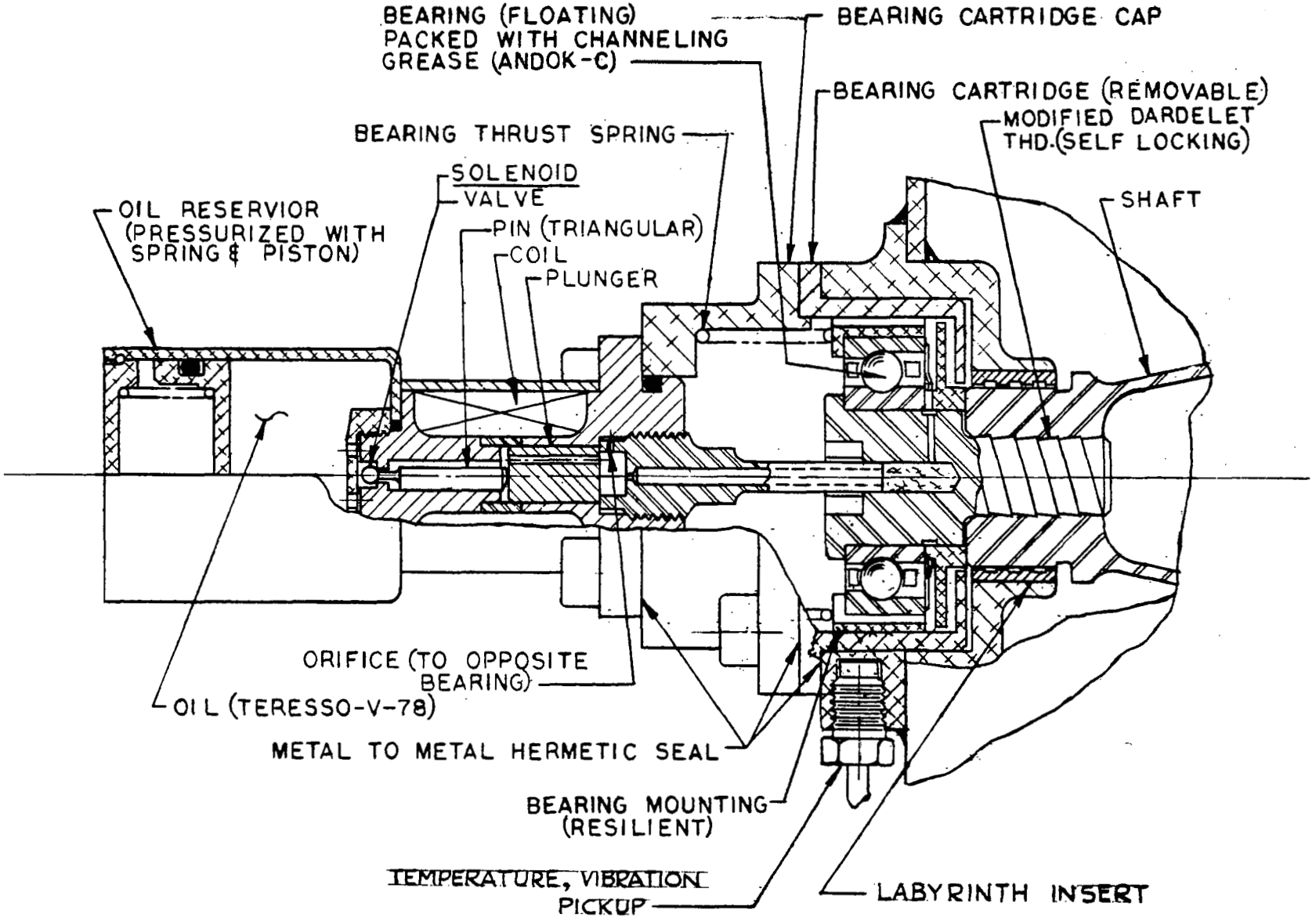

Figure 4-3. Bearing Cartridge (Motor End)

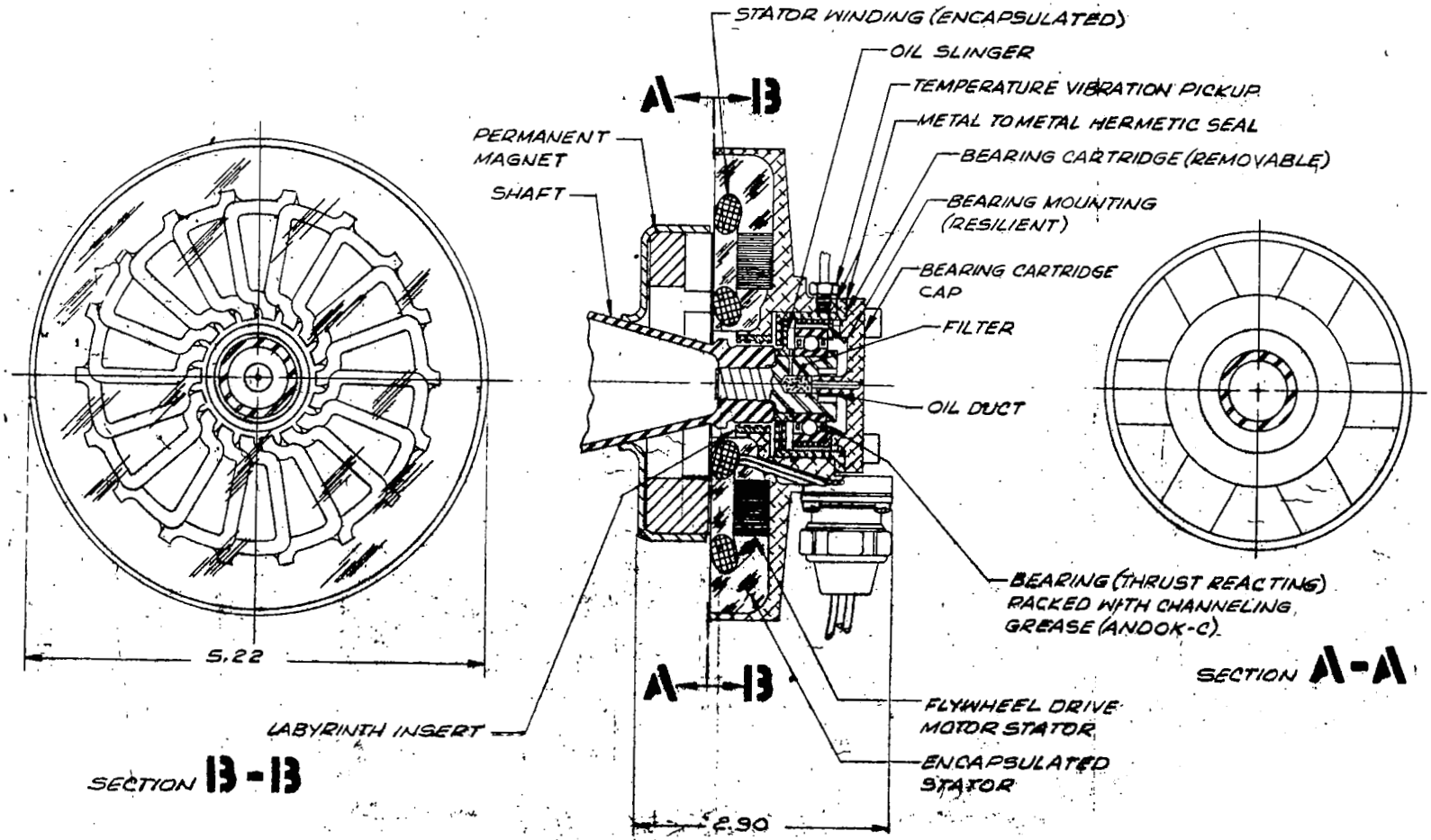

Figure 4–4. Motor and Bearing Mounting.

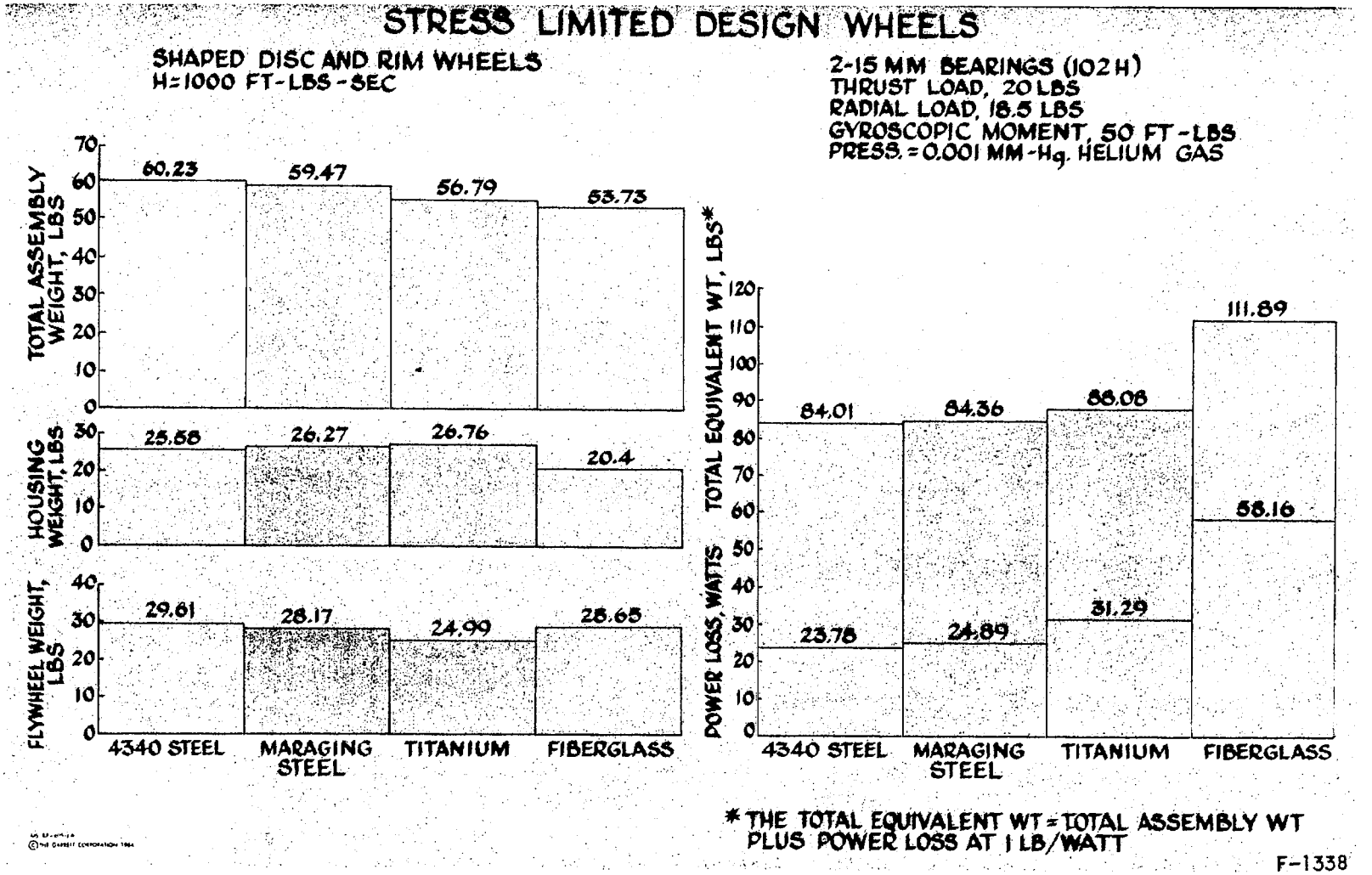

Figure 4-5. Material Selection for the Flywheel

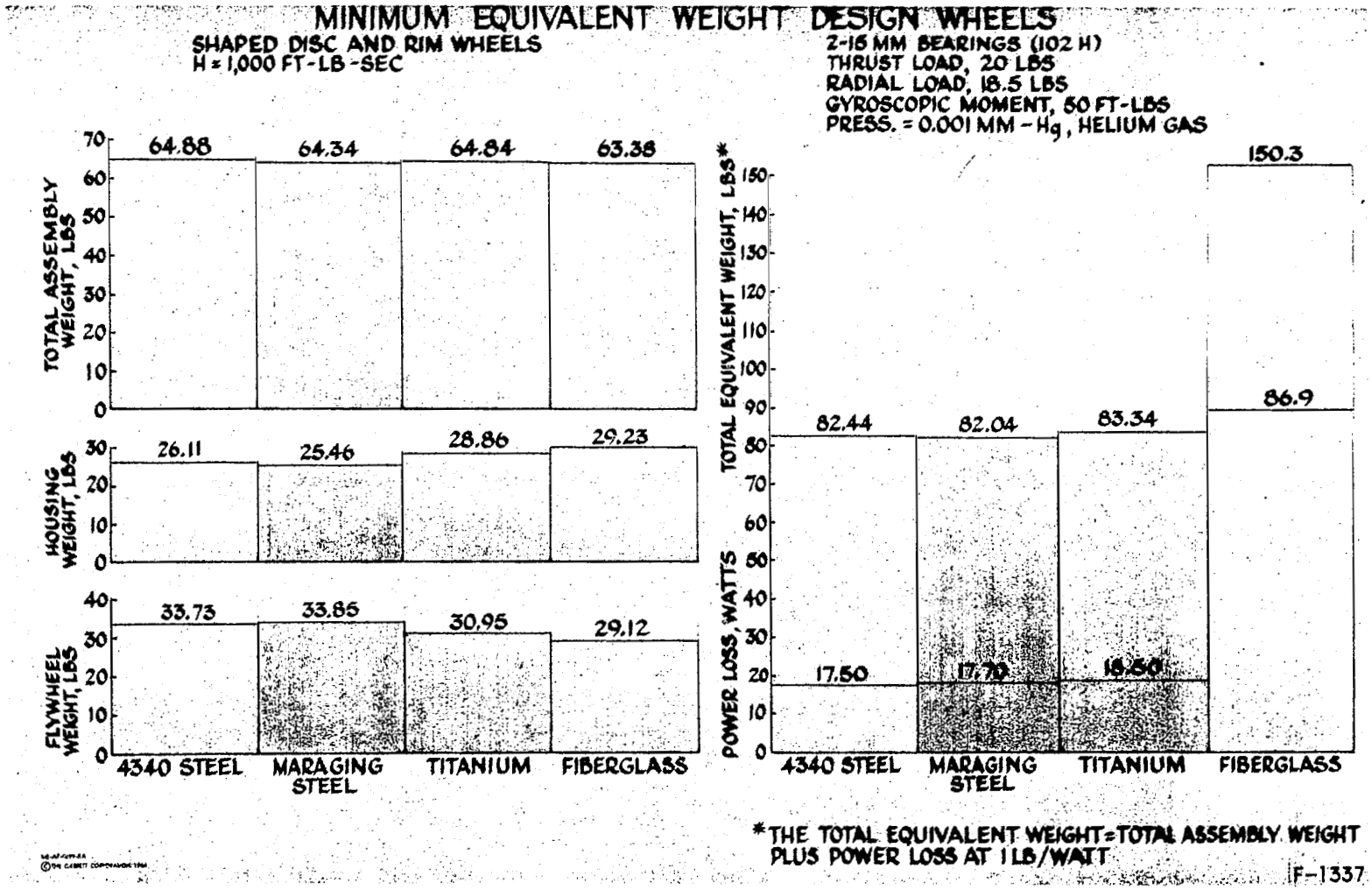

Figure 4-6. Material Selection for the Flywheel

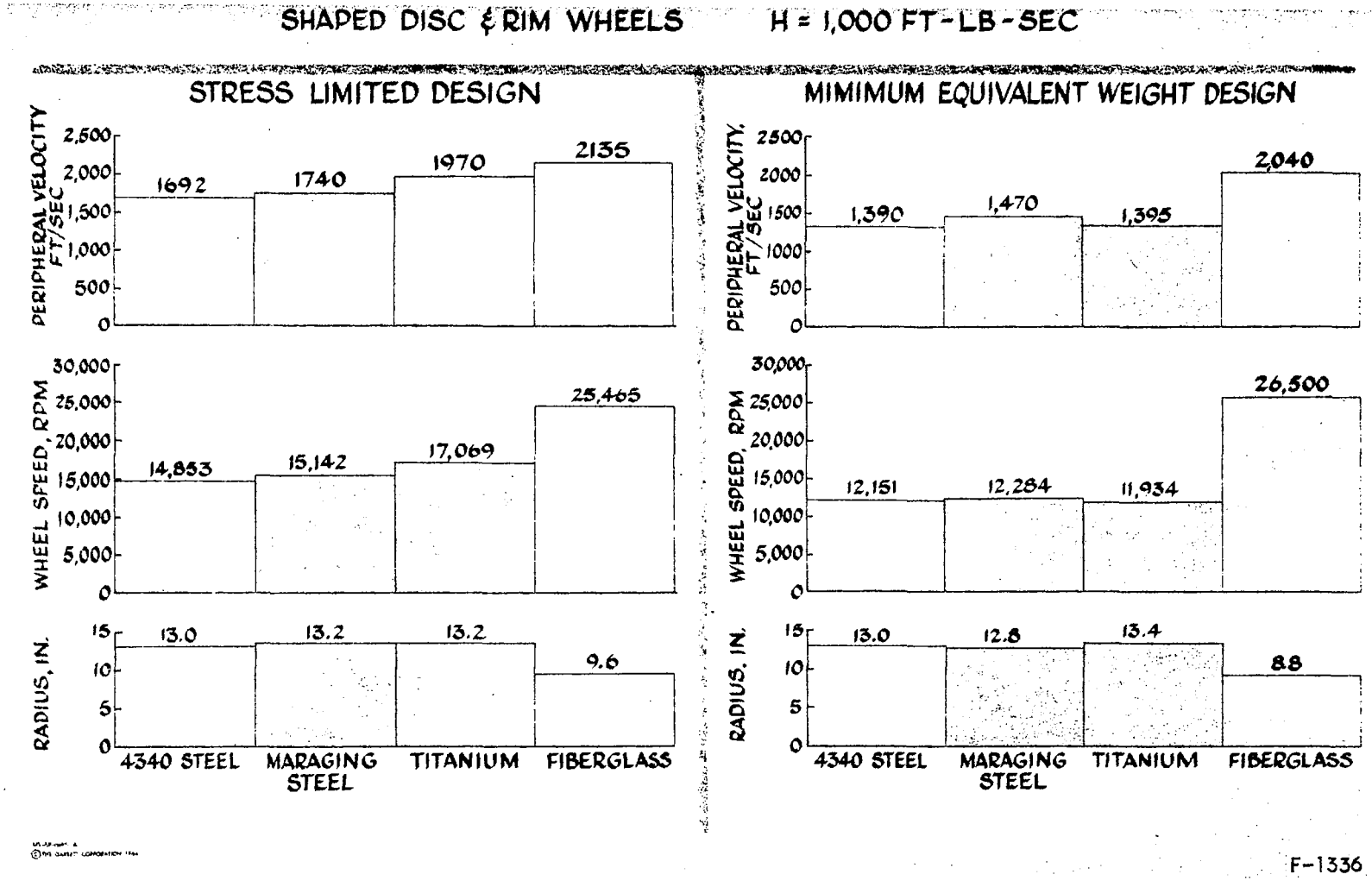

Figure 4-7. Material Selection for the Flywheel

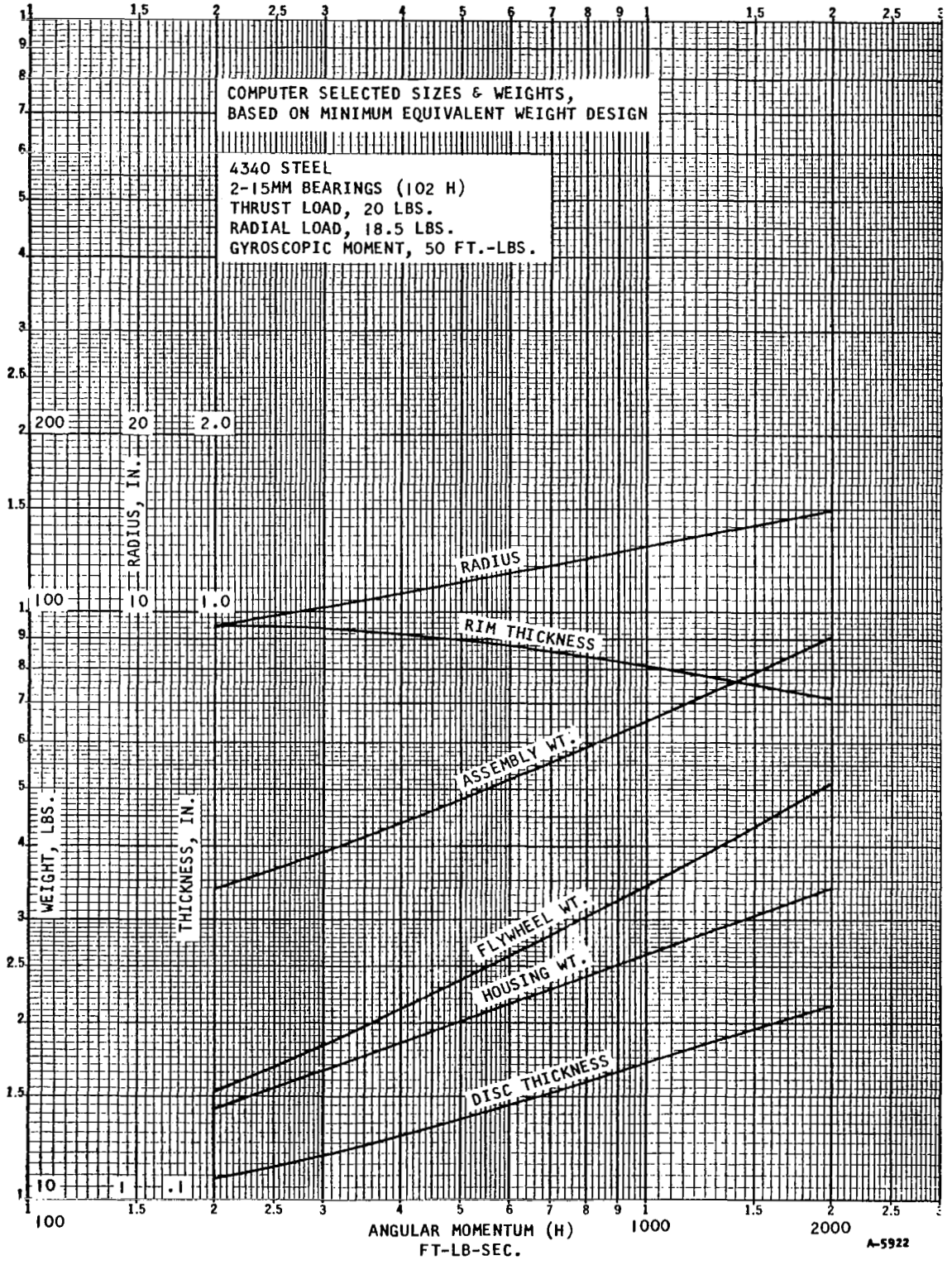

Figure 4-8. Computer Selected Sizes and Weights

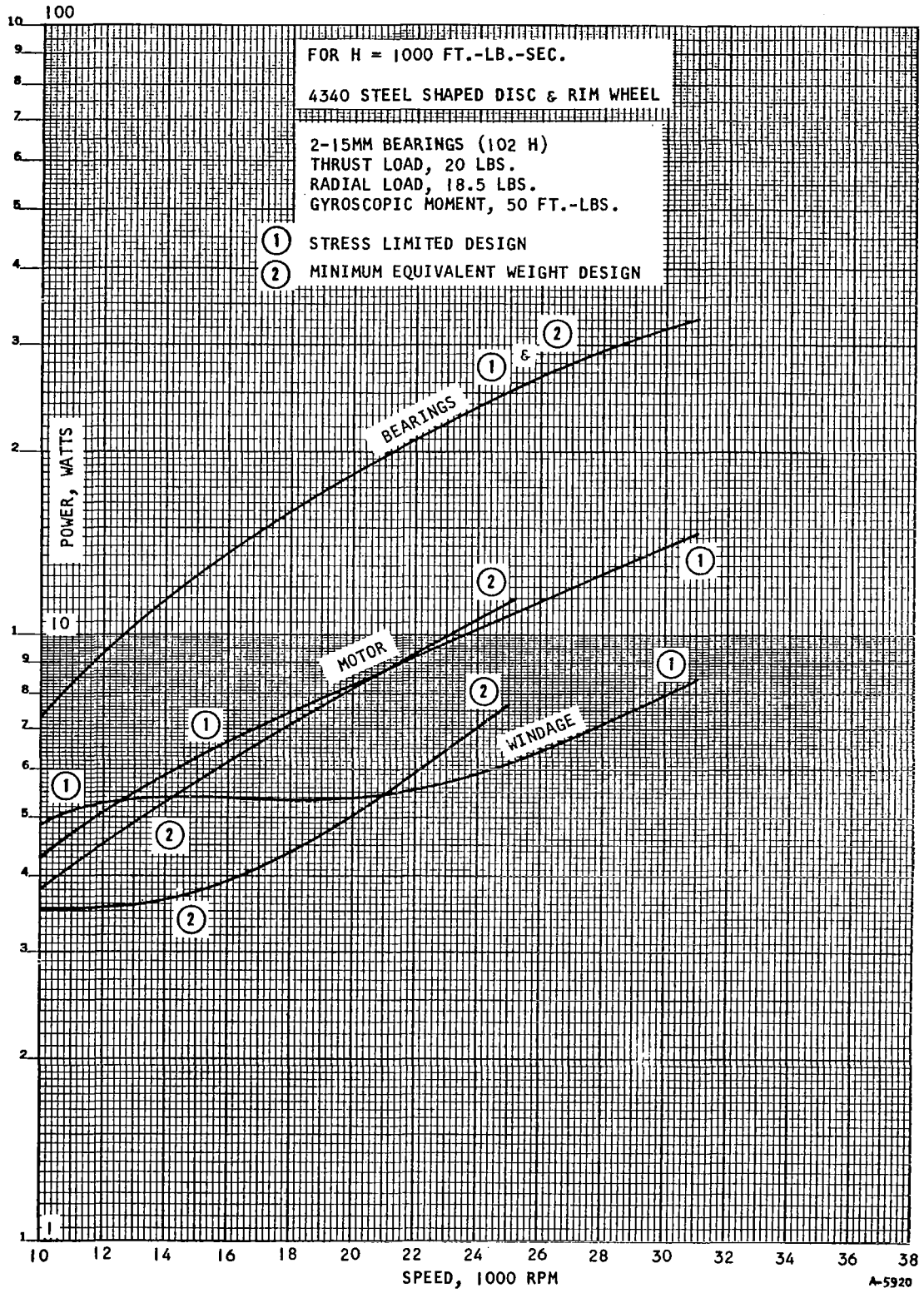

Figure 4-9. Power Loss vs Speed

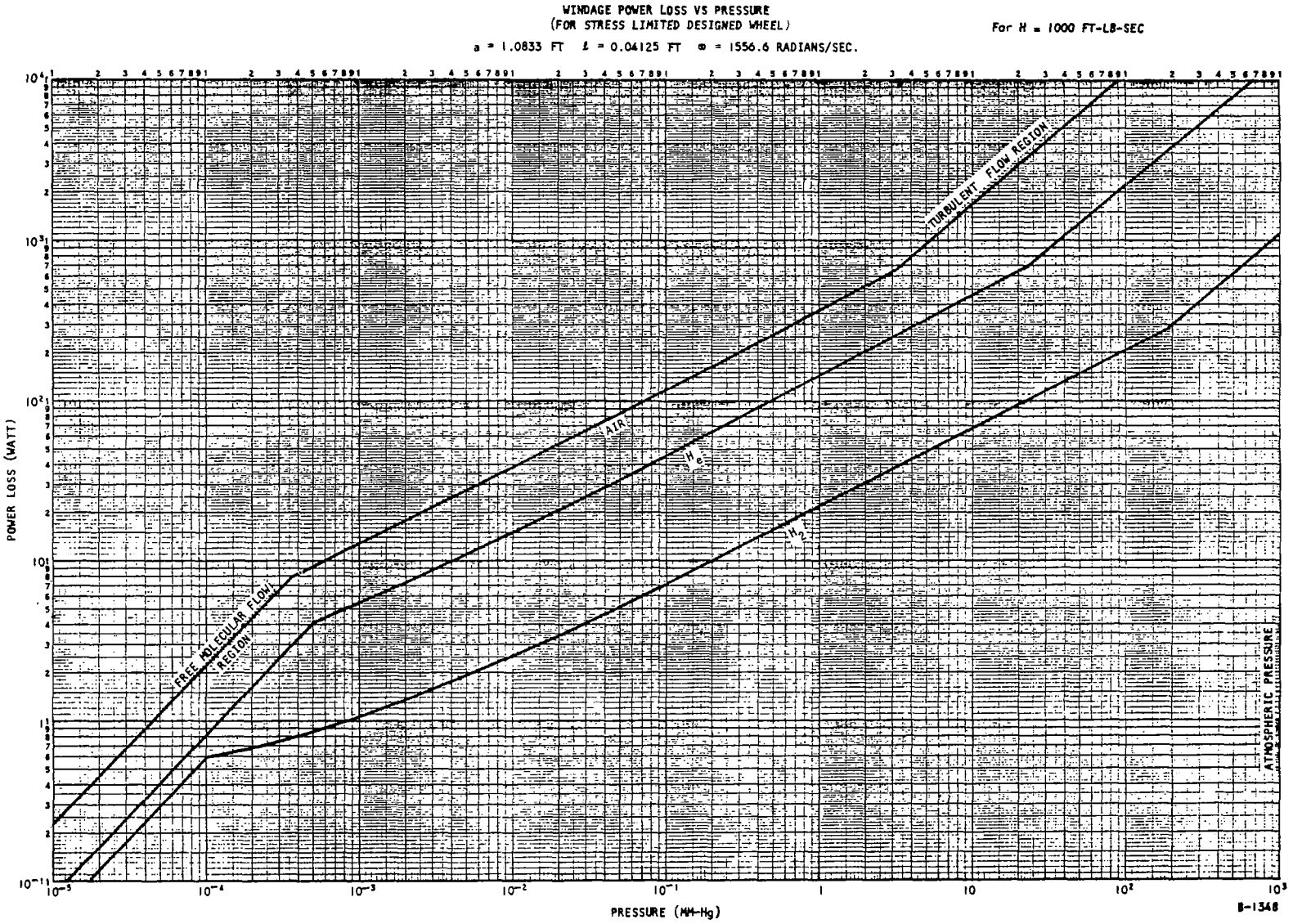

Figure 4-10. Windage Power Loss vs Pressure (Stress Limited Design)

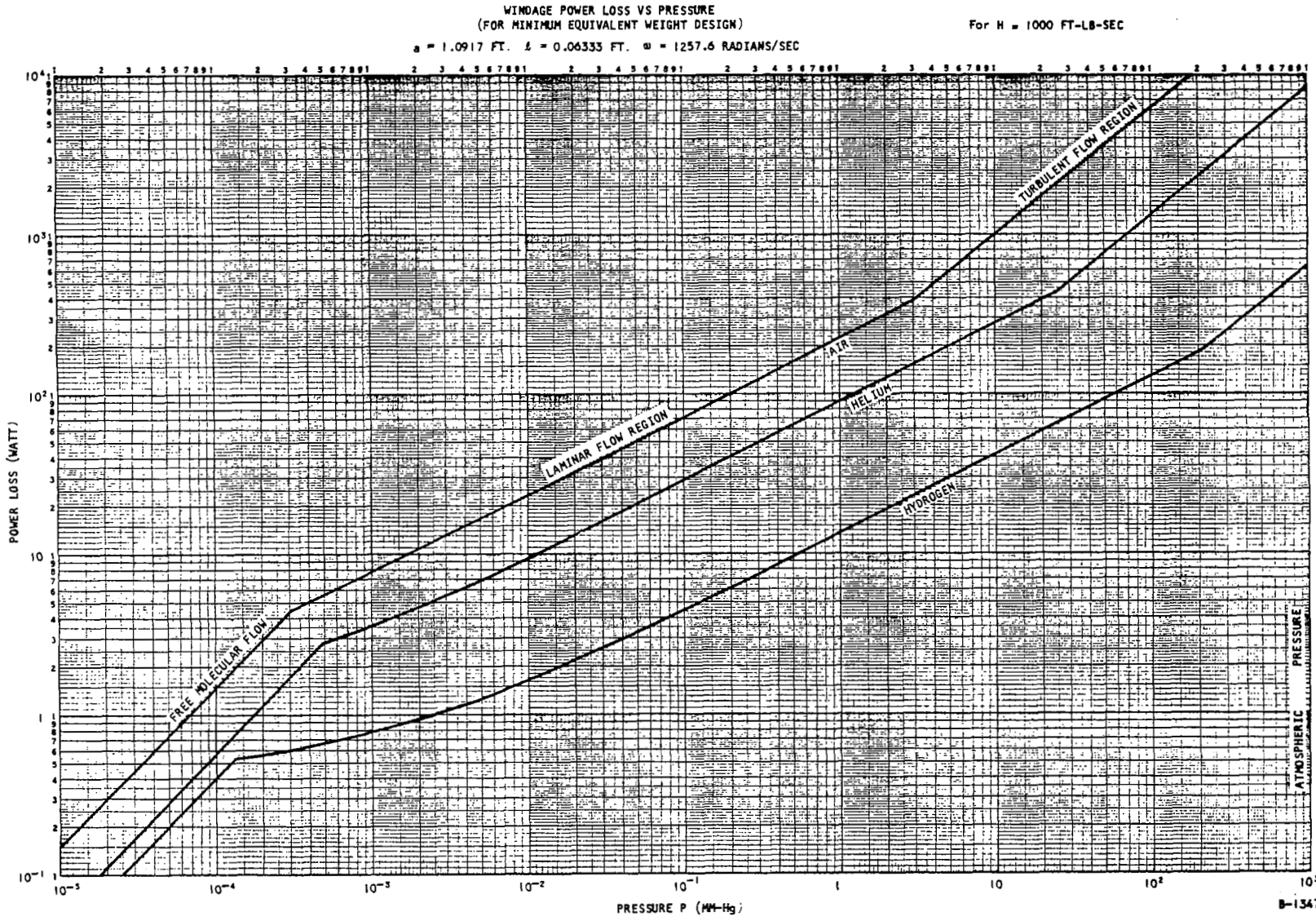

Figure 4-11. Windage Power Loss vs Pressure (Minimum Equivalent Weight Design)

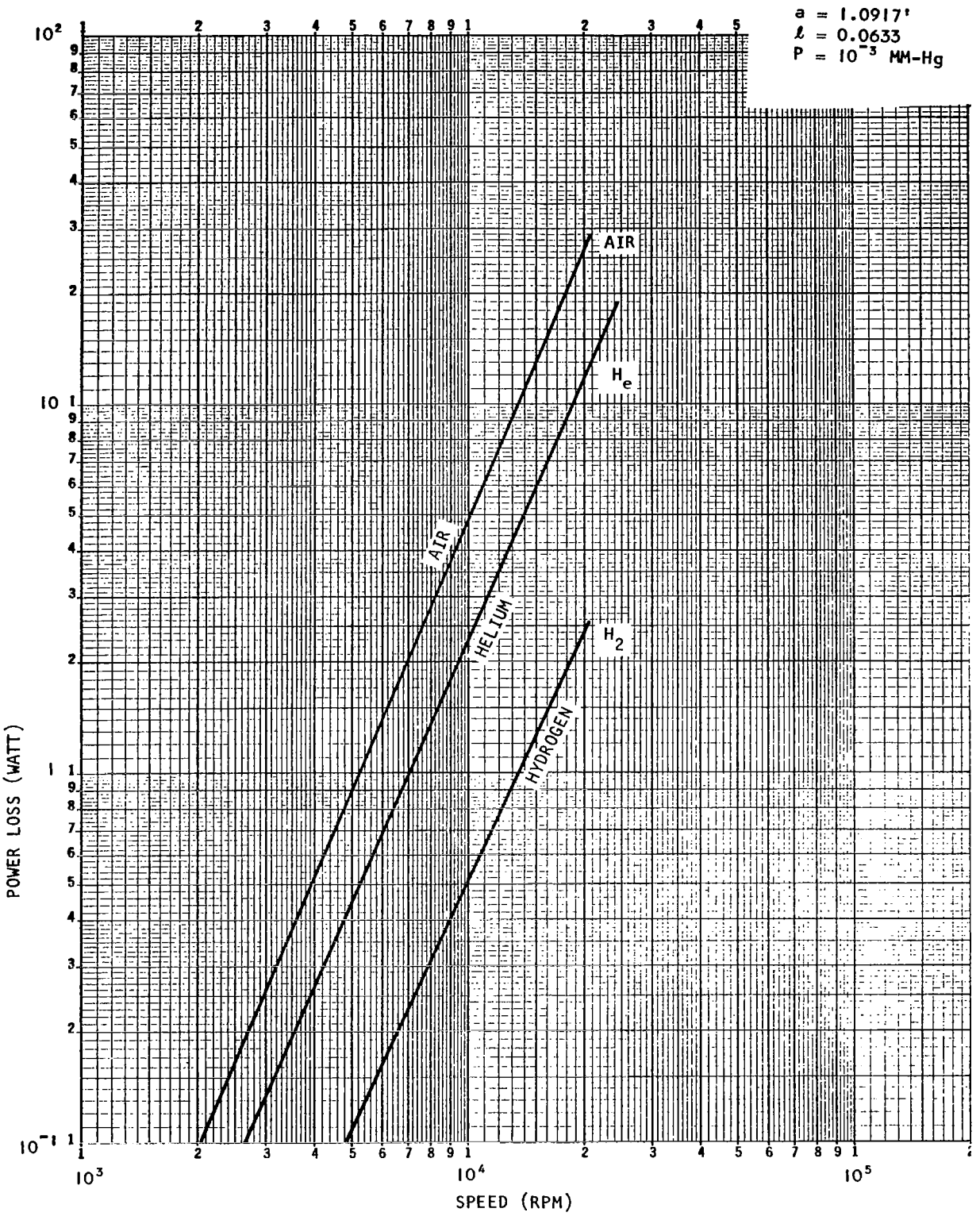

Figure 4-12. Windage Power Loss vs Speed (Minimum Equivalent Weight Designed Wheel)

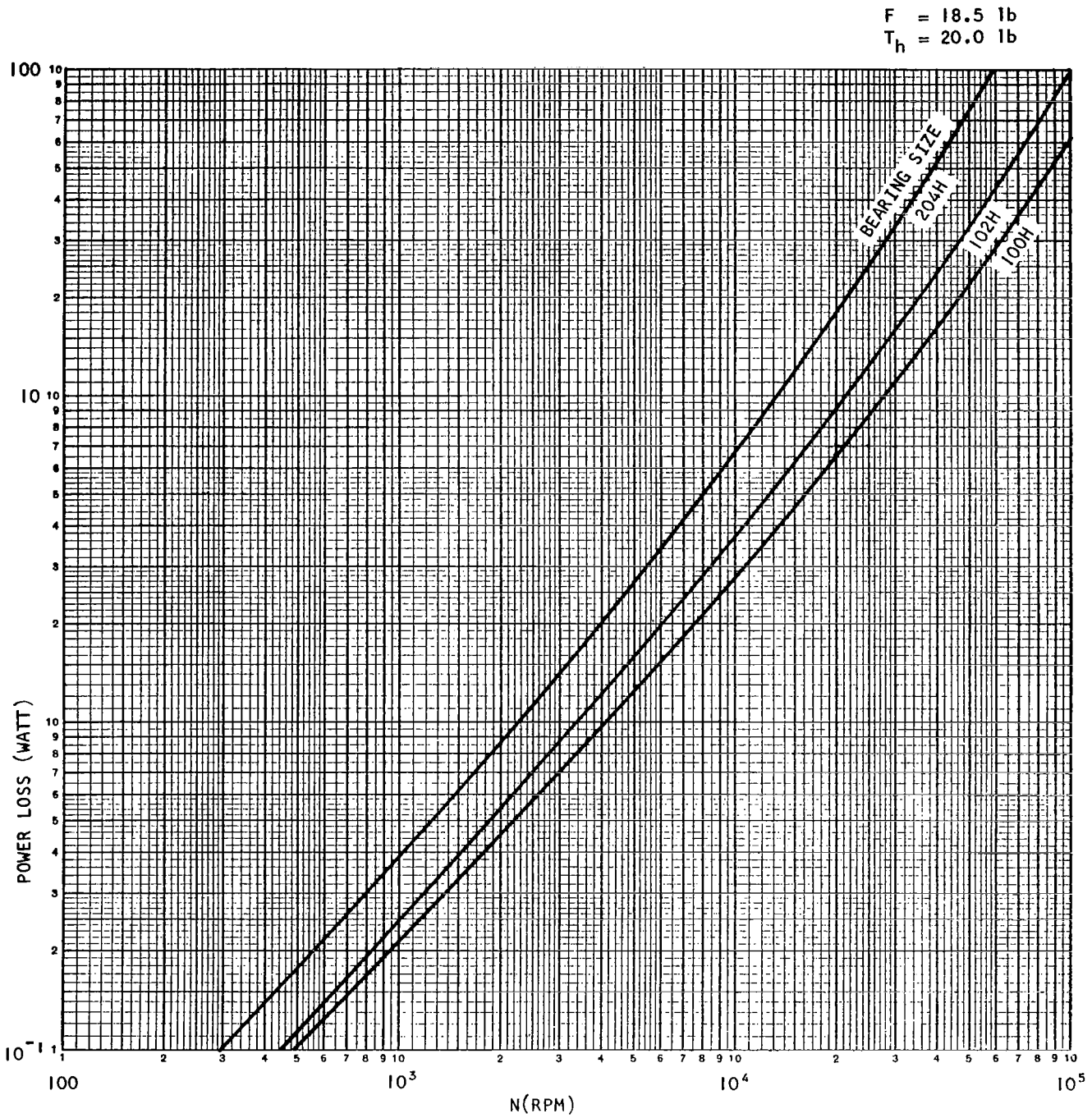

Figure 4-13. Bearing Drag - Power Loss vs Shaft Speed (Single Bearing)

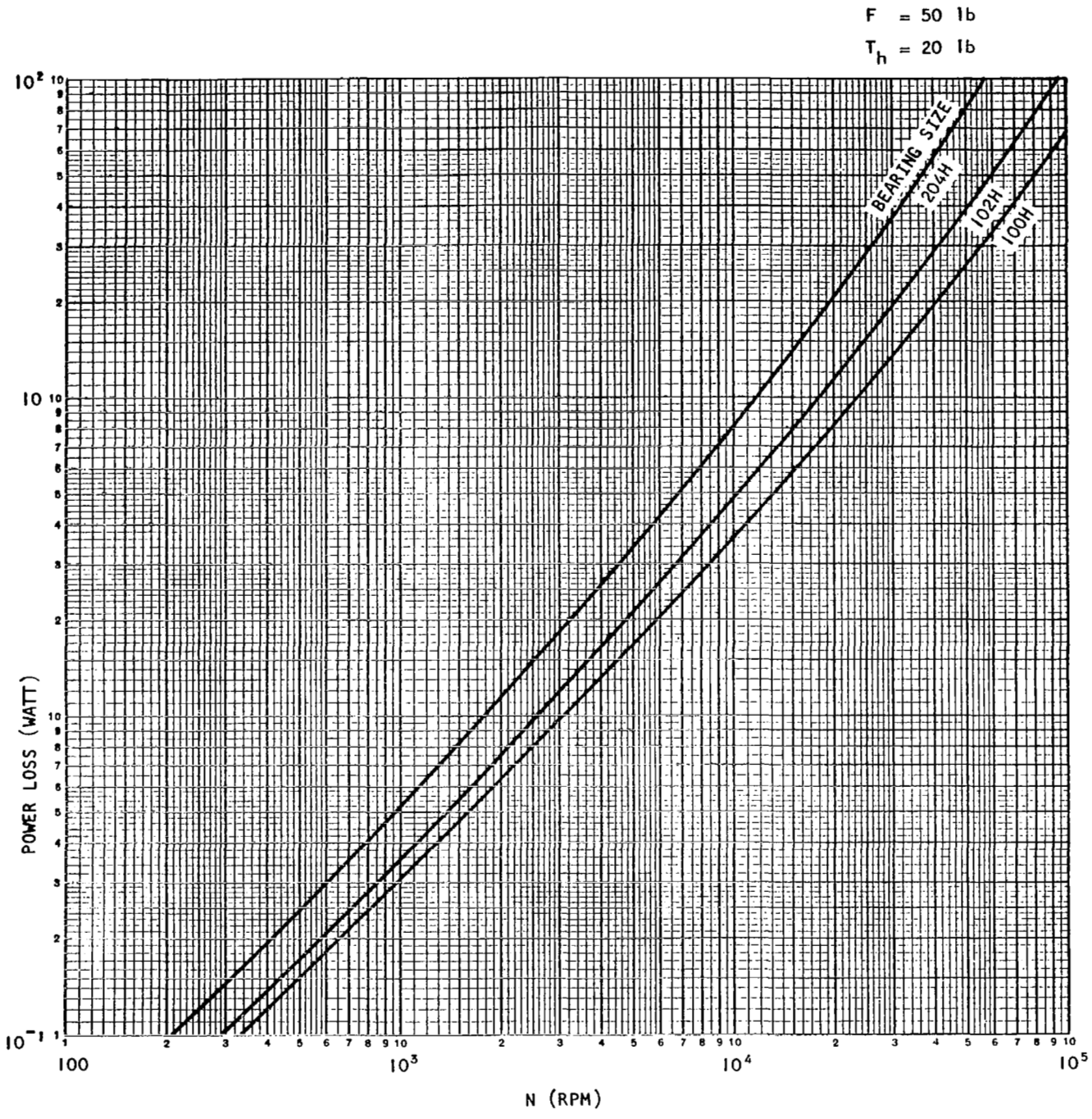

Figure 4-14. Bearing Drag - Power Loss vs Shaft Speed (Single Bearing)

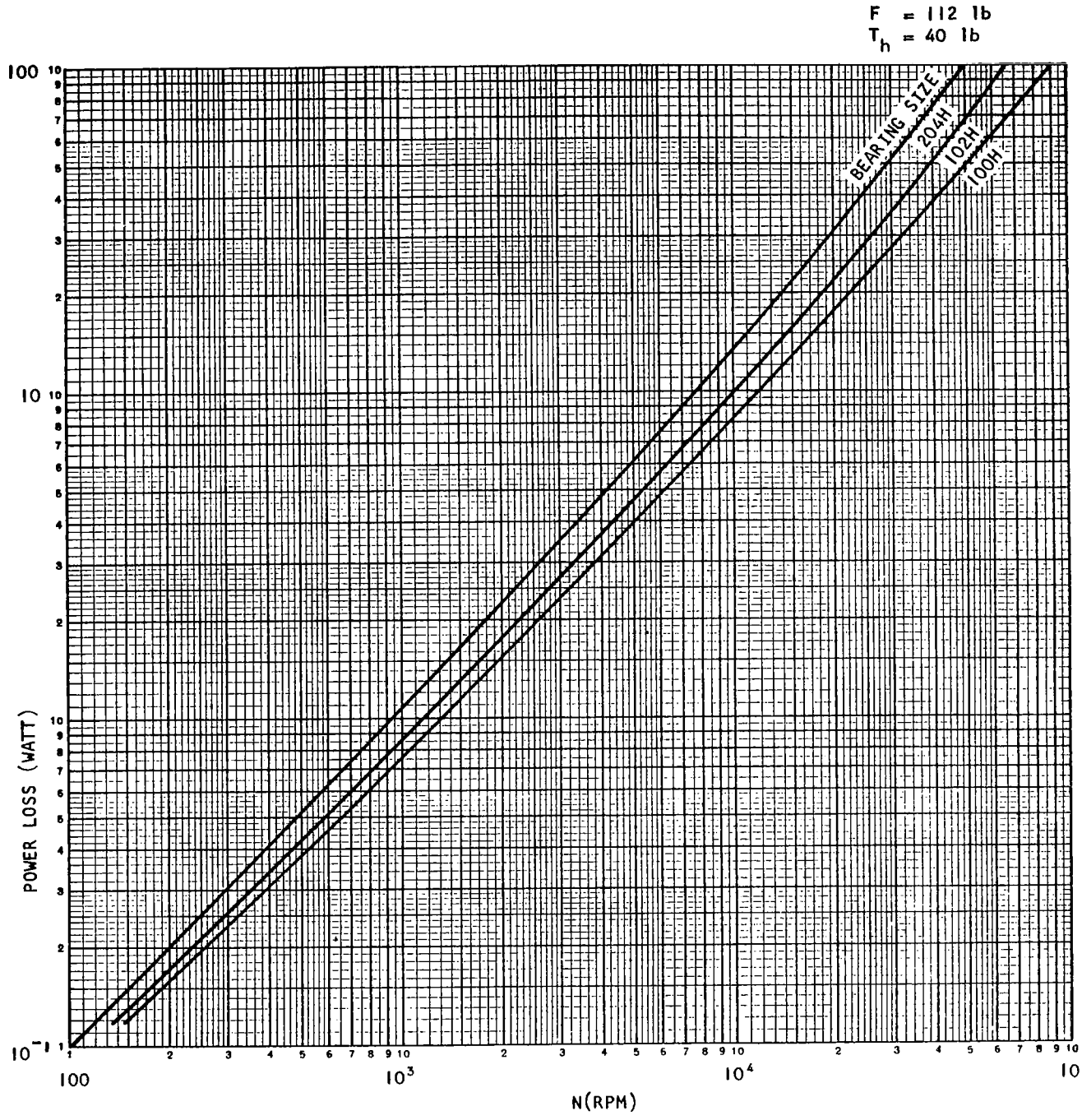

Figure 4-15. Bearing Drag - Loss vs Shaft Speed (System Bearing)

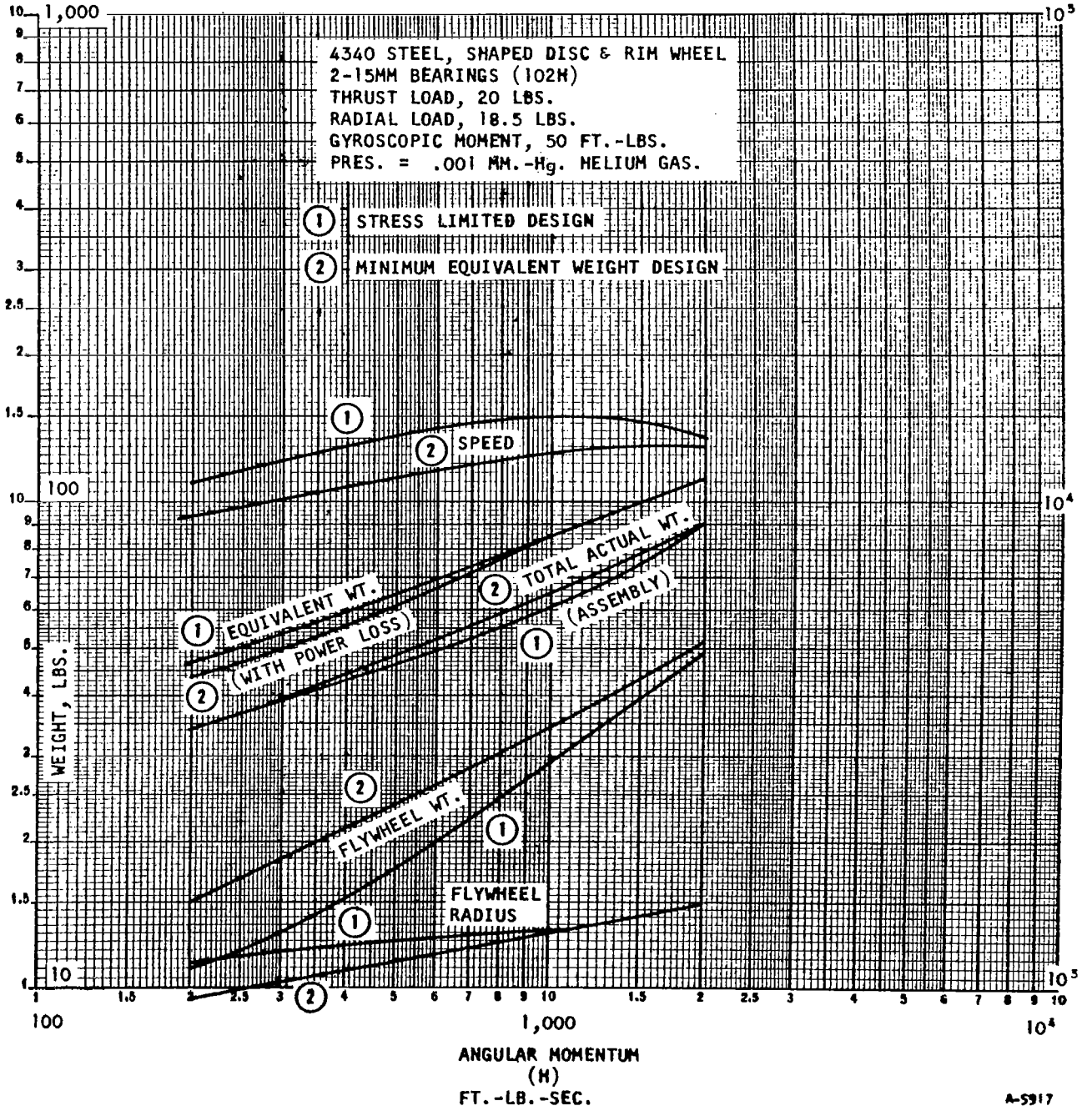

Figure 4-16. Momentum Wheel Characteristics - 4340 Steel

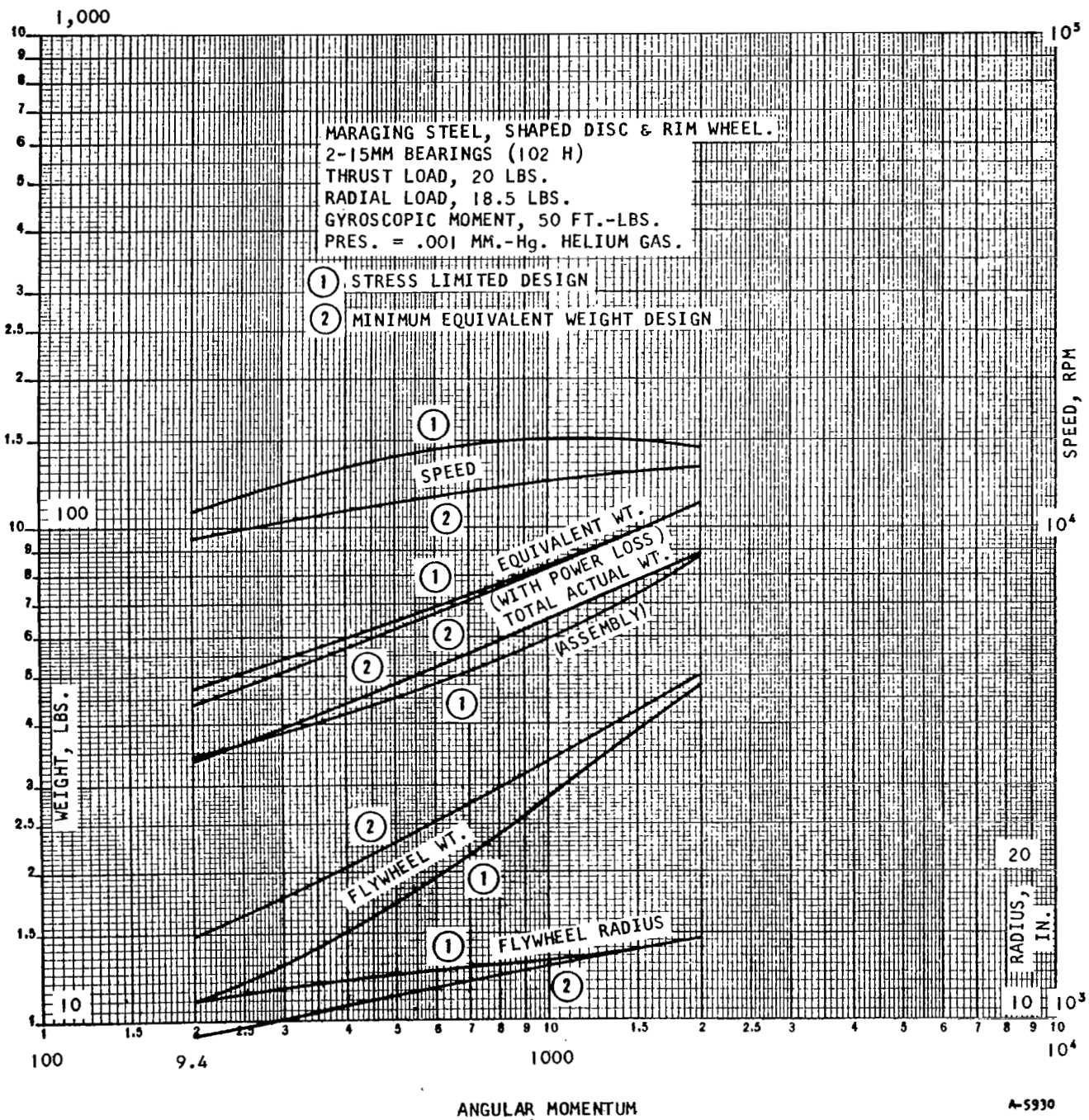

Figure 4-17. Momentum Wheel Characteristics - Maraging Steel

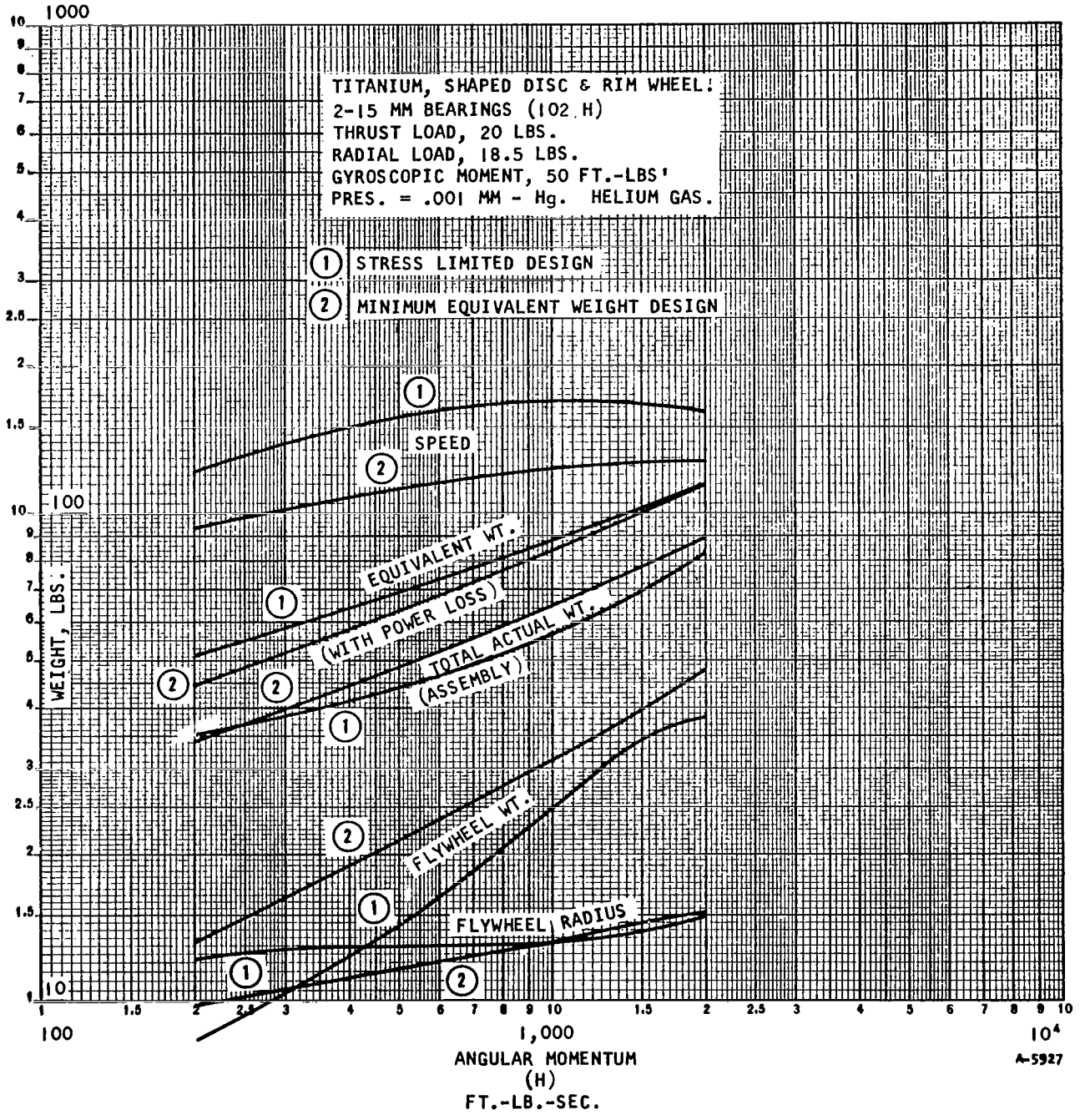

Figure 4-18. Momentum Wheel Characteristics - Titanium

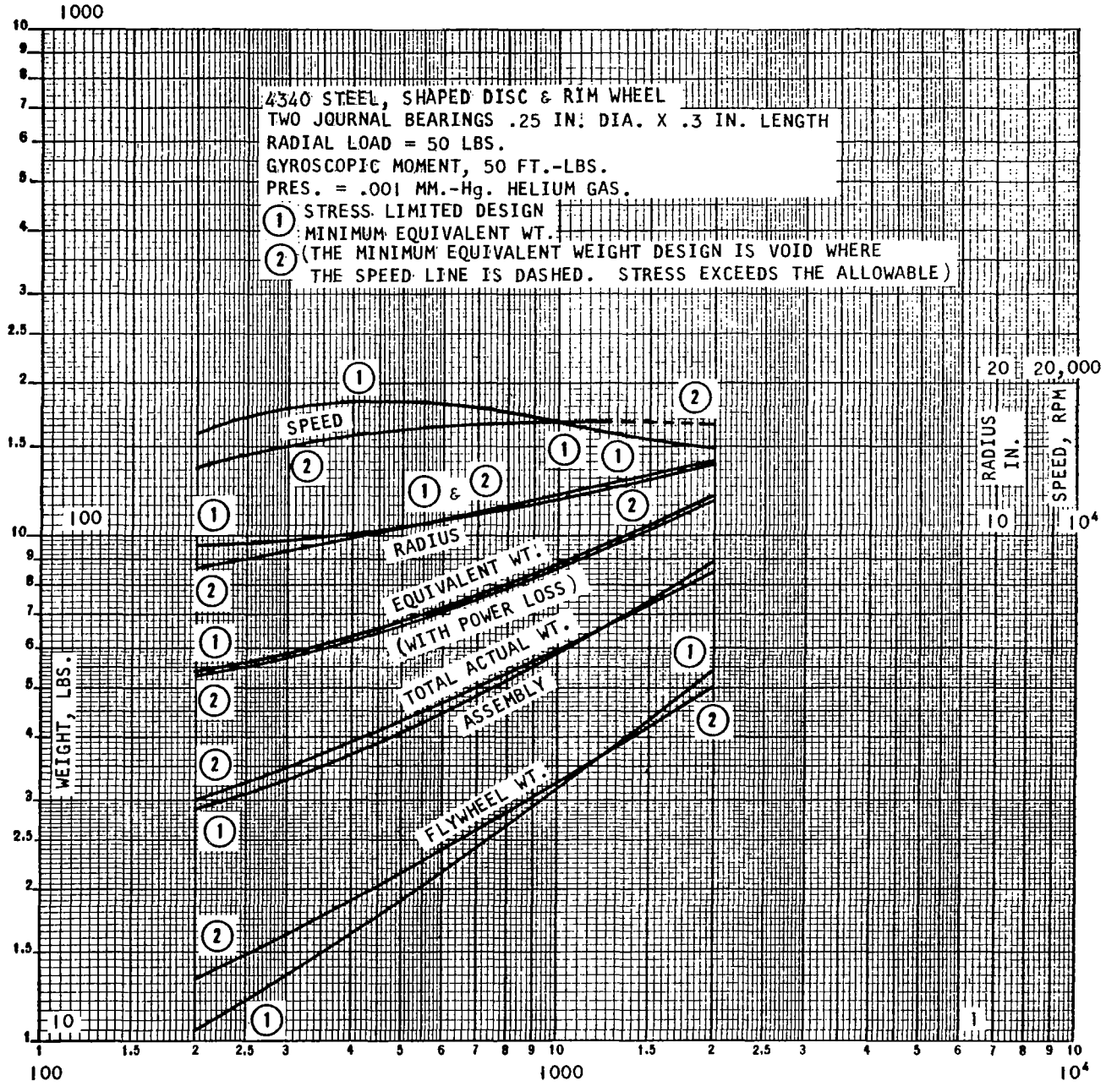
4340 STEEL, SHAPED DISC & RIM WHEEL
TWO JOURNAL BEARINGS .25 IN. DIA. X .3 IN. LENGTH
RADIAL LOAD = 50 LBS.
GYROSCOPIC MOMENT, 50 FT.-LBS.
PRES. = .001 MM.-Hg. HELIUM GAS.
(1) STRESS LIMITED DESIGN
MINIMUM EQUIVALENT WT.
(2) (THE MINIMUM EQUIVALENT WEIGHT DESIGN IS VOID WHERE THE SPEED LINE IS DASHED. STRESS EXCEEDS THE ALLOWABLE)
SPEED
RADIUS
EQUIVALENT WT. (WITH POWER LOSS)
TOTAL ACTUAL WT. ASSEMBLY
FLYWHEEL WT.
WEIGHT, LBS.
RADIUS IN.
SPEED, RPM
ANGULAR MOMENTUM (H) FT.-LB.-SEC.
A-5923

FIGURE 4-19

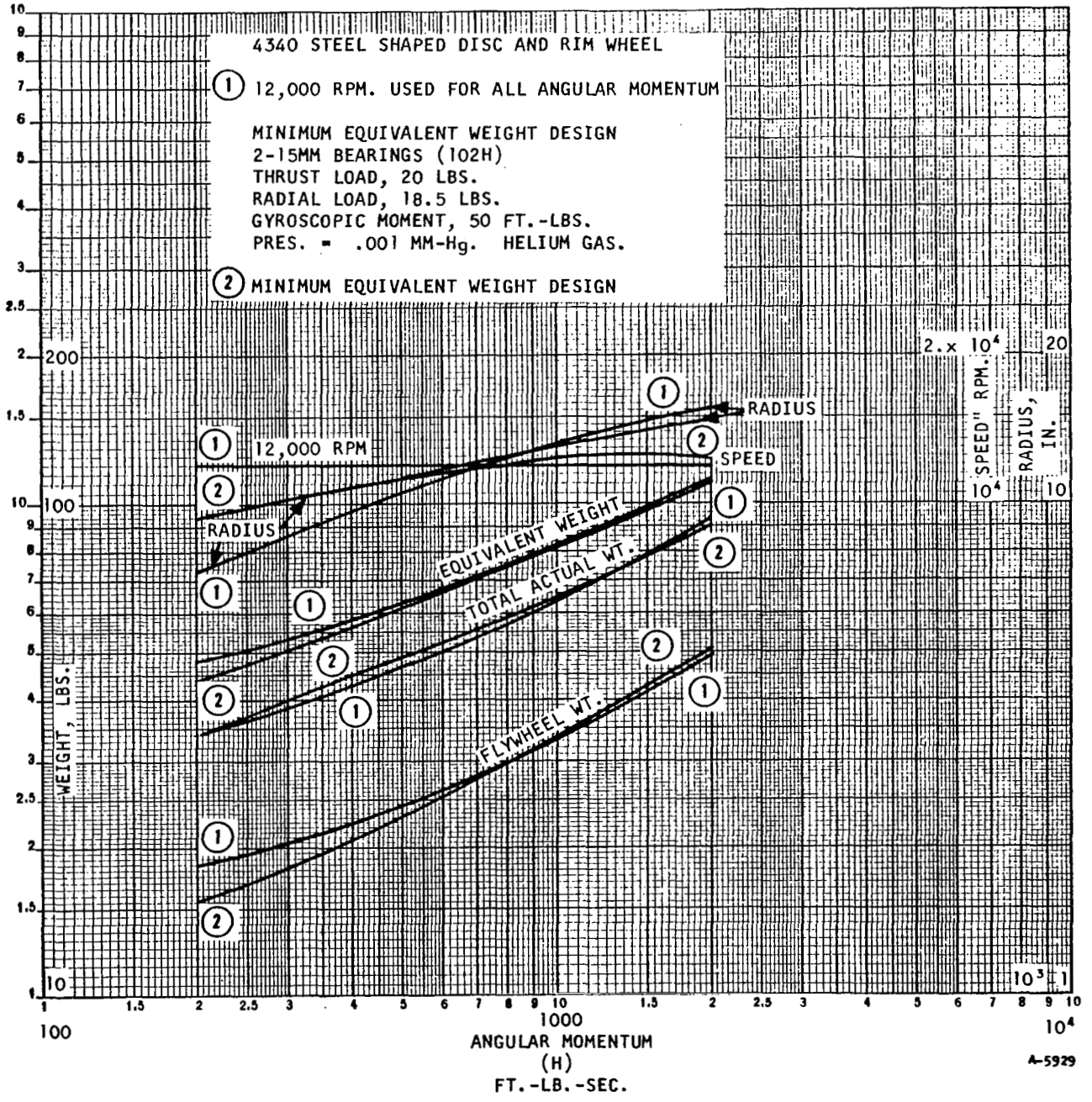

Figure 4-20. Speed Effect on Momentum Wheel - 4340 Steel

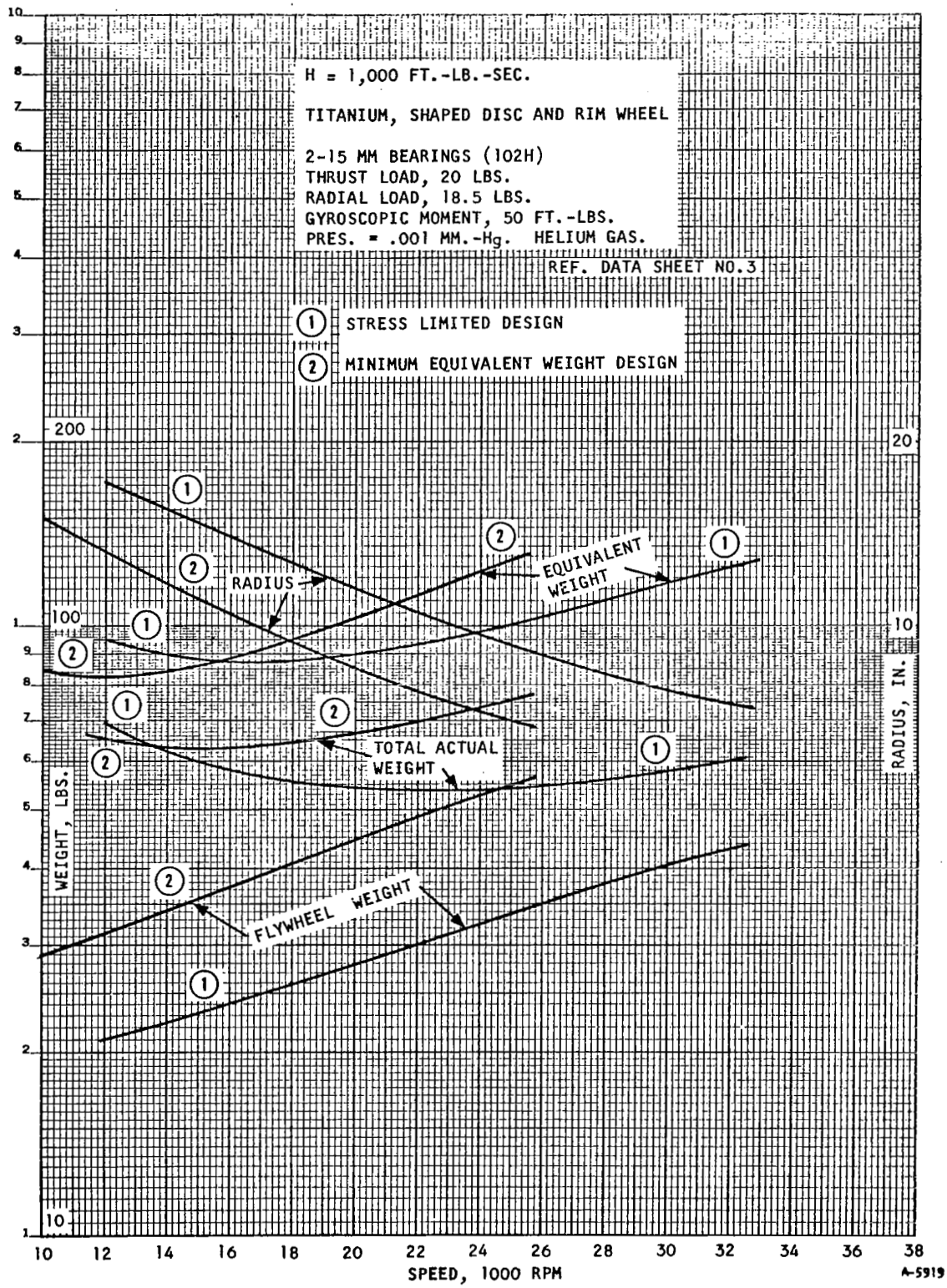

Figure 4-21. Speed Effect on Momentum Wheel - Titanium

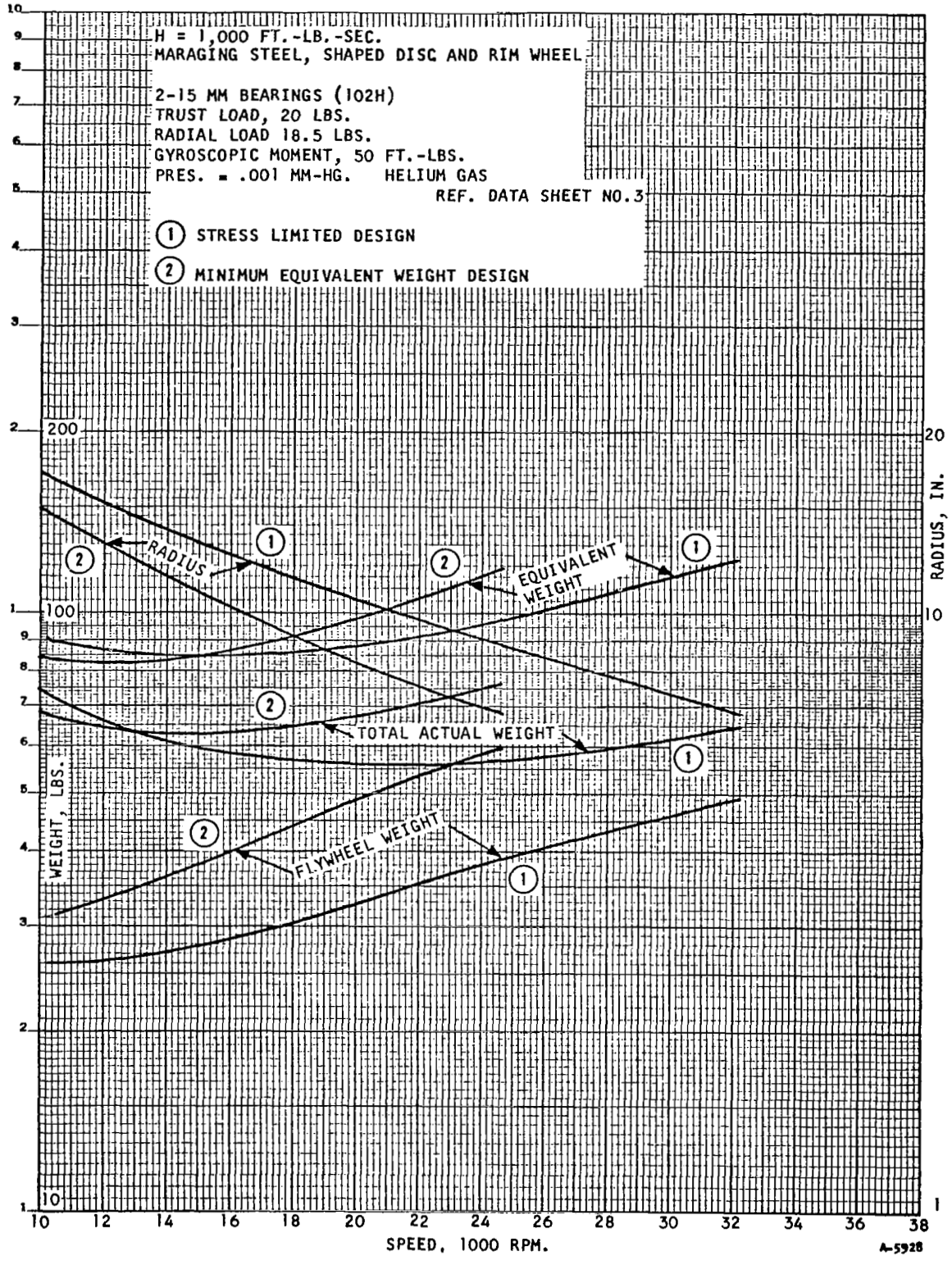

Figure 4-22. Speed Effect on Momentum Wheel - Maraging Steel

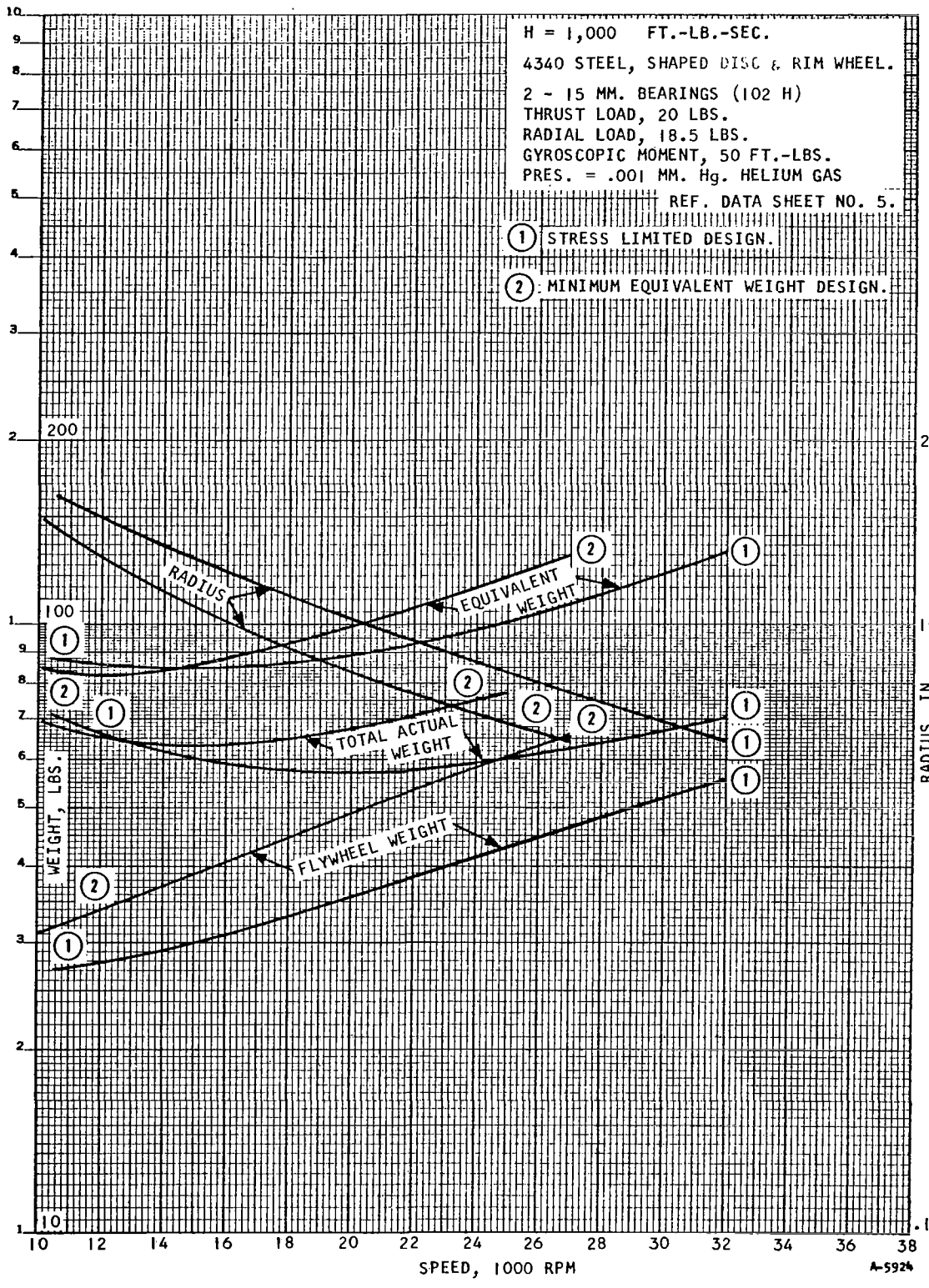

Figure 4-23. Wheel Weight and Size vs Speed

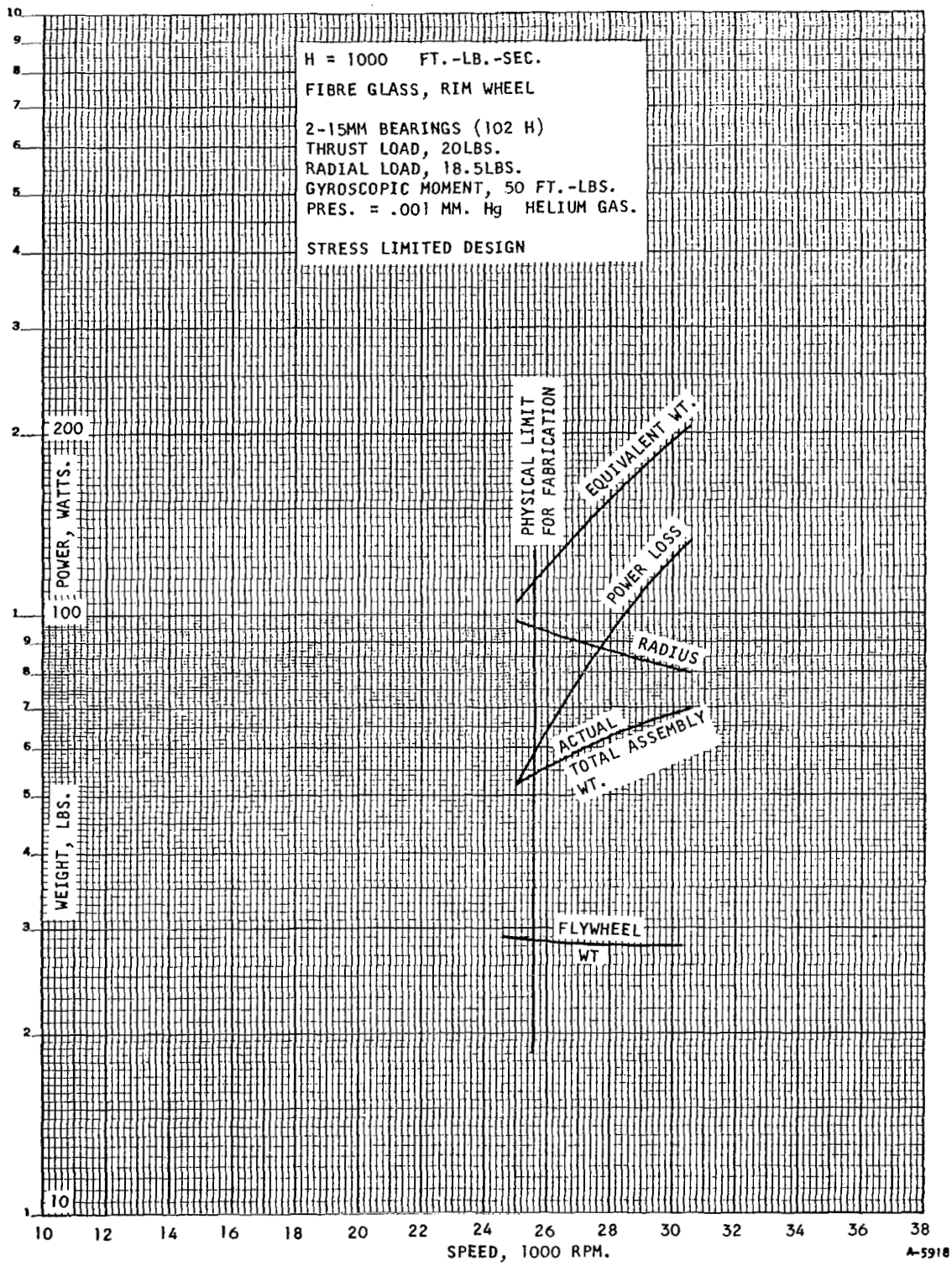

Figure 4-24. Flywheel Optimization - Fiberglass RimWheel

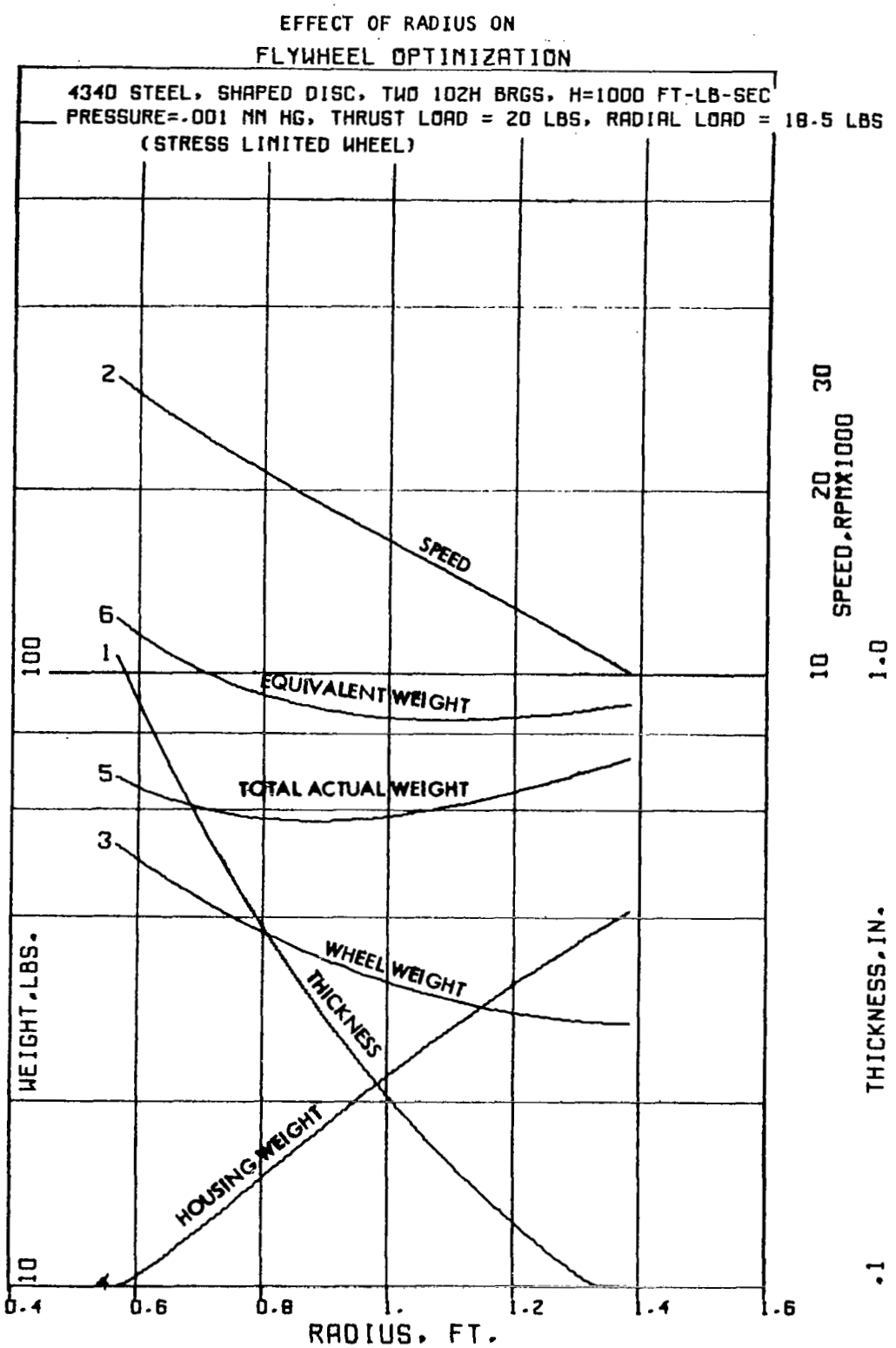

Figure 4-25. Effect of Radius on Flywheel Optimization - 4340 Steel

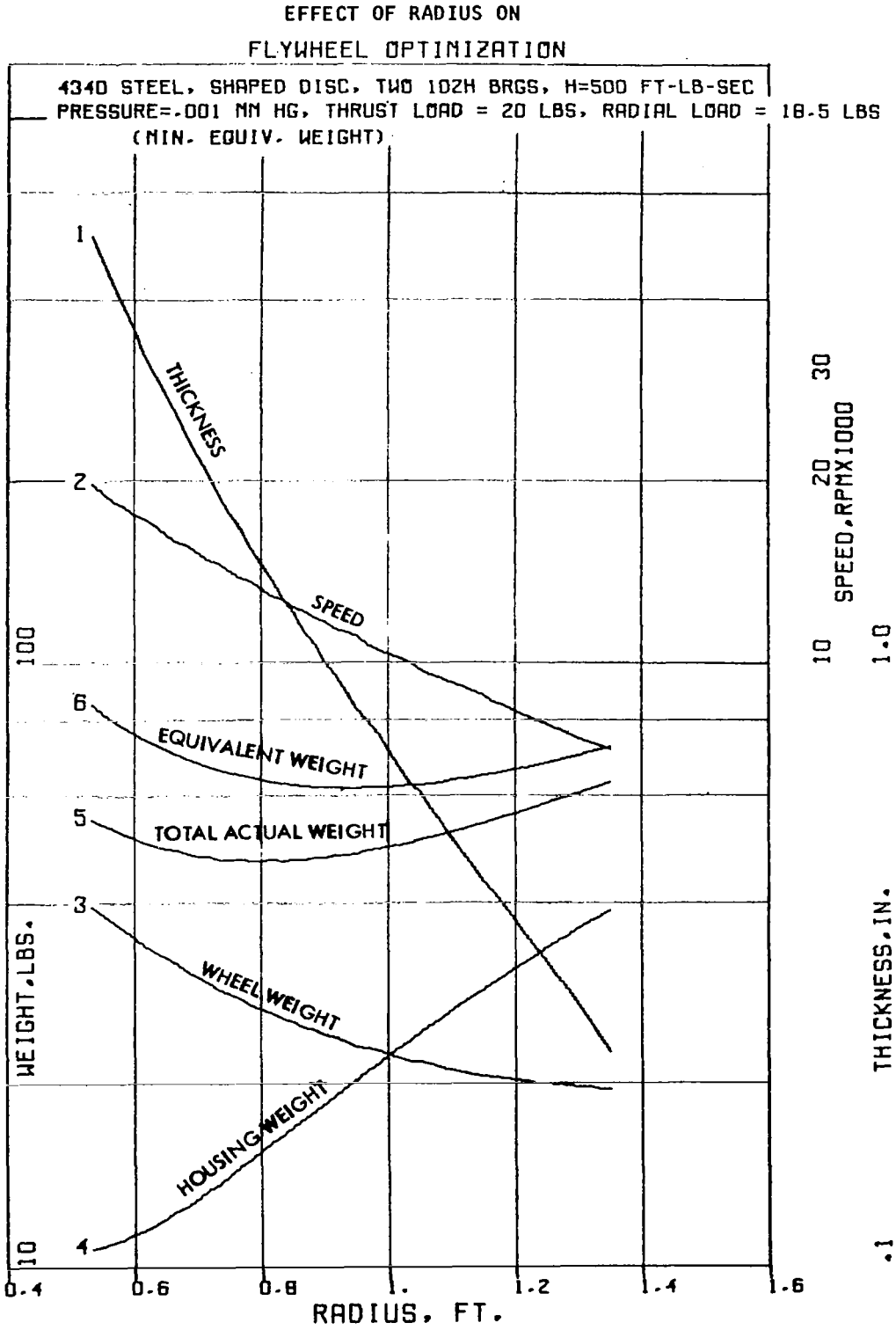

Figure 4-26. Effect of Radius on Flywheel Optimization - 4340 Steel

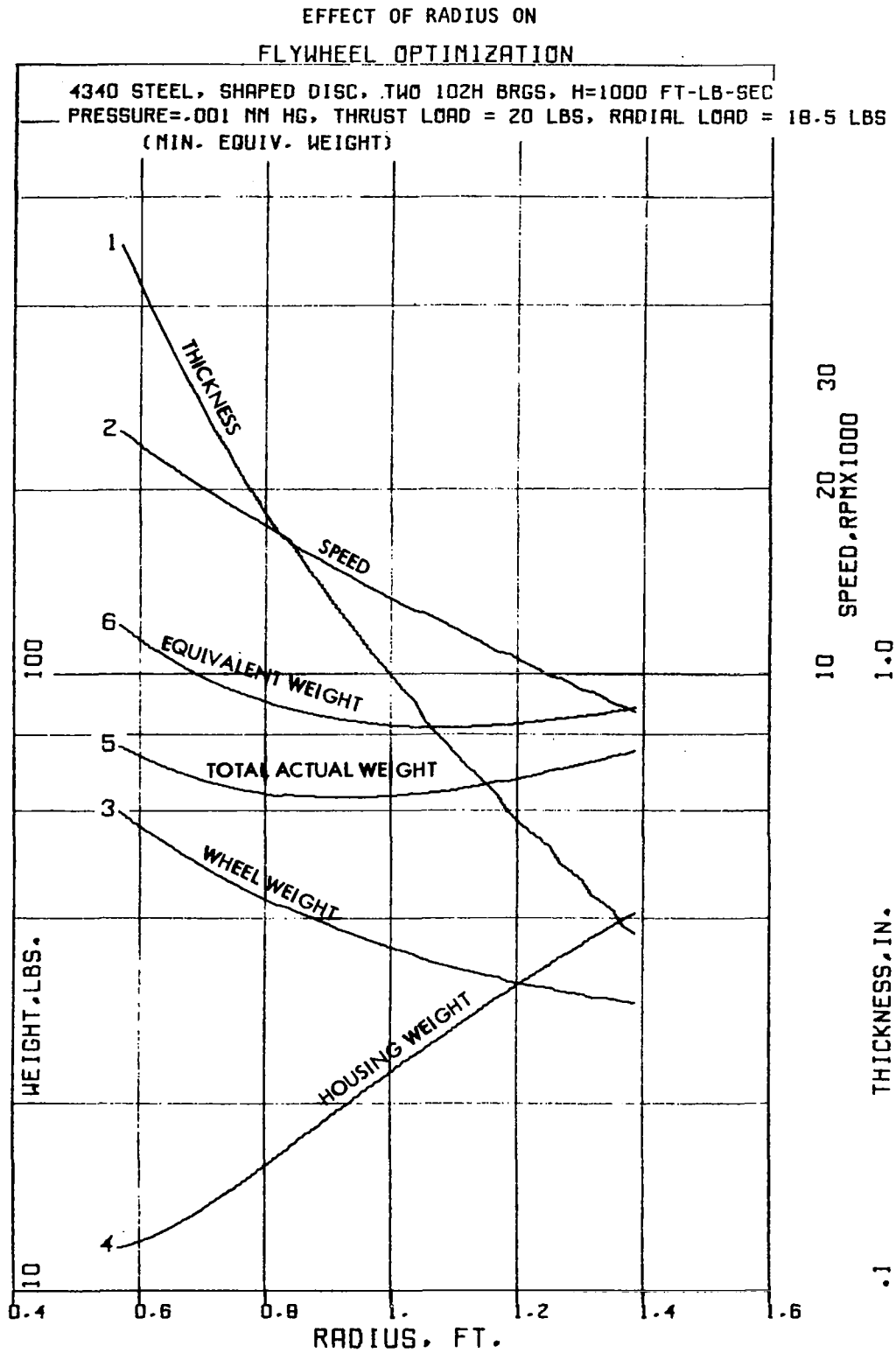

Figure 4-27. Effect of Radius on Flywheel Optimization - 4340 Steel

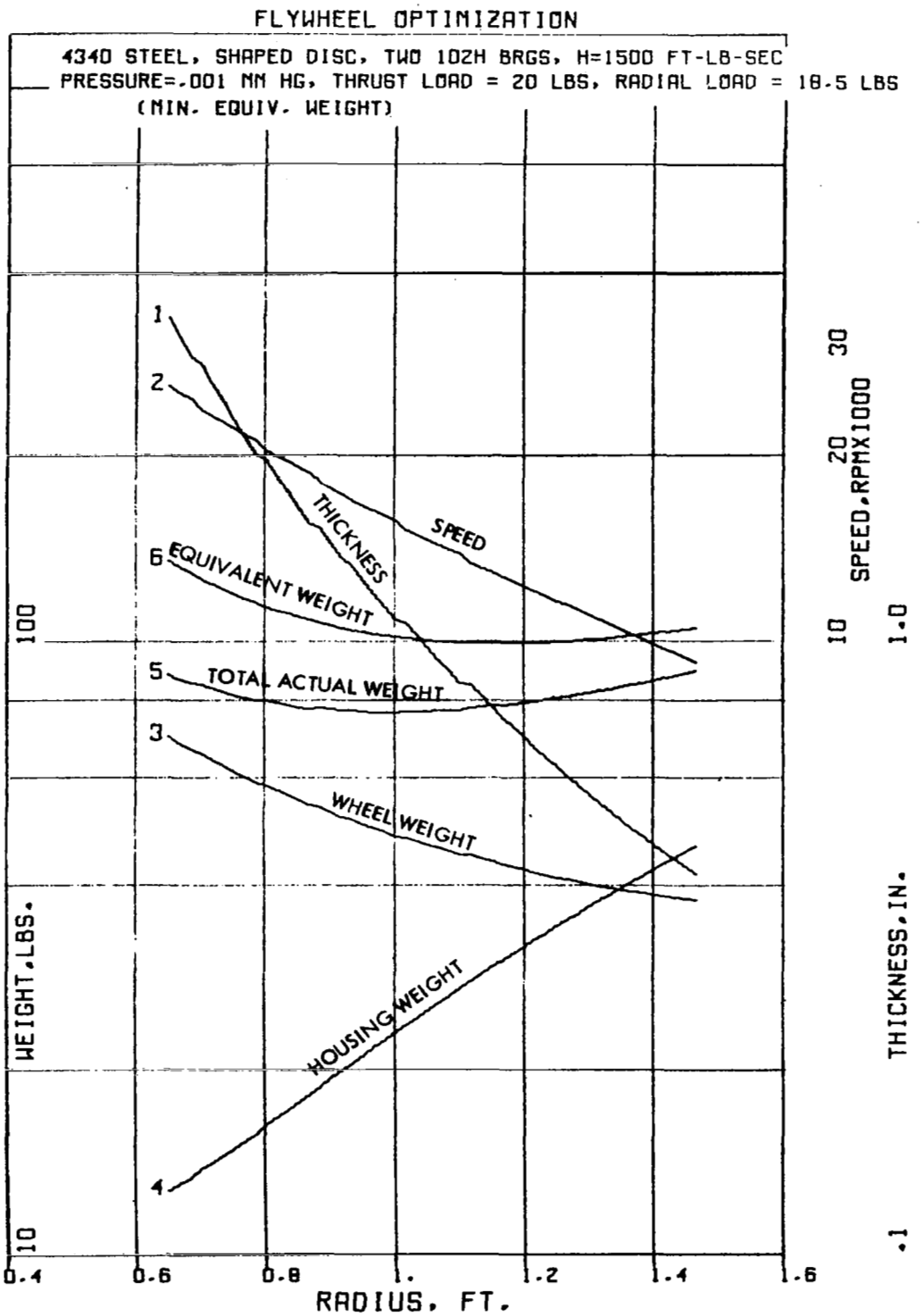

Figure 4-28. Flywheel Optimization - 4340 Steel

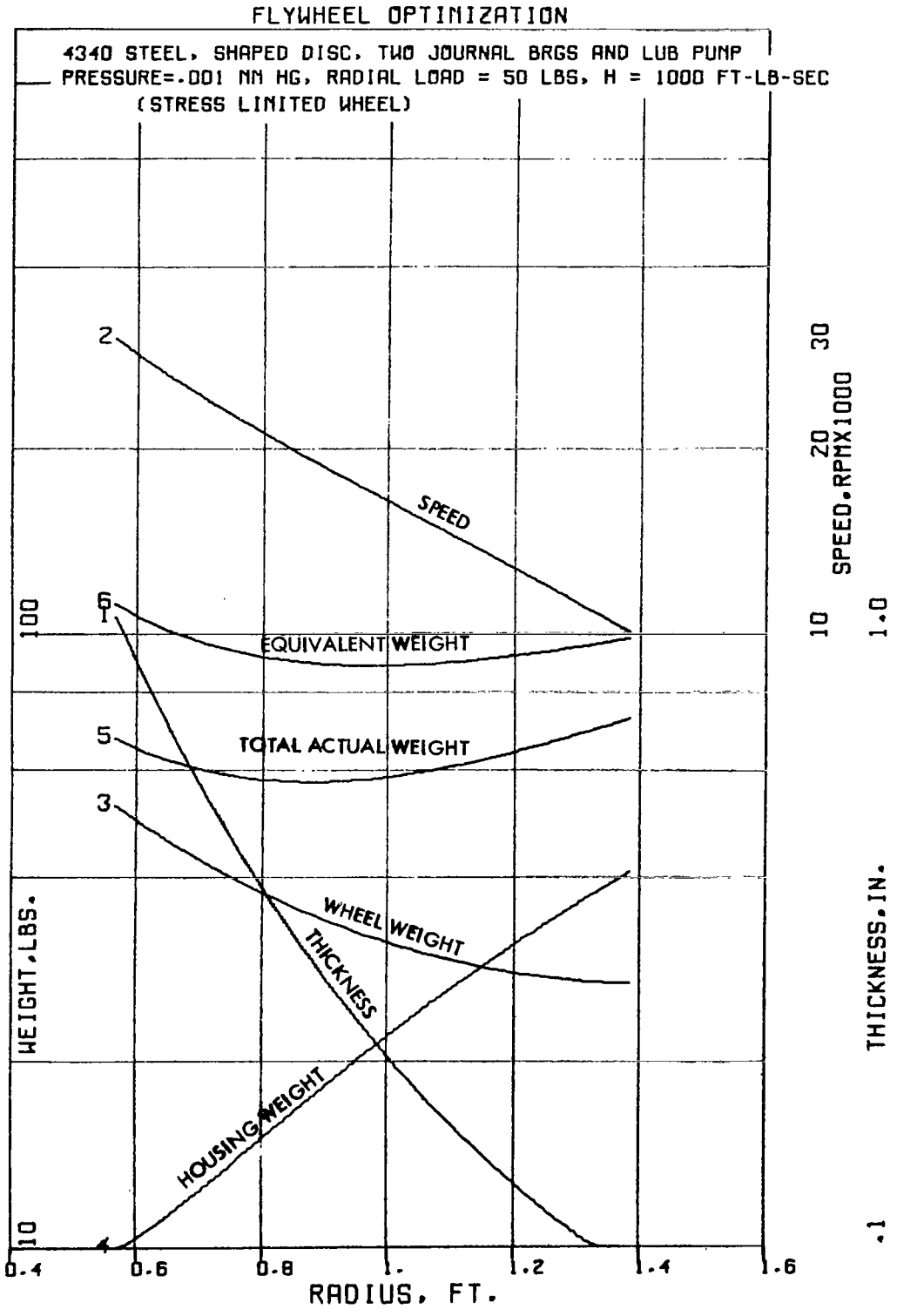

Figure 4-29. Flywheel Optimization - 4340 Steel

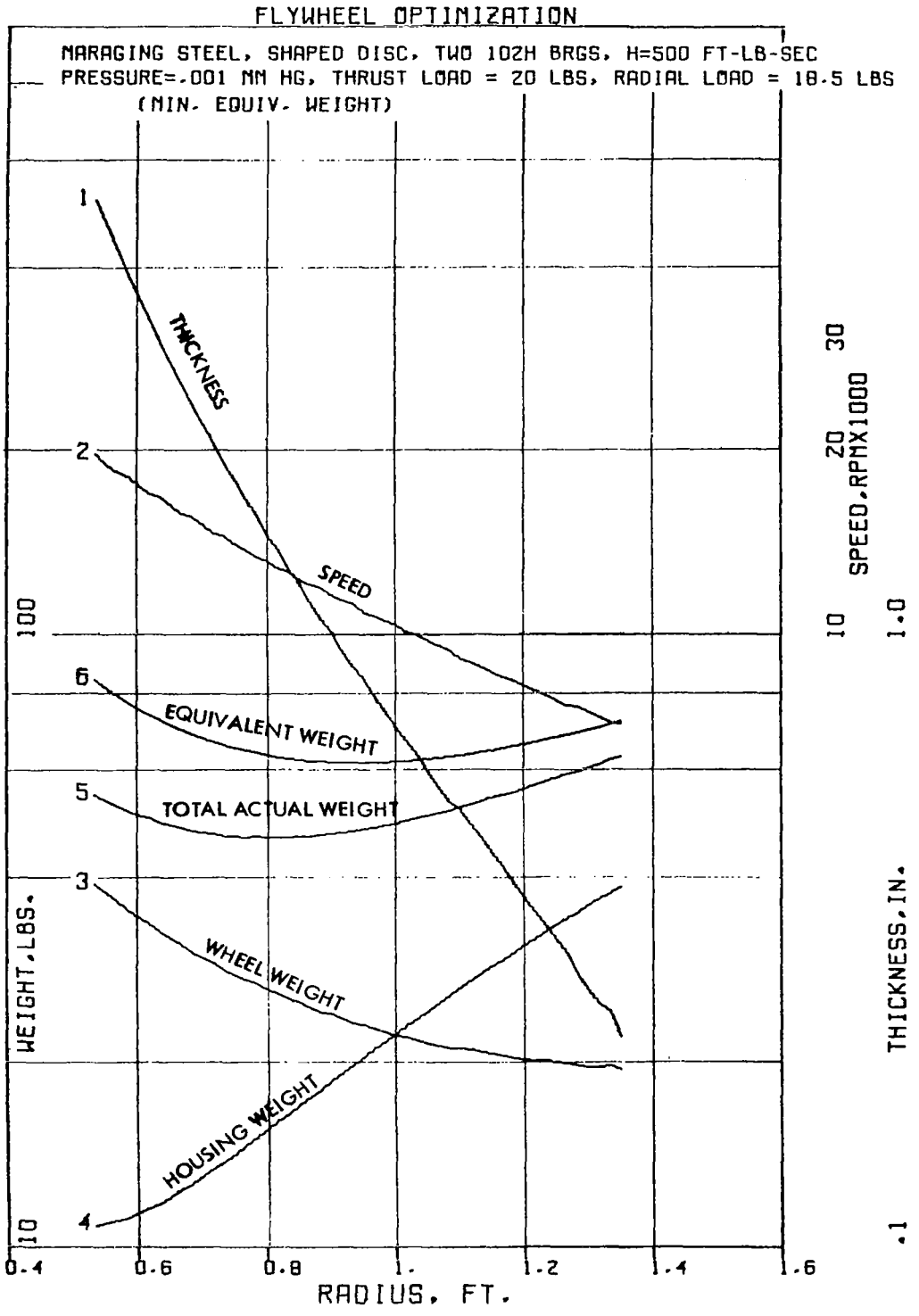

Figure 4-30. Flywheel Optimization - 4340 Steel

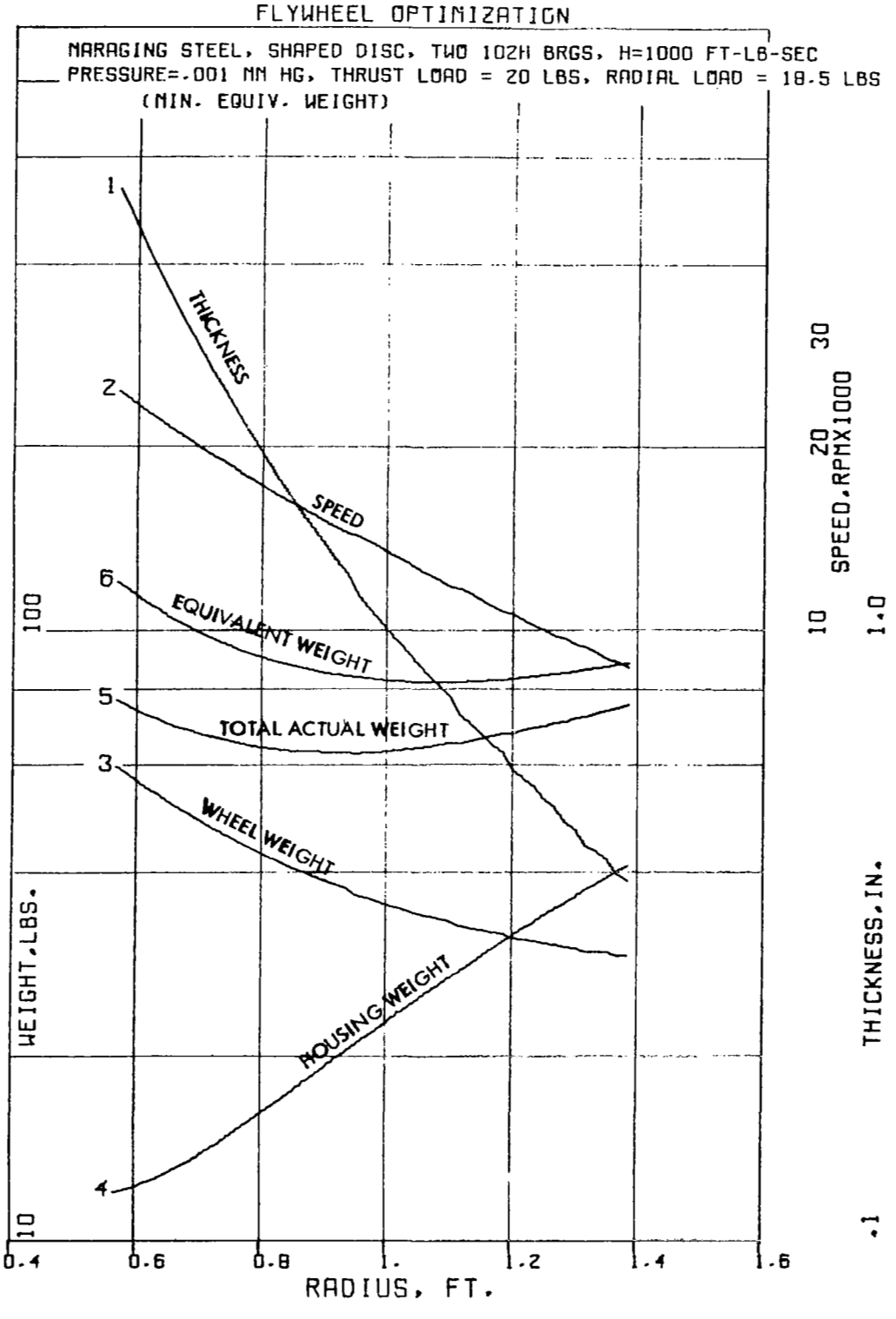

Figure 4-31. Flywheel Optimization - Maraging Steel

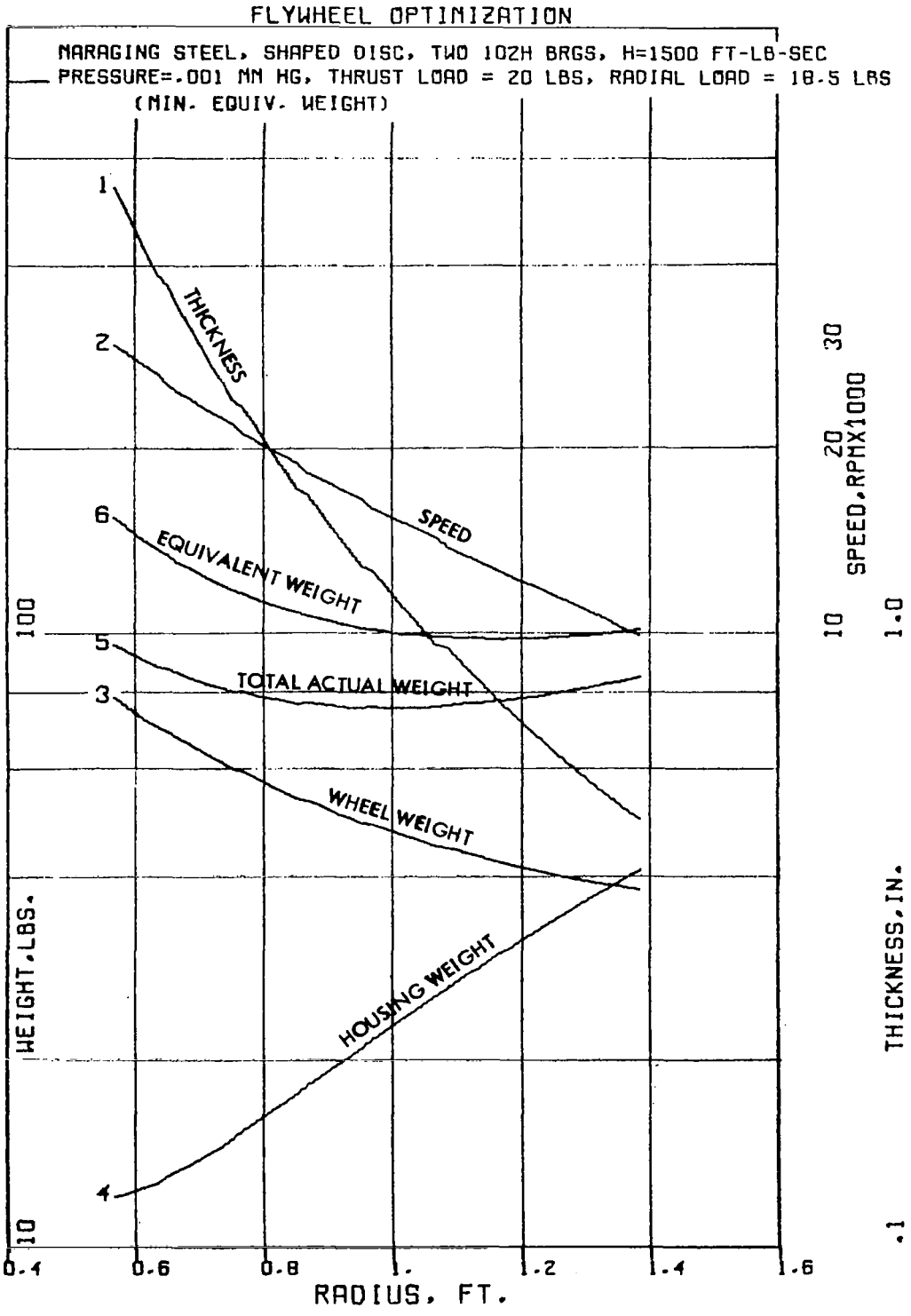

Figure 4-32. Flywheel Optimization - Maraging Steel

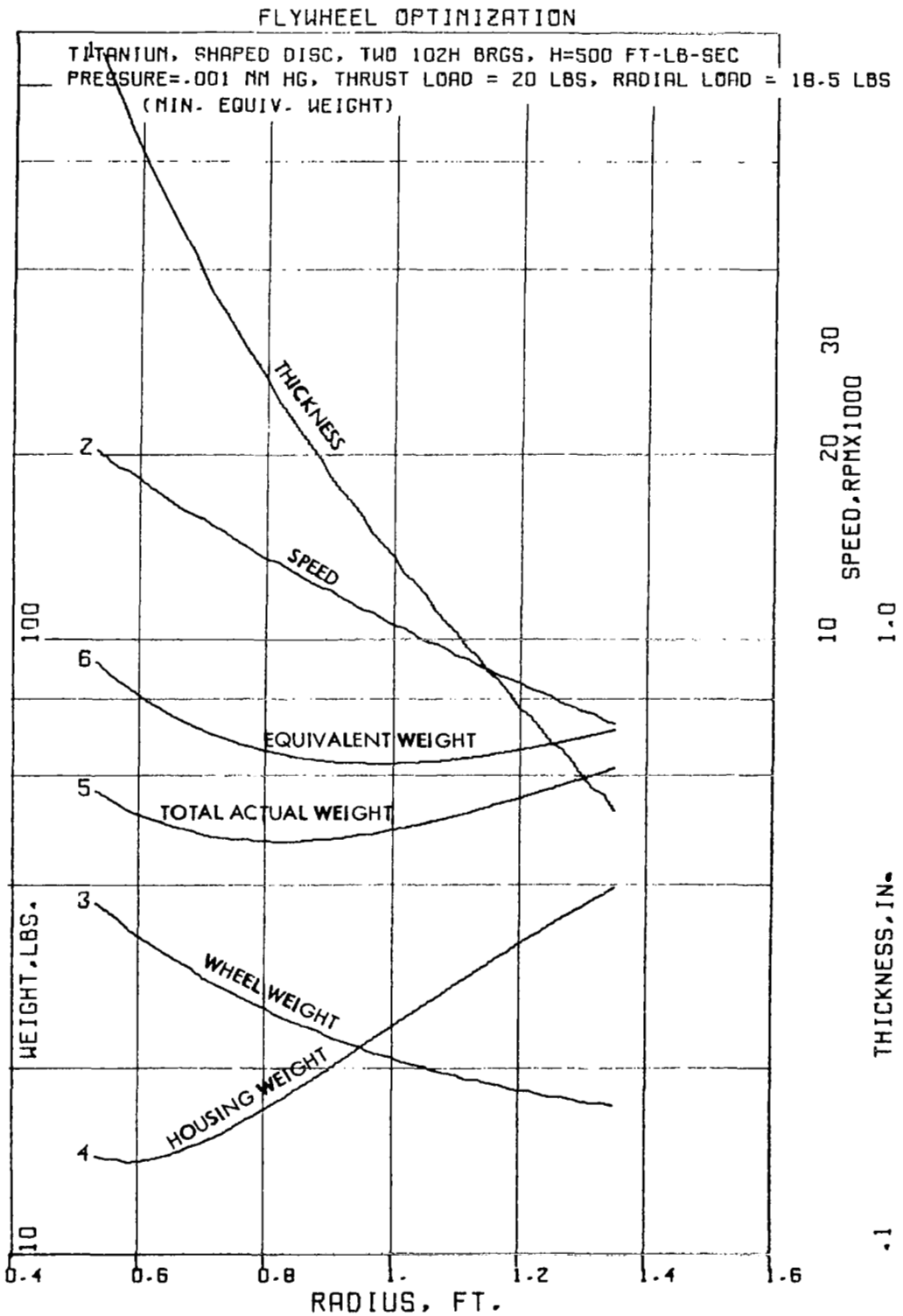

Figure 4-33. Flywheel Optimization - Titanium

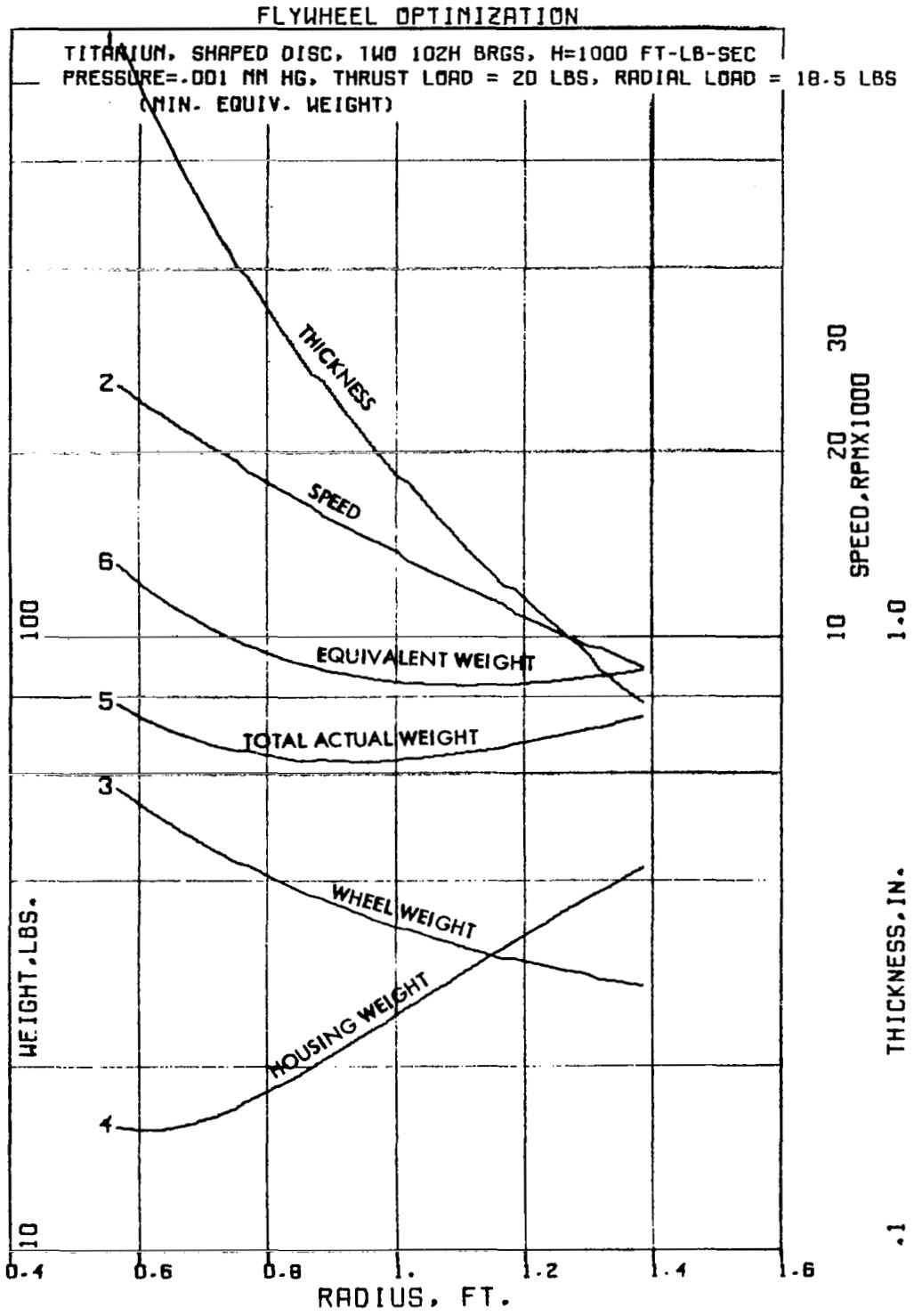

Figure 4-34. Flywheel Optimization - Titanium

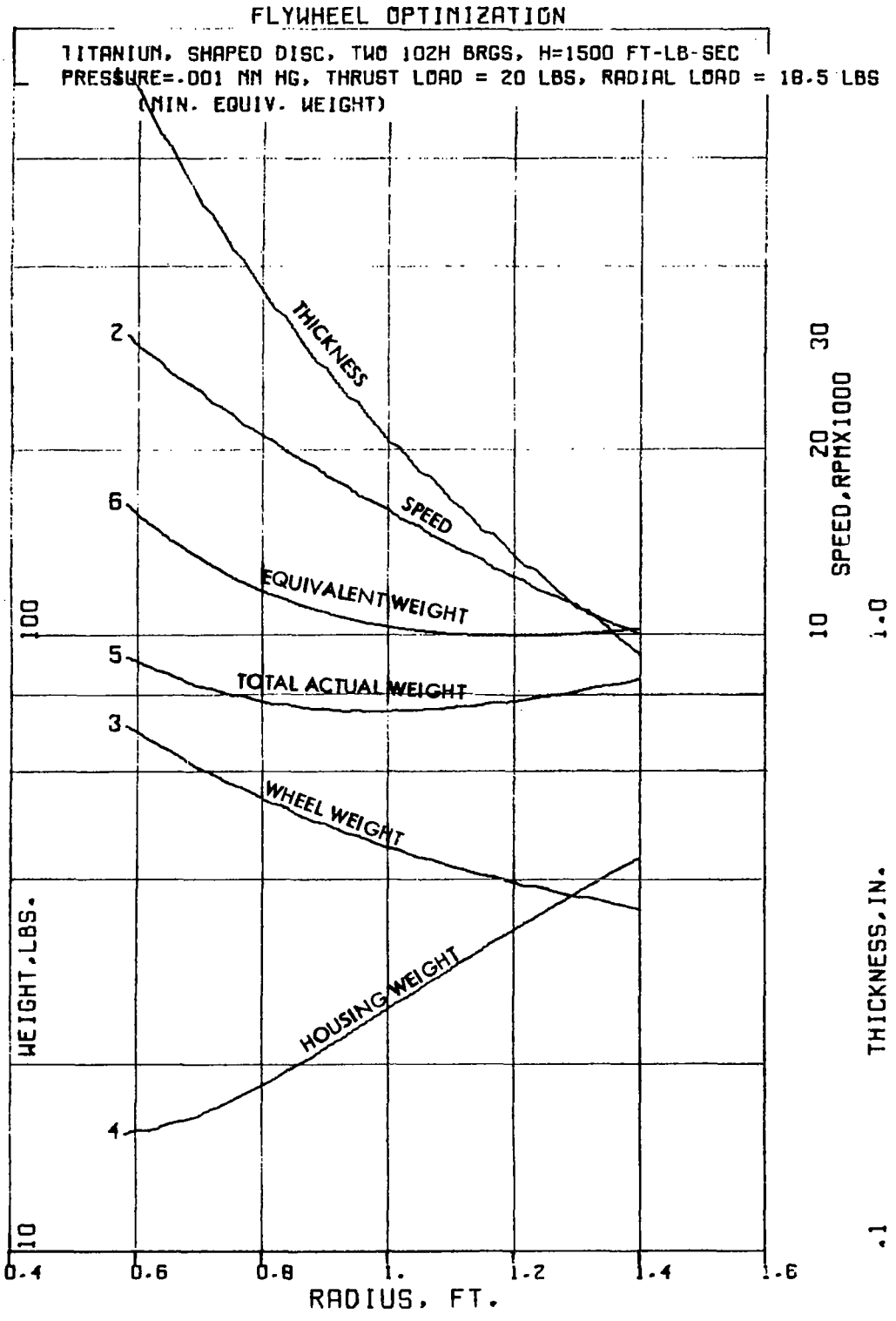

Figure 4-35. Flywheel Optimization - Titanium

SECTION 5

DISCUSSION

OPTIMUM DESIGN DESCRIPTION

Many factors had to be considered to determine the optimum design values for momentum wheel assemblies within the parametric range of this study. The results of the study, for all capacity wheels, is represented by the assembly shown in Figure 4-1. Although this drawing is for a wheel with an angular momentum of 1000 ft-lb-sec, it shows the basic shape and design features that would be used for any control moment gyro covered in this parametric study.

Since the gyroscopic moment requirement has been made the same for all angular momentum capacities considered in this study, the bearings, their distance apart, and the shaft size will be the same for all capacity wheels of this study. Figures 4-2 and 4-3 show ball bearings in a replaceable cartridge. The bearings are shown to be packed with Andok-C channeling grease. To provide for loss of oil from the grease past the labyrinth seals into the cooler flywheel chamber, a positive oiling system has been included in the design which is shown in Figure 4-3. The rate of supplying make up oil to both bearings is controlled by a solenoid operated valve which can have timed activation. When the solenoid valve is open, lubricating oil is forced into both bearing spaces through oil ducts or passages. The oil is forced into the bearings by centrifugal force. Escape of oil molecules from the bearing chamber is made difficult by use of the oil slinger and the labyrinth seal surrounding each shaft just inboard of the bearing cartridge. This labyrinth has a secondary use and that is one of acting as a journal bearing to support the momentum wheel before the ball bearings are installed. The thrust spring shown in Figure 4-3, serves the purpose of providing a thrust load on the bearings that will ensure race contact under all radial load conditions. The bearing on the oil reservoir end is floating so the bearing thrust load is transmitted to both bearings. The bearing on the motor end has a slightly higher thrust load due to magnetic pull of the permanent magnet motor. Detection of incipient bearing failure is made through use of temperature and vibration noise transducers or pickups shown in both Figures 4-2 and 4-3.

The motor used to drive the wheel is shown in Figure 4-4. This is a 4-pole, 3-phase, permanent magnet, synchronous motor with an axial gap arrangement of magnets and stator windings. Since the stator uses iron only in back of the windings, it is described as toothless. This design affords low iron power loss and permits high efficiency during the low load condition.

OPTIMUM DESIGN VALUES

The optimum design values for momentum wheel assemblies in the range of this parametric study are given in Table 4-2, and shown in graphic form in Figure 4-8. These values can be used with the basic shape, shown in Figure 2-2, to provide the basis for dimensioning any capacity wheel.

DESIGN BASIS

The wheel configuration was based on the minimum equivalent weight design which was chosen after making comparison with the stress-limited design in regard to total equivalent weight and speed. Study of Figures 4-5, 4-6, 4-7, and 4-16 shows the equivalent weight, with power loss to be slightly less or equal when comparing the minimum equivalent weight design with the stress-limited design, and the speed to be always substantially less. Also, the speed for a fairly large range of momentum capacity both less and greater than 1000 ft-lb-sec, is approximately 12,000 rpm. Since 12,000 rpm is a synchronous speed for a 400-cycle a-c power supply, there is an advantage in a basic design that requires very little compromise in using this speed.

MATERIAL SELECTION

Material selection was made by study of the graphs shown in Figures 4-5 and 4-6 which shows the three metals, 4340 Steel, Maraging Steel, and Titanium to be about equal from the standpoint of the total of assembly weight and equivalent weight of power loss. Fiberglass affords some total assembly weight reduction advantage over any of the metal wheels for either the stress limited or minimum equivalent weight designs, but the power loss associated with it is so high that it cannot be considered as a suitable material where power loss is a significant factor.

Since the minimum equivalent weight design method has been chosen, study of Figure 4-6 is useful. This graph shows the total equivalent weight to be about equal for both Maraging and 4340 Steel and not a great deal more for Titanium. The selection of the metal must then take into account other factors.

Study of Figures 4-7 and 4-16 through 4-18 disclose no significant advantage of one of these three metals over the other. Speeds and weights are close to the same. Titanium has some slightly higher speed disadvantage. Other factors such as cost, ductility, and fabrication were used to select 4340 Steel as the material for fabricating the momentum wheel.

Of the metal materials considered, 4340 Steel is by far the least expensive. It also affords other advantages in its ability to be worked or formed with relative ease. Its ductility is a highly desirable characteristic that will permit prestressing by overspeeding the wheel during the fabrication process.

BEARING SELECTION

Most of the data plotted in the study results presented in Section 4 are for designs using ball bearings. However, many computer runs were made for all four materials with designs using journal bearings. Typical results are shown in Figure 4-19.

In comparing the equivalent weight and operating speed for the two types of bearings, there is a definite advantage in use of ball bearings. The weight advantage can be determined by comparing Figures 4-16 and 4-19. This shows the

equivalent weight with ball bearings to be about 9 to 2 lb less than with journal bearings over the respective angular momentum range of 200 to 2000 ft-lb-sec. There is a decided reduction of speed by use of ball bearings, as much as 5000 rpm. A comparison in bearing power loss vs speed, for various loads and three different bearings sizes is made in Figures 4-13 through 4-15. These figures show that the larger size bearings have a substantial increase in power loss and must be avoided where they can be.

SPEED SELECTION

Figure 4-20 was plotted to study the effect of using 12,000 rpm wheel speed. It shows that this speed can be used over a wide range of angular momenta, 500 to 2000 ft-lb-sec, with a penalty of less than 1 lb additional equivalent weight. Study of Figures 4-21 through 4-23 also shows that a shift in speed, at optimum, causes only slight change in total equivalent weight. Figure 4-24 for fiberglass shows it to be very sensitive to speed.

PRESSURE AND GAS SELECTION

Figures 4-10 and 4-11 show windage power loss vs pressure for the stress limited and minimum equivalent designs respectively for three gasses, air, helium, and hydrogen. The pressure, ranging from atmospheric down to 10^{-5} mm Hg, causes three different flow regions to be encountered. At higher pressure, near atmospheric, there would be turbulent flow around the wheel and the power loss would be intolerably high. It is not until the pressure is reduced to about 10^{-2} mm Hg that the power loss becomes small. Below 10^{-3} mm Hg, free molecular flow is encountered and the power loss becomes quite small.

Hydrogen gas has the least power loss; however its flamability characteristics must be considered. Helium windage power loss can be made small enough by operating with a pressure at or under 10^{-3} mm Hg. Figure 4-12 shows the advantage of dropping the wheel speed. For all three gasses, there is a fast reduction in power loss as wheel speed is reduced.

RADIUS SELECTION

Figures 4-25 through 4-35 show that the wheel radius has only a slight effect on the equivalent weight in the region of optimum size. All the equivalent weight and total actual weight curves are very flat which will permit deviation from the optimum design without a large increase in weight. As can be seen from Figure 4-8, the optimum design wheels have radii that vary only from 9.4 to 15 in. over the entire range of angular momenta from 200 to 2000 ft-lb-sec, respectively.

POWER SUPPLY SELECTION

The power required to accelerate the flywheel to full speed can be held to a minimum by use of a variable frequency power supply. This avoids the lost power that would be encountered by starting with a fixed frequency. In starting with a frequency of 400 cps, for example, the energy loss converted

into heat would cause the temperature in the motor rotor and flywheel to rise at least 175°F to 200°F above the housing temperature since the highly polished flywheel provides a poor radiation surface. Subjecting the motor and wheel to this severe operation should be avoided. The variable frequency power supply, in addition to reducing the power loss to a very small value, allows the permanent magnet synchronous motor to be started and brought up to speed easily.

SECTION 6

CONCLUSIONS

FEASIBILITY

The field of single- and two-gimbal Control Moment Gyros has been advanced to the point where feasibility has been established for their use as torque generators and angular momentum storage for manned space vehicles. A total systems approach has led to criteria for design parameter selection which gives practical sizes and weights for desired performance, reliability, and ease of maintenance.

OPTIMIZATION

Design parameters and material selections have been established for optimum control moment gyros for manned spacecraft control.

Rotor Material Selection

Minimum equivalent weight of the assembly is obtained when a material with a high strength-to-weight ratio and high specific weight is used for the wheel. Lower density materials such as titanium and fiberglass are less optimum than steel in spite of their higher strength to weight properties. Fiberglass is unsuitable as an angular momentum storage material, mainly because of the higher speed required to compensate for its light weight. Titanium, on the other hand, along with Maraging Steel and 4340 Steel, can be used in the design with less than 3-percent discrepancy in the total equivalent weight.

Size and Speed Considerations

Graphical plots of computer results which show equivalent weight vs either wheel radius or speed reveal the gratifying fact that these curves remain very flat in the neighborhood of the minimum point so that essentially the optimum design is obtained for a range of sizes and speeds. This allows the final size and speed selections to be made in consideration of other factors, with practically no penalty in equivalent weight.

Rotor Bearing Selection

Journal bearings are somewhat less favorable than ball bearings because of the small control moment specified for the design and the more complicated lubrication pump design. The ball bearings are sized for ground testing and launch loads so that they offer ample margins of safety for the control moment schedule in space operation. Optimization of the flywheel design, which is sensitive to bearing losses, does not make use of the larger short-duration loads which the bearings can support, but is based on long-time average expected loads which determine the overall power demand of the space mission.

The bearing selection has included consideration for replacement and handling capability, selectability from lot quantities, and feasibility of manufacture.

Reliability

Each item that makes up the control moment gyro has sufficient inherent reliability to satisfy overall system requirements except possibly the low power loss rotor bearings. Although the degree of confidence in meeting the reliability goal for the rotor bearings and its lubrication scheme is high, it needs to be supplemented by further considerations such as a life test program.

The continuous monitor of bearing performance detects deterioration, and when a prescribed level has been reached, the Control Moment Gyro can be deactivated in sufficient time to allow bearing replacement with a minimum of system overstress and reduction of system reliability.

Maintainability

The projected life of the rotor bearings requires replacement during the total life of the Control Moment Gyro. In this regard, the rotor bearings are contained in easily removable and replaceable standardized cartridges. The CMG design is such that easy access is made to each bearing cartridge and when replaced, recalibration is not necessary.

Flexibility

The rotor and its gimbal design can be used equally well for single- or double-gimbal Control Moment Gyros.

SECTION 7

RECOMMENDATIONS

DESIGN PARAMETERS

Based on the results of the study contained in the analysis, the following recommendations can be made for the design of momentum wheels for CMG's of 200 to 2000 ft-lb-sec angular momentum:

1. The material for the rotor should be 4340 vacuum melted steel.

2. The rotor bearings should be ball bearings with M-50 tool steel races and a porous ball retainer. Laminated phenolic is suitable. Also worthy of consideration for a development test program is a composite material developed by Westinghouse Electric Corporation. This material consists of silver matrix 70 percent, Teflon 20 percent, and solid lubricants 10 percent. Solid lubricants are of such materials as molybdenum diselenide and tantalum diselenide. (Recommendation of the composite material should be made by Westinghouse since development in this field is still being made).

3. The housing of the inner gimbal (rotor housing) should be aluminum sheet formed in a die to achieve high strength and rigidity with low weight. Aluminum high-strength materials such as 6061 in T6 condition are suitable.

4. Housing wall thickness:

Angular Momentum Size	Thickness, in.
200 to 450 ft-lb-sec	0.075
500 to 1200 ft-lb-sec	0.090
1300 to 2000 ft-lb-sec	0.100

5. A permanent-magnet synchronous motor should be used. It should be 4-pole, 3-phase and be capable of operating on 220-v a-c power.

6. The speed of the wheel can be set at 12,000 rpm and the following data applies to a 4340 Steel wheel with an angular momentum of 1000 ft-lb-sec.

Radius	13.1
Disc thickness	
At hub	0.322 in.
At 5.568 in. radius	0.161 in.

Rim thickness	0.76 in.
Rotor weight	33.6 lb
Housing weight	26.5 lb
Total assembly weight	65.1 lb
Power loss	17.38 watts

7. A variable-frequency variable-voltage power supply should be used to bring the rotor to speed. Once up to full speed, the synchronous motor can be switched to the 400-cycle a-c power supply to avoid a continuous power loss of about 2 watts from the power supply.

AREAS FOR FURTHER STUDY

To implement the results of the study contained in this report, three areas of further study are strongly recommended. Since each is generally independent of the other, all three can be accomplished simultaneously. From a schedule point of view and the need to finalize the control portion of the complete vehicle preliminary design, it would be desirable to initiate each study concurrently and as soon as possible. Only in this fashion can maximum assurance be established for the use of Control Moment Gyros as control elements in manned space vehicles.

Rotor Bearings and Lubrication System Study

A bearing design study and verification test is required in order that lubricant demand rate be minimized and that the bearings operate in a stable manner for reasonable periods of time in the event of interruption of the lubricant supply. The design and test of a suitable lubrication system and the selection of the optimum lubricant need be performed. Means of reducing the probability of early fatigue failure must be developed and proved. Gyroscopic ball spin control must be studied and a solution advanced which will ensure that bearing operation is within a stable regime.

Fabrication and Test of Control Moment Gyro

In order to fully substantiate the findings of the optimization study contained in this report, one or more optimum CMG's should be fabricated and tested. In addition, the maintenance situation involving personnel with skills commensurate with those of the vehicle occupants can be evaluated.

Torquer Consideration

Torquer methods for single- and double-gimbal Control Moment Gyros need be studied in order that for specific applications, the CMG torquers be of the lowest weight, lowest power and have desired response time. A serious problem of power and weight exists if direct drive torquers greater than 20 ft-lb are used as coupling between the vehicle and the CMG. The use of gear

trains or other torque multiplication techniques must be compared with the gimbal torquers of single-gimbal CMG's. Gimbal torquers for double-gimbal CMG's must be studied with the intent of resolving gyroscopic coupling.

SECTION 8

RELIABILITY

RELIABILITY CONSIDERATIONS

The approach outlined in this report reflects the continuous consideration given to the objective of designing as simple a wheel as possible, consistent with the objectives of minimum weight, power, and reliability penalties. Three facets of the approach adopted illustrate the following elements of good design: (1) the considerable reduction in the magnitude of the radial loads impressed upon the bearings, in relation to their rating, (2) the positive but simple method of achieving reliable and thoroughly adequate lubrication of these bearings, and (3) the elimination of a special power supply for continuous operation of the wheel once a start has been achieved by means of the variable frequency power supply. Structural integrity against burst has been obtained and optimized by methods described in Section 3 of this report.

In the field of reliability, electronic devices such as the variable frequency power supply always are considered to be potential weak links, and an inability to start the wheel, once in orbit, is second only to a wheel burst in its reliability and mission success implications. Therefore, it is recommended that this power supply be modularized into a pull-out plug-in unit which can be replaced by a second unit carried as a back-up spare and which requires no great specialized ability on the part of the astronaut to remove and replace.

RELIABILITY FACTOR

To establish estimated reliability factors on a design that has not been completely detailed, comparison with similar mechanisms or components must be made. On this basis, comparison can be made with induction motor driven fans which have a background of successful operation for many years.

One example of comparable machinery is the Titan II fan which used a 52 watt 2-phase induction motor rotating at a speed of 19,500 rpm. Grease packed bearings were used. Testing with 11 samples over a 2-year period established a Mean-Time-Between-Failure of 60,000 hours. It is believed that the lower speed of 12,000 rpm, greater bearing load margin, and better method of lubrication will yield a MTBF for the wheel drive motor of some value in excess of 88,000 hours.

SECTION 9

GENERAL DESIGN SPECIFICATION

The following material is a general design specification that provides data, established requirements, and design criteria pertinent to the development and fabrication of the momentum wheel. Preceding sections discuss in depth the various parameters of design to be developed or optimized. The information included in this specification is outlined below:

1.0 GENERAL
- 1.1 Scope
- 1.2 Purpose
- 1.3 Definitions

2.0 APPLICABLE DOCUMENTS
- 2.1 Applicability
- 2.2 Reference Documents

3.0 DESIGN REQUIREMENTS - GENERAL
- 3.1 General
- 3.2 Performance Criteria
- 3.3 Selection and Application of Materials, Parts, and Processes
- 3.4 Non-Specification
- 3.5 Interchangeability
- 3.6 Maintainability
- 3.7 Modular Construction

4.0 TEST REQUIREMENTS
- 4.1 Test Program
- 4.2 Reliability Assessment
- 4.3 Waiver of Tests
- 4.4 Criteria for Success
- 4.5 Failures - Analysis and Feedback System
- 4.6 Notice of Tests
- 4.7 Witnessing of Tests
- 4.8 Adjustments and Repairs During Tests
- 4.9 Test in Progress Data
- 4.10 Test Procedures
- 4.11 Applicable Procedures for Tests

5.0 DATA AND DOCUMENTATION REQUIREMENTS
- 5.1 General
- 5.2 Installation and Maintenance Instructions
- 5.3 Assembly and Operating Instructions
- 5.4 Drawings
- 5.5 Parts Listing
- 5.6 Reports

6.0 PREPARATION FOR DELIVERY
- 6.1 General
- 6.2 Article Packaging
- 6.3 Intermediate Packaging
- 6.4 Special Instructions
- 6.5 Marking

1.0 GENERAL

1.1 Scope - This document contains the information required to provide control and implementation of the detail design of an Angular Momentum Wheel and its Associated Control System, for use in spacecraft.

1.2 Purpose - The primary objective of the information presented herein is to assure the proper and maximum direction of design effort in achieving the detail design goals desired.

1.3 Definitions - The following list of words as used in this document, shall be defined as follows:

(a) Contractor - That agency which is procuring the subject equipment or design thereof

(b) Subcontractor - That agency which has contracted to perform the design and/or manufacture of subject equipment

(c) Subject equipment - That equipment as defined in Paragraph 1.1, namely, the Angular Momentum Wheel and its Associated Control System

(d) Article - Any item, part, component or other physical subdivision of the subject equipment

2.0 APPLICABLE DOCUMENTS

2.1 Applicability - The following documents shall form a part of this specification to the extent specified herein.

SPECIFICATION

Military

MIL-C-9435A	Chamber, Explosion-Proof Testing, dated March 14, 1956
MIL-I-26600	Interference Control Requirements
MIL-D-70327	Interchangeability Drawing Requirements
MIL-E-5400	Electronic Equipment, Military Aircraft
MIL-P-17555	Preparation for Delivery
MIL-Q-9858	Quality Control System Requirements

STANDARDS

Military

MIL-STD-202	High Potential Testing
MIL-STD-704	Electric Power, Aircraft
MIL STD-810	Environmental Test Methods

PUBLICATIONS

NASA - National Aeronautical and Space Administration

NPC 200-2 Quality Assurance Provisions for Space Contractors, dated April 1962

2.2 Reference Documents

Military

MIL-R-27542 Reliability Program Requirements for Aerospace Systems, Subsystems, and Equipment

3.0 DESIGN REQUIREMENTS - GENERAL

3.1 General - Specification MIL-E-5400 is applicable as a requirement of this document. Where requirements of MIL-E-5400 and this document conflict, the requirements of this document shall govern.

3.2 Performance Criteria - The Angular Momentum Wheel shall meet the following requirements:

3.2.1 Angular Momentum Capacity - 1000 ± 1.0 ft-lb-sec

3.2.2 Torque Capacity

(a) Normal maximum - 32 ft-lb

(b) Overload - 48 ft-lb

(c) Maximum test overload - 64 ft-lb

3.2.3 Speed

(a) Normal maximum - 12,500 rpm

(b) Overspeed - 15,500 rpm

(c) Maximum limit, no burst - 21,000 rpm

3.2.4 Gimbal Action

(a) Torque per actuator - 32 ft-lb

(b) Full torque capacity of the momentum wheel shall be transmittable through either gimbal actuator.

(c) Net power at ouput shaft - 0.01 hp

(d) Gimbal assembly and actuators shall be contained in a spherical dimension of the diameter 33.6 in.

3.2.5 Electric Motor Drive

(a) Synchronous type motor shall be used.

(b) Power frequency - 400 cps

(c) Acceleration zero to full speed in 2 hours

(d) Minimum power capability - 100 watts

(e) Decelerate to full zero speed in 2 hours

(f) Braking shall be accomplished by using the dynamic characteristics of the motor.

(g) Operation of the motor shall require no cooling liquids.

(h) Maximum energy required for acceleration to full speed - 500 watt-hours

(i) At full speed operation, the steady-state temperature shall not exceed 100^0F above ambient.

(j) During acceleration and deceleration the temperature rise shall not exceed 115^0F above ambient.

(k) Maximum temperature in the motor in an environment of 120^0F at 1/2 atmosphere shall not exceed 400^0F.

3.2.6 Bearings

(a) Bearings must be easily replaced as a cartridge.

(b) A lubricating system shall be provided to permit continuous operation for at least one year.

(c) The bearings and lubricant shall be capable of operation in a pressure of 10^{-3} mm Hg at a temperature of 160^0F.

3.2.7 Power Supply

(a) The power supply shall be capable of accelerating the flywheel to full speed without producing adverse heating effects in the motor or flywheel.

(b) It is desirable that the power supply system be capable of returning at least 60 percent of the energy of the flywheel to the main electrical power system during deceleration by dynamic braking. Provision shall be made to dissipate all all electrical energy associated with the dynamic braking that is not returned to the main power system.

(c) Motors shall operate from either direct or alternating current source.

(d) Direct current power shall be:

Regulated	28 ± 0.5 volts
Unregulated	24 to 31 volts

(e) Alternating current power shall be either 115 volts, 400 cps, or 200 volts, 400 cps, 3 phase, wye connected.

3.2.8 Physical Characteristics

(a) Flywheel weight shall not exceed 40 lb.

(b) Flywheel assembly, including housing, motor, bearings, and shaft weight shall not exceed 70 lb.

(c) Flywheel diameter shall not exceed 24 in.

(d) The housing shall be capable of being sealed to allow evacuation to a pressure of 10^{-3} mm Hg.

(e) Slip rings shall be provided in the gimbal asembly to give transmission of power and electrical signals.

(f) The mass center shall not exceed 0.0001 in. from center of rotation.

3.3 Selection and Application of Materials, Parts and Processes - During the design, development, and construction of subject equipment, the subcontractor shall investigate the suitability of materials, parts, and processes to be used. The suitability shall be determined by the intended use and the ability to satisfy the requirements of this specification. The incorporation of suitable materials, parts, and processes shall consider anticipated availability to meet reasonable production schedules.

3.3.1 Nonmagnetic Materials - Nonmagnetic materials shall be used for all parts of subject equipment, except where magnetic materials are essential or unavoidable.

3.4 Non-specification - Details of design and construction other than those specified herein shall be at the option of the subcontractor, insofar as they do not conflict with the content or intent of this document.

3.5 Interchangeability - Articles manufactured in accordance with this specification shall be functionally, physically, and structurally interchangeable. Each article shall be assigned a specific part number. Any change in an article shall be attended by a change in Supplier's part number to identify the new configuration.

3.6 Maintainability - This equipment shall be designed with the objective that installation, repair, and servicing can be accomplished without special tools or handling equipment. Where special tools and equipment cannot be avoided, due to the uniqueness of the structure, then their design and construction require prior approval of the Contractor. As an additional object, the equipment shall incorporate features and packaging procedures which make feasible the replacement of faulty components and subassemblies by personnel of the lowest possible skill levels.

3.6.1 Maintenance Periods - Scheduled maintenance periods which require the interruption of operation of subject equipment, shall be no more frequent than one year between scheduled dates.

3.7 Modular Construction - Modular design concepts shall be utilized wherever feasible for electronic and mechanical components to provide for ease of interchangeability and maintainability. The electronic circuitry modules shall be "plug-in" for ease of removal.

3.8 Reliability Factor - The entire system including associated electronics shall have a reliability of (0.99). Redundancy is permissible to achieve the reliability goal.

3.9 Test Point Accessibility - The equipment design shall permit ease of accessibility to critical test points without interruption or impairment of equipment operation. Critical test points may be used to interrogate mechanical as well as electronic operations.

4.0 TEST REQUIREMENTS

4.1 Test Program - In general, the test programs may be classified as follows:

(a) Development tests

(b) Qualification tests

(c) Acceptance tests

4.1.1 Development Tests - These tests are conducted to satisfy the following requirements:

(a) Evaluation of materials, parts, components, and circuits to determine their application suitability

(b) Acquisition of design and process information

(c) To develop assurance that the product will successfully complete the qualification tests

4.1.1.1 The tests shall be designed to identify failure modes, determine effects of critical single and combined environments, functional stresses, combinations of tolerances, and to determine design margins.

4.1.2 Qualification Tests - Qualification tests of appropriate parts, components, subassemblies, and higher levels of assembly shall be performed to verify the inherent capability of the design to meet the performance and environmental requirements stipulated in Section 3 of this document and the applicable procurement specification. The qualification tests shall be performed on items produced with the same tooling processes and under the same conditions as those intended for quantity production. The order and number of equipment items to be subjected to these tests are defined in the procurement specification.

4.1.3 Acceptance Tests - These tests shall be performed (by the Subcontractor on all hardware presented for qualification and delivery) to verify that materials, construction, workmanship, dimensions, design, and performance comply with the requirements of the applicable drawings and specification. Specific tests to be employed will vary for each equipment, depending upon the ability of avilable methods to measure the acceptability of the parameters being evaluated. Where functional tests alone cannot provide assurance of acceptability, low-level environments such as vibration; or nondestructive tests including X-ray, infrared, ultrasonic, magnaflux or others; may be employed. Specific test requirements are contained in the procurement specification for each item. Acceptance test procedures shall be submitted to the contractor for approval prior to implementation.

4.2 Reliability Assessment - Although each of the defined test programs are designed primarily to provide engineering information, they are also planned to make available a maximum practical amount of detail for assessment of reliability. The subcontractor shall assess achieved reliability. Some of the methods employed to accomplish this objective may include (but are not limited to) the following:

(a) Performance parameter variation analysis (e.g., probability of significant parameters remaining within specified limits as a function of time and environmental stresses)

(b) Margin of safety evaluation (e.g., total life reliability operating life requirement, strength versus stress, etc.)

(c) Mean-time-between-failure at most meaningful confidence levels

(d) Attribute data evaluation (e.g., number of successful tests total attempts)

4.2.1 Comparative Analysis - A comparative analysis showing results obtained by utilizing more than one (or combinations) of the aforementioned methods may also be presented.

4.3 Waiver of Tests - Applicable portions of the qualification tests defined in the procurement specification may be waived, after contractor approval, if the following substantiating data are provided:

(a) Evidence of equipment compliance with the qualification test program requirements or applicable portions thereof

(b) Substantiating data verifying that similar equipment has successfully passed tests equivalent to or more stringent than those required herein

4.3.1 Test Waiver Request - Any test waiver is completely at the discretion of the contractor. Evidence to be submitted in support of requests for such waivers shall include the following information:

(a) Complete description of similar items including photographs, drawings, and performance data

(b) Test reports and test data describing previously conducted functional and environmental tests on actual or similar equipment (development tests included)

(c) A detailed comparison between the proposed article and the item for which similarity is claimed, listing sufficient reasons and justification to establish the validity of the similarity request

4.4 Criteria for Success - Equipment will be considered as having successfully completed the environmental, functional, and life tests defined in the procurement specification when the following specific conditions have been satisfied. (Additional criteria for success may be obtained from referenced Specification MIL-R-27542.)

(a) Operation throughout all tests shall be within the tolerance limits stated in the design requirements section of the applicable procurement specification.

(b) No deterioration (internal or external) has occurred which could in any manner prevent the equipment from meeting its functional requirements during service usage.

4.5 Failures - Analysis and Feedback System - The subcontractor or supplier shall have a system for collecting, analyzing, and recording all failures and reliability data such as operating time, cycles, and variables data during those phases of the program in which they have primary responsibility.

4.5.1 Failure Reporting - The failure reporting system shall provide a means by which effective corrective action can be taken on a timely basis thereby reducing or preventing recurrence of the failures. The subcontractor or supplier shall report failures occurring on operating equipment during receiving inspection, in final assembly checkout, and during acceptance and qualification testing. Quality discrepancies revealed in inspection shall not be construed as failures. For reporting purposes, an unscheduled adjustment other than a calibration made during maintenance shall be defined as a failure. Corrective action initiated to prevent recurrence of failures shall be prepared in detail and submitted to the Contractor for concurrence.

4.6 Notice of Tests - The contractor shall be advised not less than 48 hours in advance of a scheduled test. No tests shall be delayed if the contractor's representative fails to appear.

4.7 Witnessing of Tests - The contractor reserves the right to witness any test, in whole or in part, or to designate witnesses (in addition to those selected by the supplier) who have a "need to know" (consultant or government agencies).

4.8 Adjustements and Repairs During Tests - A declaration of intent to adjust or repair any item must be made by the supplier or subcontractor prior to conducting any test. Adjustments, repairs, or maintenance shall not be allowed during tests unless they are a part of scheduled maintenance and providing such adjustements, repairs, and maintenance are not the result of faulty design, materials or workmanship, and have not been caused by the test conditions imposed.

4.9 Test in Progress Data - Copies of information regarding tests in progress shall be made available, in a central location at the subcontractor's or supplier's facility, for review by contractor personnel at any time.

4.10 Test Procedures - Detailed test procedure delineating the method and sequence of tests to be performed, schematics and flow diagrams, and test equipment descriptions are required by the contractor. The detailed test procedures shall state exactly how each test and each measurement will be made.

4.10.1 Specimen Identification Function - Test specimens shall be permanently identified by numbers or other symbols (in addition to part numbers) in order to permit identification of individual items. Specimens shall be permanently marked "FOR TEST ONLY".

4.10.2 Pre-test Performance Record - The performance characteristics of each test specimen shall be measured under ambient conditions prior to each test sequence. Specimens that fail the pre-test check shall not be subjected to further tests until corrective action is accomplished and formal approval to proceed has been granted by the contractor.

4.10.3 Operational Environmental Tests - Operational environmental tests require the equipment to function while being subjected to the environment. The equipment operation shall be with the input and output values varied over the ranges specified by the design requirements. The number of operating parameters to be monitored during a test and the performance requirements thereof, will be defined in the equipment procurement specification.

4.10.4 Nonoperational Environmental Tests - Nonoperational environmental tests are employed under the following two general conditions:

(a) For those environments encountered during transportation, storage and stand-by periods.

(b) For equipment that operates only while the vehicle is on the ground or is not expected to operate in service (e.g., equipment in the spacecraft command module may not have to operate during earth entry, but it cannot fail structurally during this phase or upon landing, and endanger the astronauts).

4.10.5 Post-Test Performance Check - Specimen performance characteristics shall be measured under ambient conditions at the completion of specified test sequences. Should the next test sequence occur within 24 hours after successful completion of the post-test performance check, pre-test performance checking will not be required.

4.10.6 Teardown Inspection - After its final test, and with the approval of the contractor, each specimen will undergo a teardown inspection in order to make a full analysis of test deterioration. The final test report shall include a description of the findings and photographs of the deterioration as necessary. Unless otherwise noted, all test speciments shall be returned to the contractor with the final test report.

4.11 Applicable Procedures For Test - The procurement specification shall specify the required ranges and tolerances allowable under the test conditions prescribed in each method. Below are listed the general test categories that shall be required:

(a)	Low Pressure	Method 500, MIL-STD-810
(b)	High Temperature	Method 501, MIL-STD-810
(c)	Low Temperature	Method 502, MIL-STD-810
(d)	Humidity	Method 507, MIL-STD-810
(e)	Salt Fog	Method 509, MIL-STD-810
(f)	Sand and Dust	Method 510, MIL-STD-810
(g)	Explosion	Method 511, MIL-STD-810
(h)	Acceleration	Method 513, MIL-STD-810
(i)	Vibration	Method 514, MIL-STD-810
(j)	Acoustical Noise	Method 515, MIL-STD-810
(k)	Shock	Method 516, MIL-STD-810
(l)	Low Pressure-Solar Energy	Method 517, MIL-STD-810
(m)	Electrical Interference Control	MIL-I-26600

5.0 DATA AND DOCUMENTATION REQUIREMENTS

5.1 General - The quantities, detailed contents, and specific dates of submission of required documents shall be specified in the purchase order.

5.2 Installation and Maintenance Instructions - The Subcontractor shall submit subject instructions for review and approval by the Contractor. The instructions shall include, but not to the exclusion of other information that may be deemed pertinent later, a listing and complete description of all test equipment and other tools required to assemble, install, repair and maintain subject equipment. The recommended test set-up and procedures shall also be provided in sufficient detail to adequately check out the equipment. Should no tools or instruments be required, then a statement to that effect shall suffice.

5.3 Assembly and Operating Instructions - The Subcontractor shall submit subject instructions for review and approval by the Contractor. The instructions shall include, but not to the exclusion of other information that may be deemed pertinent later, a complete description, sufficiently illustrated with drawings and the like, which depict the part-by-part assembly of subject equipment. The operating instructions shall include complete procedures and a detail description of the functional operation of each major assembly and/or system of the equipment.

5.4 Drawings - Drawings furnished by the Contractor or Subcontractor, when applicable, shall become a part of this specification, but only when such drawings are in accordance with the specification herein. Drawings so furnished may be in an acceptable commercial format.

5.4.1 Wiring Diagrams - The Subcontractor shall also furnish detailed electrical schematics of all electronic and electrical equipment, including cabling, and wiring charts.

5.5 Parts Listing - The Subcontractor shall furnish a complete parts list, identifying each part or component required in the construction of the end-item. This identification shall include a part description, manufacturers part number, manufacturers name, and quantity of each part required.

5.6 Reports

5.6.1 Progress Reporting - A letter type progress report shall be submitted, each month giving a complete but concise summary of work accomplished during the reporting period, plans for ensuing period, special problems encountered and their solution or proposed solution.

5.6.2 Qualification Test Report - Upon completion of the qualification test program, a test report shall be submitted, delineating the results of the test operation. Commercial format shall suffice.

5.6.2.1 Contents of Report - Reports shall include a description of the test set-up, the test procedure, a summary of results, sample calculations, and supporting test data. Graphic, tabular and photographic entries shall be made as required for clarity and completeness. In addition, the test report shall contain sufficient cutaway drawings to clearly define the construction, materials, finishes and operation of the article. The supporting test data shall include a narrative history, or log, of the test, which records all incidents of the test which required revision or repair of the test article or test set-up, or rerun of a part of the test.

5.6.1.1 Certification of Report - Test reports shall be certified by the signature of an officer or an authorized employee within the Subcontractor's company. When testing is subcontracted to a testing laboratory, the test reports shall be certified by the signature of an officer of the testing subcontractor's company or by an authorized employee of the testing subcontractor's company.

5.6.3 Final Technical Report - A final report shall be furnished giving a complete summary of all work accomplished under the contract. A preliminary copy of this document shall be submitted for technical and format review and concurrence prior to final production and release of the report.

5.6.4 Subcontractor Initiated Design Changes - The Subcontractor shall notify the Contractor whenever design and development activities result in any detail of article configuration or function that differs from the configuration as disclosed in the Contractor design specification. Prior approval of the Contractor shall be obtained before incorporating any prospective design change. It shall be the Subcontractor's responsibility to coordinate with the Contractor whenever in the course of the design activities there is any indication that a particular design may be contrary to the requirements or intent of this document.

5.6.5 Correspondence Identification - The Subcontractor shall mark each separate drawing item or design information, test report,or piece of correspondence to show that the material pertains to a particular source control part number.

6.0 PREPARATION FOR DELIVERY

6.1 General - Preservation, Packaging, Handling and Shipping of subject equipment shall be in accordance with Section II of NPC 200-2.

6.2 Article Packaging - Individual containers shall be so constructed as to allow removal of parts for inspection purposes without damage to the container or labels. Materials and methods used in packaging the article shall be suitable to ensure protection of the article from handling damage or storage deterioration.

6.3 Intermediate Packaging - Where size or other considerations result in more than one article being packaged within a shipping carton, the individual articles shall be individually packaged within the shipping carton. This precaution is required in order to provide suitable protection and identification during storage and handling after removal of the individual articles from the major shipping container. Any deviation from the above required individual packaging requirement must in all cases be approved by the Contractor prior to shipment.

6.4 Special Instruction - Where the Subcontractor is aware that certain non-obvious characteristics of the specified article will require special handling procedures, it shall be the responsibility of the contractor to notify the Contractor to that effect and thereafter to affix and appropriate removable instruction tag to each such production article delivered.

6.5 Marking - All containers including individual packages and outer cartons shall be marked with the following information:

(a) Subcontractor's name

(b) Name of Article

(c) Quantity in container

(d) Source control part number

SECTION 10

TEST PROGRAM FOR MOMENTUM WHEEL ASSEMBLY

This assembly shall consist of a flywheel, shaft, bearings, electric motor, frequency converter, housing, gimbals, and torquers to apply moment to the inner and outer gimbals.

Testing procedures are listed below:

1. Acceleration test - turning on the power to converter starts the acceleration phase

    1.1 Power input vs time

    1.2 Speed vs time

    1.3 Temperature recordings at various points of wheel, shaft, converter, motor, bearings, and housing. Determine maximum transient temperature gradients.

    1.4 Vibration should be monitored at the bearing supports to determine frequency and magnitude of resonant vibrations. If vibration is excessive or if resonance is detected at frequencies other than those calculated, the mode of shaft motion should further be determined by transducers mounted in two perpendicular directions of each monitoring plane.

    1.5 Total time to reach full speed

2. Full speed performance test

    2.1 Measure power input

    2.2 Measure vibration level

    2.3 Determine angular momentum (speed) variations due to power fluctuations

    2.4 Apply variously scheduled torquer input and measure the following:

        2.4.1 Error in gimbal rates from computed results

        2.4.2 Time lag in gimbal response

        2.4.3 Drift in gimbal angles

        2.4.4 Increase in power demand

        2.4.5 Increase in vibration level or appearance of new mode of vibration

2.4.6 Speed fluctuations and feasible degree of precision which can be maintained by the control circuit

2.4.7 Temperature increase in the bearings

2.4.8 Dynamic stresses in the rotor as recorded from strain gage output

2.4.9 Structural deflections due to applied moments

2.4.10 Structural vibrations, if any

2.4.11 Transverse vibrations of the rotor disc, if any

2.4.12 Maximum attainable gimbal angle (designed for ±60 degrees)

2.5 Reduce lubricant supply and determine effectiveness of bearing failure monitoring devices

2.6 Cycle with maximum torquer input and determine endurance limit and failure mode

2.7 Determine steady-state temperature distribution.

3. Structural test

3.1 The housing should be subjected to 2 atmospheres external pressure differential to demonstrate stability.

3.2 The assembly should be subjected to launch environment vibration and "g" loads. Subsequent start-up must show no significant deviation from pre-test performance.

3.3 Overspeed test - The rotor should be spun to a speed where the local maximum stress exceeds the yield strength by about 3 percent. There should be no measurable permanent set after such a test. This test may be conducted in an evacuated whirl pit.

3.4 Burst test - A rotor should be spun to destruction in a whirl pit. If burst did not occur for any reason, the rotor must still be retired from any further assembly testing.

4. Deceleration test

4.1 Record speed vs time with all power removed from the converter; this should require approximately 32 hours for the H = 1000 ft-lb-sec design.

4.2 Determine vibration levels during coast down.

SECTION II

MAINTENANCE

One of the constraints of the optimization study was to have reliability sufficiently high to eliminate maintenance due to wearout and unpredictable failures. Most of this can be accomplished except for the rotor spin bearings and the evacuation of the rotor housing. Routine programmed maintenance, however, will not be required. Bearing replacement will be anticipated by deterioration detection from temperature and noise sensors. Replacement corrective action can be taken before other problems have a chance to develop.

The design of the CMG is such that the rotor bearings are contained in a preadjusted and standardized cartridge. Bearings will have been previously calibrated and matched so that the keyed insertion of a new cartridge will give balanced operation within the limits established. Access to the cartridge is made easy so that the skill level of the crew member is low and only a limited number of simple tools are required. The axial preload on the bearings will have been determined beforehand and each bearing cartridge will have been previously calibrated and adjusted to have the required amount.

In order to perform a cartridge change, the flywheel must be stopped. This can be accomplished by using the permanent magnet motor as a generator for dynamic braking and by opening the evacuation fitting to let in atmosphere to increase the windage loss. The housing should be blown clean of the oil that has settled on the members which leaked past the housing labyrinth. After the cartridge has been changed, the air is purged from the assembly with helium gas and a pressure of 10^{-3} mm Hg is established. The evacuation fitting is closed and the unit is ready for restart and use.

It is expected that the hermetic seal of the rotor housing will be sufficient so that the desired pressure of 10^{-3} mm Hg can be retained. If, in the final design this is not possible, the action to re-evacuate may be signaled by measurement of motor power loss. Pressure increase will cause increased windage loss. Because of limited gimbal angle, the plumbing for the evacuation fitting can be permanently installed and a fitting on the frame can be made available to the vacuum pump.

It is anticipated that oil replacement in the grease will be required, as it slowly evaporates from the bearing chamber into the flywheel housing space. To provide for this, a spring-loaded piston and oil cylinder is attached to the housing with a small solenoid-operated valve. A timing device included in the control system can supply a few drops of oil to the bearings every 10 days.

SECTION 12

CONTROL

A separate study of the control methods possible with the momentum wheel used as a control movement gyro is covered in Report F-8037.